Susana Costa Saraiva

ANALYSIS OF THE PREFRONTAL CORTEX PROTEOME OF MICE EXPOSED TO PSYCHOTROPIC MEDICATION

Dissertação de Mestrado em Biotecnologia Farmacêutica, orientada pelo Doutor Bruno Manadas (Centro de Neurociências e Biologia Celular) e pelo Prof. Doutor Sérgio Simões (Universidade Coimbra) e apresentada à Faculdade de Farmácia da Universidade de Coimbra

Setembro de 2014

· U C ·

UNIVERSIDADE DE COIMBRA

Susana Costa Saraiva

ANALYSIS OF THE PREFRONTAL CORTEX PROTEOME OF MICE EXPOSED TO PSYCHOTROPIC MEDICATION

Dissertação de Mestrado em Biotecnologia Farmacêutica, orientada pelo Doutor Bruno Manadas (Centro de Neurociências e Biologia Celular) e pelo Prof. Doutor Sérgio Simões (Universidade Coimbra) e apresentada à Faculdade de Farmácia da Universidade de Coimbra

Setembro de 2014

· U C ·

UNIVERSIDADE DE COIMBRA

"If you never try, you´ll never know!"

Author Unknown

AGRADECIMENTOS

Quando mais uma etapa da minha vida é concluida com sucesso é importante realçar o contributo daqueles que me apoiaram e acompanharam durante este percurso e ao longo de toda a minha vida.

Assim, sem mais demoras tenho que agradecer em primeiro lugar ao Doutor Bruno Manadas pela oportunidade de participação neste projecto, pela excelente orientação, pela confiança depositada, pela óptima transmissão de conhecimentos, pela disponibilidade e constante boa disposição, um obrigado muito especial.

Ao meu orientador interno Doutor Sérgio Simões pela disponibilidade e boa orientação durante o decorrer do projecto.

Às minhas colegas do grupo de Proteómica e Metabolómica que me acompanharam durante estes meses. À Cátia Santa e Sandra Anjo pela partilha de conhecimento e pela ajuda nas várias fases do projecto, assim como a ajuda na revisão do documento. À Vera Mendes pela preocupação demostrada, a simpatia e o excelente profissionalismo. À Matilde Melo e Mariana Marcos pela convivência e os momentos de descontração. À Liliana Loureiro e Lúcia Sabala, apesar de não terem estado sempre presentes também foram importantes para mim. À Liliana Loureiro por me ter motivado e inspirado na escolha desta área, pela amizade e bons conselhos, foi bom termo-nos reencontrado novamente. À Lúcia Sabala pelas garagalhadas e constante boa disposição que lhes são características. À Joana Pinto e à Margrida Coelho pela amizade, pelas viagens emocionantes, pelas compras inesperadas, pelas conversas e o apoio constante, um grande obrigada.

Aos meus amigos, os de perto e os de longe, que nunca se esquecem de mim, pelo interesse e preocupação, pelo apoio e motivação, pelos momentos especiais e por aqueles que não pude estar presente, não seria nada sem eles.

À minha família, pelo carinho, preocupação, apoio, paciência e principalmente por todo o esforço que empenham em mim, a quem nunca quero desiludir. E por fim, ao meu namorado, por estar sempre do meu lado e por me fazer feliz.

RESUMO

O principal tratamento para os doentes com esquizofrenia é a medicação psicotrópica, contudo os mecanismos de acção destes medicamentos ainda não são completamente compreendidos. Assim, neste projecto foi realizado o subfraccionamento do proteoma de amostras de cortex prefrontal de ratinhos cronicamente tratados com medicação psicotrópica (Haloperidol, Citalopram e Clozapina). A fracção solúvel foi primeiramente analisada por cromatografia líquida acoplada à espectrometria de massa sequencial (LC-MS/MS) e aproximadamente 1500 proteínas foram identificadas no controlo e em cada condição de medicamento. Posteriormente, 489 proteínas foram quantificadas com elevada confiança usando um método quantitativo sem recurso a marcação (SWATH). A clozapina apresentou 39, o citalopram 23 e o haloperidol 19 proteínas diferencialmente reguladas (usando um $p < 0.05$ e/ou um aumento ou diminuição de 1.5× como limite) e isto pode explicar os diferentes efeitos observados pelos medicamentos revelando diferentes mecanismos de acção. Nas três condições foram encontradas 14 proteínas com $p < 0.05$ e 3 dessas apresentavam $p < 0.01$. A maioria das proteínas alteradas estão no metabolismo, embora outros processos relacionados com a esquizofrenia também foram identificados (via apoptótica, imune e homeostase do cálcio). A elevada expressão da proteína CaMKIIα por todos os medicamentos e da proteína EAAT2 em consequência da administração de clozapina, bem como, a diminuição da calretinina pelo uso da clozapina pode ser importante, uma vez que pode ser um mecanismo de compensação na doença. Todas estas descobertas podem abrir novos caminhos estratégicos para o tratamento e prevenção da progressão da esquizofrenia, uma vez que apontam para novas direcções no conhecimento das alterações relacionadas com a doença.

Palavras chave: Medicação psicotrópica, esquizofrenia, cortex prefrontal, subfraccionamento do proteoma, LC-MS/MS, análise SWATH.

ABSTRACT

Psychotic medication is the main treatment for schizophrenia (SCZ) patients, however their long-term mechanisms of action are not completely understood. Thus, in this project a subproteome fractionation was performed using prefrontal cortex samples of mice, chronic treated with psychotropic drugs (Haloperidol, Citalopram and Clozapine). The soluble fraction were firstly analyzed by liquid chromatography-tandem mass spectrometry (LC-MS/MS) and around 1500 proteins were identified in control and each drug condition. Then, 489 proteins were quantified with high confidence using a label free quantitative method (SWATH). The clozapine presented 39, the citalopram 23, and Haloperidol 19 differentially regulated proteins (using a $p < 0.05$ and/or 1.5 fold change as cut off) and this could explain the different effects observed by the drugs revealed different mechanisms of action. In the three drug conditions 14 proteins presented a $p < 0.05$ and 3 of them a $p < 0.01$. The majority of the changed proteins were involved in the metabolism, although other processes related with SCZ were identified (apoptotic, immune pathways and calcium homeostasis). The increased expression of the proteins CaMKIIα by all the drugs and the EAAT2 in consequence of clozapine administration, as well as, the down regulation of the Calretinin by the use of clozapine could be important, once it may be a compensatory mechanism of the regulation in the disease. Altogether, these findings can give new insights of future strategies for the treatment and prevention of the progression of SCZ once it shows new directions for recognizing disease-related changes.

Keywords: Psychotropic medication; schizophrenia, prefrontal cortex; subproteome fractionation; LC-MS/MS, SWATH analysis.

TABLE OF CONTENTS

LIST OF ABREVIATIONS

2DE	Two-dimensional polyacrylamide gel electrophoresis
BPD	Bipolar disorders
CaMKIIa	Calcium/Calmodulin-dependent Kinase type II subunit alpha
CID	Collision-Induced Dissociation
COMT	Catechol-o-methyl transferase
CV	Coefficient of variation
DA	Dopamine
DAAO	D-amino acid oxidase activator
DAO	D-amino acid oxidase
DAT	Dopamine transporter gene
DIA	Data independent acquisition
DISC1	Disrupted in schizophrenia 1 gene
DTNBP	Dysbindin
EAAT1	Excitatory amino acid transporter 1
EAAT2	Excitatory amino acid transporter 2
EPS	Extrapyramidal-side-effects
ESI	Electrospray ionization
FGAs	First generation antipsychotics
GABA	Gamma-amino-butyric-acid
HPLC	High-performance liquid chromatography
IDA	Information dependent acquisition
iDG	Immature dentate gyrus
iRTs	Indexed Retention Time
LC	Liquid chromatography
m/z	Mass-to-charge ratio
mGluR	Metabotropic glutamate receptor
MMTS	S-methyl methanethiosulfonate
MS	Mass Spectrometry
MS/MS	Tandem mass spectrometry
NMDAR	Ionotropic n-methyl-d-aspartate receptor
NRG1	Neuregulin-1

PET	Positron emission tomography
PFC	Pre-frontal-cortex
Q	Quadrupole
RGS4	Regulator of G protein signaling 4
RP	Reversed phase
SCZ	Schizophrenia
SD	Standard deviation
SGAs	Second Generation Antipsychotics
SSRIs	Selective serotonin re-uptake inhibitors
SWATH	Sequential window acquisition of all theoretical fragmentation spectra
TCA	Tricyclic antidepressants
TCEP	Tris(2-carboxyethyl)phosphine
TEAB	Triethylammonium bicarbonate buffer
TOF	Time-of-flight
Tris	Tris(hidroximetil)aminometano
XIC	Extracted ion chromatograms

INTRODUCTION

1. INTRODUCTION

1.1. Schizophrenia

In 1911 Paul Eugen Bleuler introduced the term "schizophrenia" as a description of a brain disease, which replaced Kraepelin's term *dementia praecox* (Bob and Mashour, 2011). This new name comes from the Greek *schizen*, that means to split, and *phren* that means soul (Fusar-Poli and Politi, 2008).

Schizophrenia (SCZ) is a severe form of mental illness, which is categorized as a psychotic disorder (Frangou, 2008). This disease is a complex and multifactorial clinical disorder (Jablensky, 2013), characterized by a wide phenotypic and etiological heterogeneity (Tandon, Nasrallah and Keshavan, 2009), and exhibiting a variety of course and outcome patterns, ranging from debilitating chronic illness to recurrent episodes with remissions of symptoms in between or, in a small proportion of cases, complete recovery (Jablensky, 2013).

According to the World Health Organization SCZ is ranked as the seventh greatest cause of disability worldwide (Frangou, 2008) and the prevalence rate for this disease is approximately 1% (Karam *et al.*, 2010).

The incidence of schizophrenia increases rapidly after puberty, peaking in the mid-twenties. Its onset in males is particularly early, with a peak of incidence between 15 and 24 years, while on females it increases more gradually over the age range, about 5–7 years later (Tiffin and Welsh, 2013).

Patients with a diagnosis of schizophrenia tend to die 12–15 years before the average population, with this mortality difference increasing in recent decades (Os, van and Kapur, 2009). Moreover the risk of suicide is much higher when compared with the general population (Chien and Yip, 2013). However, the main reason for increased mortality is related to physical causes, resulting from decreased access to medical care and increased frequency of routine risk factors (poor diet, little exercise, obesity, and smoking) (Os, van and Kapur, 2009).

Although the precise societal burden of schizophrenia is difficult to estimate, because of the wide diversity of accumulated data and methods employed (Os, van and Kapur, 2009), the overall U.S. 2002 cost of schizophrenia was estimated to be $62.7 billion, with $22.7 billion excess direct health care cost ($7.0 billion on outpatient, $5.0 billion on drugs, $2.8 billion on inpatient, and $8.0 billion on long-term care) (Wu *et al.*, 2005).

Schizophrenia is characterized by an admixture of positive, negative, disorganization, mood, psychomotor, and cognitive symptoms (Carpenter and Tandon, 2013). Positive

symptoms involve impaired reality testing and include delusions, hallucinations, and other reality distortions (Tandon *et al.*, 2009).

Negative symptoms involve a blunting or loss of a range of affective and conative functions. These include impairments in affective experience and expression, abulia (loss of motivation), alogia (poverty of speech), anhedonia (inability to experience pleasure), avolition (lack of initiative), apathy (lack of interest), and reduced social drive (Elis, Caponigro and Kring, 2013).

Disorganization includes disorganized thoughts and speech (neologisms, poverty of thought content or incoherent verbal communication) and disorganized behavior (inappropriate or unusual actions) (Elis *et al.*, 2013).

In what concerns mood symptoms schizophrenia patients could exhibit increased emotional arousal and reactivity in conjunction with positive symptoms, as well as, significant depressive symptoms during the course of the disease (Tandon *et al.*, 2009).

Slowness of psychomotor activity is common in schizophrenia, it is variably associated with negative and depressive symptom clusters, and means a poor outcome. Excessive motor activity, often apparently purposeless, is more often associated with exacerbations of positive symptoms (Tandon *et al.*, 2009). Individuals with schizophrenia show significant deficits in a number of different cognitive domains, including executive function, working memory and episodic memory (Barch and Ceaser, 2012).

The course of schizophrenia can be divided into premorbid, prodromal, first-episode, and chronic phases (Abbott and Keith, 2010). In premorbid phase patients often have a subtle and nonspecific cognitive, motor and/or social dysfunction (Frangou, 2008), in prodromal phase they have a gradual onset of symptoms (misperceptions, over-valued beliefs, ideas of reference) prior to the onset of psychotic symptoms (Abbott and Keith, 2010). The first psychotic episode indicating formal onset of schizophrenia, and finally, there is a stable phase or plateau, when psychotic symptoms are less prominent and negative symptoms and the stable cognitive deficits increasing (Tandon *et al.*, 2009).

1.1.1.   Etiology and Pathophysiology of Schizophrenia

While an etio-pathophysiological nosology of schizophrenia and related psychotic disorders is currently elusive (Carpenter and Tandon, 2013) and there is, as yet, no validated biological marker that could assist diagnosis (Jablensky, 2013), diagnosis criteria remains essentially based on the Diagnostic and Statistical Manual of Mental Disorders, 5th edition from

2013 (Tandon *et al.*, 2013) and on the International Classification of Diseases, 10th revised edition from 2003 (Tandon and Maj, 2008), which is expected to be updated in 2015 (Gaebel, Zielasek and Cleveland, 2013).

Once the diagnosis is subjective, neuroimaging and cognitive testing may help to rule out alternatives, such as schizophrenia-like psychotic features secondary to brain or other medical disease (Jablensky, 2013).

Many studies have demonstrated that the hippocampus (Föcking *et al.*, 2011; Harrison, 2004) and cortex (Williamson and Allman, 2012) have a central role in the neuropathology and pathophysiology of schizophrenia. Different approaches have been used to provide evidences of that importance, both *in vivo* (neuropsychology, structural and functional imaging) (Kasai *et al.*, 2002) and *post mortem* (histology, morphometry, gene expression, and neuro-chemistry) (Harrison, 2004).

Several imaging technologies, such as functional magnetic resonance imaging, diffusion tensor imaging (Ross *et al.*, 2006), structural magnetic resonance imaging, magnetic resonance spectroscopy, event-related potentials, magnetoencephalography (Kasai *et al.*, 2002), positron emission tomography (PET), single-photon emission computed tomography (Chana *et al.*, 2013) and others, are techniques that allow to identify the brain abnormalities in patients with schizophrenia.

Although the findings have been frequently inconsistent and the results are difficult to replicate, most studies have found widespread lateral and third ventricular enlargement (Kasai *et al.*, 2002; Os, van and Kapur, 2009; Ross *et al.*, 2006), and volume reduction of the hippocampus (Haren, van *et al.*, 2012; Harrison, 2004; Honea *et al.*, 2000) and cortex (Kasai *et al.*, 2002; Ohtani *et al.*, 2013; Owens *et al.*, 2012; Williamson and Allman, 2012). The regions demonstrated as being affected by this disease are involved in cognitive, emotional, and motivational aspects of human behavior (Kasai *et al.*, 2002).

A major confounding factor in neuroimaging studies in general, and in studies investigating brain volume change over the time in particular, is the cumulative intake of psychotic medication. It is difficult to establish whether these changes in structural brain abnormalities are caused by the disease or are an effect of treatment (Haren, van *et al.*, 2012).

It is well known that schizophrenia aggregates in families. Although over two-thirds of the cases occur sporadically, having an affected family member substantially increases the risk of developing schizophrenia (Tandon, Keshavan and Nasrallah, 2008). Several genes and environmental factors have been associated with this disease (Bertolino and Blasi, 2009; Bray *et al.*, 2010; Hosak, 2013; Modinos *et al.*, 2013). About 60% of schizophrenic patients do not

have an affected first-degree relative, and about 40% of the monozygotic twins of schizophrenia patients remain healthy, leading to an estimated heritability of around 60–80 % demonstrating that genetic risk alone does not explain the full picture (Akdeniz, Tost and Meyer-Lindenberg, 2014). In schizophrenia, environmental factors are proposed to play a role up to 60% (Schmitt *et al.*, 2014). The risk of schizophrenia increases with some factors such as cannabis abuse, urbanicity, immigration, physical and psychological abuse, parental lost, obstetric complications and inflammation during pregnancy (Os, van and Kapur, 2009; Ratajczak, Wozniak and Nowakowska, 2013; Schmitt *et al.*, 2014; Akdeniz *et al.*, 2014; Tandon *et al.*, 2008).

It is now generally accepted that schizophrenia is a polygenic disorder (Bray *et al.*, 2010) although, finding these susceptibility genes has proven to be extremely difficult (Bertolino and Blasi, 2009; O'Tuathaigh *et al.*, 2007).

The nature of human psychopathology seriously confounds efforts to create valid animal models of schizophrenia at the level of behavior (Kirby, Waddington and O'Tuathaigh, 2010). The literature describe four basic groups of animal models of schizophrenia, such as: models created by pharmacological intervention, genetic models, lesion models, and models of developmental disorders of primary brain structures. None of the models is perfect as none of them reflects the full clinical picture observed in humans (Ratajczak *et al.*, 2013).

Nevertheless gene disruption, either by deletion (knockouts) or insertion/over-expression (transgenic/knock-in), with increasing conditional control over the spatial or temporal expression of the mutation are used for the breeding of mutant mice with the objective to clarify the functional roles of genes and their encoded proteins at a mechanistic level, to identify novel therapeutic targets and to feed into clinical studies so as to resolve phenotypic relationships and evaluate those targets (Kirby *et al.*, 2010). Given the likely polygenic basis of the disorder, neither partial or complete loss of function nor overexpression of any single gene in mice is likely to produce an animal model with construct validity for schizophrenia (O'Tuathaigh *et al.*, 2007).

Altered neurotransmission has been appointed as one of the principal pathophysiological mechanism underlying the expression of schizophrenia symptoms (Frangou, 2008). Many studies established that the dopaminergic system is implicated in schizophrenia (Broome *et al.*, 2005; Chana *et al.*, 2013; Jean Lud Cadet, Subramaniam Jayanthi, Michael T. McCoy, Genevieve Beauvais and Cai, 2010). Dopamine (DA), is the most abundant catecholamine neurotransmitter in the basal ganglia, it participates in the regulation of motor functions and of cognitive processes such as learning and memory (Jean Lud Cadet, Subramaniam Jayanthi, Michael T. McCoy, Genevieve Beauvais and Cai, 2010). Multiple indices of dopamine

transmission have been found altered (Abi-Dargham *et al.*, 2009), giving rise to the "dopamine hypothesis in schizophrenia (Eyles, Feldon and Meyer, 2012). This hypothesis suggests that too much dopamine stimulation in the anterior cingulate cortex causes positive symptoms and too little dopamine stimulation in the dorsolateral frontal lobe causes negative symptoms/cognitive impairment (Eggers, 2013).

This is supported by the observation that drugs such as amphetamine, cocaine and methamphetamine all increase dopaminergic transmission and are capable of inducing psychosis (Chana *et al.*, 2013). Thus, given that the psychotic symptoms of schizophrenia are uniquely human and thus not accessible in animals, one approach adopted to induce in these a certain behavior like the disease is through the administration of these drugs (pharmacologically based models) (Kirby *et al.*, 2010; O'Tuathaigh *et al.*, 2007).

Other studies use genetic models related to putative dopaminergic pathophysiology. Given evidences for intensified activation of sub-cortical D2 DA receptors in schizophrenia, it is notable that the phenotype of transgenic mice with selective over-expression of D2 receptors in the striatum is characterized by locomotor hyperactivity in a novel environment. Also a hyperactive phenotype has been widely reported in mutants with knockouts or knockdown of the dopamine transporter (DAT) gene, this may be related to disrupted DAT–D2 receptor interaction (Kirby *et al.*, 2010).

Another evidence that this system is implicated is the dysregulation in the candidate susceptibility gene for catechol-o-methyl transferase (COMT). This gene is linked to the 22q11 susceptibility region, a microdeletion of chromosome 22 is associated with velocardiofacial syndrome or Di George syndrome, which has been linked with increased risk for schizophrenia (O'Tuathaigh *et al.*, 2007; Monks *et al.*, 2014). COMT, encoding for the enzyme that degrades dopamine (Chana *et al.*, 2013), is critically involved in DA metabolism, particularly in the prefrontal cortex (PFC) where functional specificity of COMT to DA metabolism has been proposed to derive from the low levels of DA transporters at synapses in PFC relative to the striatum (O'Tuathaigh *et al.*, 2007; Kirby *et al.*, 2010).

The cholinergic system has also gained importance in this disease (Chana *et al.*, 2013; Scarr *et al.*, 2013), once cholinergic neurons innervate anatomical structures implicated in schizophrenia and participate in processes that are altered in patients such as attention, working memory, and motivated behaviors (Karam *et al.*, 2010). All functions of the cholinergic system are controlled by the interaction of acetylcholine with the nicotinic and muscarinic receptors (Scarr *et al.*, 2013) and the most reproduced findings suggest that the problems in the cholinergic system in schizophrenia are not simply due to changes in levels of acetylcholine

(Scarr *et al.*, 2013) but a widespread decrease in levels of muscarinic receptors (Chana *et al.*, 2013; Scarr *et al.*, 2013).

Gamma-amino-butyric-acid (GABA) has been implicated for a number of years in this disorder because of the reductions in GABAergic markers such as glutamic acid decarboxylase-67, the synthesizing enzyme for GABA, in the cortex and hippocampus (Chana *et al.*, 2013; Kannan, Sawa and Pletnikov, 2013).

Although studies on the serotonin system are far less abundant, serotonin transporter density has been found unaltered in schizophrenia. Whereas the stimulatory 5-HT$_{2A}$ receptors are decreased in drug naive patients, and the inhibitory 5-HT$_{1A}$ receptors showing increased densities in postmortem studies, in PET studies were found both increased and decreased binding (Hirvonen and Hietala, 2011).

"NMDA hypofunction hypothesis of schizophrenia" is derived from the observations that drugs such as ketamine and phencyclidine that primarily block ionotropic n-methyl-d-aspartate receptors (NMDARs) are capable of causing negative and positive symptoms (Karam *et al.*, 2010). This evidences, as well as, the observation that the kainate receptor expression is decreased in the cortex while hippocampal expression of subunits of the NMDA receptor are altered, led to the involvement of the glutamatergic system in schizophrenia (Chana *et al.*, 2013).

Recent reviews have documented both the status of putative metabotropic glutamate receptor (mGluR) dysfunction in the pathophysiology of schizophrenia and the phenotype of mutation for members of this receptor family (mGluR1–8) (Kirby *et al.*, 2010).

Furthermore, many of the genes that have consistently been associated with schizophrenia, such as neuregulin-1 (NRG1), regulator of G protein signaling 4 (RGS4), dysbindin (DTNBP), and D-amino acid oxidase activator (DAAO) are involved in regulation of glutamatergic neurotransmission (Bray *et al.*, 2010; Chana *et al.*, 2013; Kannan *et al.*, 2013; O'Tuathaigh *et al.*, 2007).

The neuregulins are a family of growth and differentiation factors whose effects are mediated via four neuregulin genes (NRG1-4) that bind to the ErbB family of tyrosine kinase transmembrane receptors (ErbB1-4) (O'Tuathaigh *et al.*, 2007). NRG1 signaling, via ErbB receptors and regulation of both NMDA receptors and postsynaptic density 95, has been implicated in neuronal differentiation and migration, synapse formation and plasticity and regulation of neurotransmitter expression and function (O'Tuathaigh *et al.*, 2007; Ross *et al.*, 2006). A mutant mouse line that expressed only 5% of normal levels of the NMDA receptor subunit NR1 were developed, and exhibited hyperactivity that responded to the typical

antipsychotic haloperidol, but they also exhibited impaired social behaviors and reproducing that were partially reversed by the atypical antipsychotic clozapine (Ross *et al.*, 2006). The functional role of NRG1 in schizophrenia is still uncertain, particularly since many different alleles and haplotypes have been implicated (O'Tuathaigh *et al.*, 2007; Owen, Craddock and O'Donovan, 2005; Ross *et al.*, 2006).

The functional role of RGS4 in the central nervous system is largely unknown. RGS4 is widely expressed throughout this system and is involved in the regulation of G protein-coupled receptors which mediate signal transduction of DA, glutamate, GABA and several other neurotransmitters (O'Tuathaigh *et al.*, 2007). There is now some evidence to suggest association between genetic variation at the RGS4 gene and schizophrenia, although it would appear that any contribution of RGS4 to schizophrenia susceptibility is modest (O'Tuathaigh *et al.*, 2007).

Dysbindin binds to both α- and β-dystrobrevin, which are components of the dystrophin glycoprotein complex. The dystrophin complex is found in the sarcolemma of muscle but is also located in postsynaptic densities in several brain areas, particularly mossy fibre synaptic terminals in the cerebellum and hippocampus (Owen *et al.*, 2005). Although its functions are largely unknown, reduced levels of expression of dysbindin messenger RNA or protein have been found in schizophrenic brains raising the possibility that polymorphisms in dysbindin associated with schizophrenia may modulate expression level of the protein (Ross *et al.*, 2006). Moreover, some data suggest that variation in DTNBP1 might confer risk by pre-synaptic effects on glutamate trafficking or release (Owen *et al.*, 2005).

The chromosome 13 locus has strong linkage regions to schizophrenia. Among other genes, this locus contains the G72 gene, now called the D-amino acid oxidase activator gene. DAOA activates D-amino acid oxidase (DAO), which oxidizes D-Serine, a coagonist at NMDA glutamate receptors (Ross *et al.*, 2006). Thus, there is some biologic plausibility for DAOA and DAO in contributing to risk for schizophrenia, based on the glutamate hypothesis, once an increase in DAO enzyme activity and gene expression has been reported in post-mortem brain tissue from patients with schizophrenia (Kirby *et al.*, 2010).

There is also evidences that support the involvement of the disrupted in schizophrenia 1 (DISC1) gene at 1q42.1, which was originally identified in a family which displayed a variety of psychiatric disorders with a chromosome translocation (Zhang, Feng *et al.*, 2006). This gene encodes for a protein of 854 amino acids, with no obvious homology to other proteins of known function (Zhang, Feng *et al.*, 2006). Examination of protein expression in post-mortem brain of patients with schizophrenia has also revealed altered subcellular distribution of a

DISC1 isoform in orbitofrontal cortex (O'Tuathaigh *et al.*, 2007). Mutant DISC1 is proposed to contribute to schizophrenia susceptibility by disrupting intracellular transport, neurite modeling, and neuronal migration (Zhang, Feng *et al.*, 2006).

The evidences in all these studies are sufficient to suggest that schizophrenia is a progressive brain disease (Haren, van *et al.*, 2012) and is not a neurodegenerative disease (Harrison, 2004; Martins-de-Souza, 2012). None of the original reports for the genes mentioned above is compelling alone, and there is insufficient follow-up to make informed judgments (Owen *et al.*, 2005).

There is lack of clarity concerning the relative schizophrenia risk quotient associated with even the most widely considered susceptibility genes regarding emergent genome-wide association studies (Kirby *et al.*, 2010).

1.2. Current Approaches in Schizophrenia Treatment

Until the early 1950s, the treatments used in schizophrenia were: inducing a condition of shock with cardiazol, insulin or electrical current, or cutting the connections between the frontal cortex and the deeper brain regions (lobotomy) (Ellenbroek, 2011).

The current approaches to treatments for schizophrenia still apply electroconvulsive shock, in a controlled manner, for specific treatment resistant cases (Ellenbroek, 2011) and more recently different approaches to psychosocial interventions have been used successively (Elis *et al.*, 2013). However, the main-stream and standard treatment for nearly all patients is psychotropic medication, especially antipsychotic drugs (Miyamoto *et al.*, 2005). And since subsyndromal symptoms of depression in patients with schizophrenia are common and clinically important, another class of psychotropic medication commonly prescribed is antidepressants (Dawes *et al.*, 2012).

An antipsychotic (or neuroleptic) is a tranquilizing psychiatric drug used primarily to manage psychosis. Antipsychotic drugs have been used to treat patients with schizophrenia and other psychotic disorders like bipolar disorders (Park, E. J. *et al.*, 2013). These drugs can be divided into three groups: typical or first-generation, atypical or second-generation, and third-generation antipsychotics (Park, E. J. *et al.*, 2013).

Antipsychotics are shown to be effective against positive symptoms in patients with schizophrenia, however, their use alone may be limited by their inability to tackle the frequently occurring negative symptoms and cognitive impairments (Chien *et al.*, 2013).

Moreover a continuous long-term antipsychotic therapy is required for patients with schizophrenia to control symptoms and reduce relapse rates (Park, E. J. *et al.*, 2013).

Antipsychotic drugs are monoamine receptor antagonists (Nguyen *et al.*, 1992). All the currently available antipsychotics, except the third generation antipsychotics (Ellenbroek, 2011), block the dopamine D2 receptor family (Kapur and Seeman, 2000). The third-generation antipsychotic are a partial dopamine agonist, it means, it is an antagonist in brain areas with high dopamine levels and it is an agonist in areas with low dopamine activity (Ellenbroek, 2011). All antipsychotic medications are associated with an increased likelihood of sedation, sexual dysfunction, postural hypotension, cardiac arrhythmia, and sudden cardiac death (Muench and Hamer, 2010).

So far, previous studies have not been able to elucidate all effects of these drugs (Chien *et al.*, 2013) Therefore a promising route of investigation into the causes of the schizophrenia is to study how psychotic drugs alter brain function, as it can help to unravel neural mechanisms involved in the pathogenesis of this disorder (Critchlow *et al.*, 2006; Konradi and Heckers, 2001).

1.2.1. First Generation Antipsychotics

Chlorpromazine was the first antipsychotic drug and its use in schizophrenic patients marked the beginning of a revolution in the treatment of schizophrenia in 1950's (Chien *et al.*, 2013; Ellenbroek, 2011). Subsequently several other first generation antipsychotics (FGAs) were introduced into the market including haloperidol, and this widespread use led to a rapid decline in the number of patients in psychiatric institutions (Chien *et al.*, 2013; Ellenbroek, 2011).

First generation antipsychotics also known as typical, conventional, classical or traditional antipsychotics, are classified according to their chemical structure: the *Butyrophenones* to which haloperidol belongs to; the *Phenothiazines* such as Chlorpromazine; and the *Thioxanthenes* (Park, E. J. *et al.*, 2013).

Most of all, FGAs are a relatively low-cost treatment and commonly used medication (Chien *et al.*, 2013). They have satisfactory efficacy in positive symptoms reduction, however there is limited evidence to support their efficacy against the negative and cognitive symptoms (Chien *et al.*, 2013).

Major adverse events induced by FGAs generally include sedation, movement disorders, endocrine disturbance, and metabolic and electrocardiogram changes (Chien *et al.*, 2013).

Nevertheless, the extrapyramidal-side-effects (EPS) may be considered the most debilitating side effects of these drugs, which include: pseudoparkinsonism, akathisia (characterized by a restless feeling), acute dystonia, and tardive dyskinesia (repetitive involuntary movements) (Muench and Hamer, 2010). This is primarily true for medications that bind tightly to dopaminergic neuro-receptors, such as haloperidol, and less likely with FGAs that have weaker dopamine blockade (Muench and Hamer, 2010).

Haloperidol

Haloperidol, which structure is represented in Figure1.1, was synthesized in 1958 by the Janssen Pharmaceutica (Ban, Healy and Shorter, 2004), which is now part of Johnson & Johnson Pharmaceutical Research and Development.
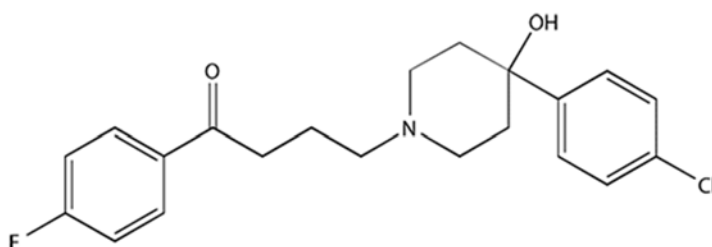
Figure 1.1 - Chemical structure of Haloperidol (Ebrahimzadeh *et al.*, 2013). The chemical designation is 4-[4-(p-chloro-phenyl)-4-hydroxypiperidino]-4'—fluorobutyrophenone and it has the following molecular formula: $C_{21}H_{23}ClFNO_2$ and molecular weight: 375.864223g/mL.

Also known by the commercial name of Haldol, is a butyrophenone derivative and was first marketed in the United States in 1967 (Gerace *et al.*, 2012).

This drug is a first-generation antipsychotic that is widely used clinically (Park, J. *et al.*, 2012a). It is an effective antipsychotic agent commonly used in the treatment of schizophrenia and in the treatment of acute psychotic states, such as drug-induced psychosis (LSD, psilocybin, amphetamines, ketamine, phencyclidine) and psychosis associated with high fever or metabolic disease (Ebrahimzadeh *et al.*, 2013) and delirium (Gerace *et al.*, 2012).

Haloperidol exert its therapeutic properties mainly by blocking D2 receptors and exhibits low activity at 5-HT$_{2A}$, D1, and α1 and α2 adrenergic receptors, and only minimal affinity to 5-HT$_{1A}$ and histamine receptors, in contrast with second generation antipsychotics (Karl *et al.*, 2006; Schmetzer, 2008).

In schizophrenia, haloperidol reverses positive symptoms but is not particularly effective against negative symptoms or cognitive deficits (Karl *et al.*, 2006).

Adverse reactions to haloperidol, like other FGAs, include drowsiness, blurred vision, extrapyramidal effects, tachycardia, hypotension and muscular rigidity (Gerace *et al.*, 2012).

Haloperidol is metabolized to a haloperidol pyridinium ion that is toxic and can increase oxidative stress and induce plasma membrane damage, which may partially explain the pathogenesis of haloperidol induced extrapyramidal side effects such as parkinsonism symptoms (Bošković *et al.*, 2013). It has also been widely cited to induce changes in brain volume, including enlargement of the caudate nucleus and reductions in cortical gray matter (Vernon *et al.*, 2012).

Though a number of theories have been proposed, the precise pathophysiological mechanisms responsible for the development of these adverse drug reactions are not known (Crowley *et al.*, 2013). Moreover, molecular and cellular adaptations responsible for its mechanism of action remain largely unknown. Understanding this involves the study of long-term effects of haloperidol, not only on neurotransmitters and their receptors, but also on the signal transduction pathways that translate their actions on neuronal activity (Dlaboga, Hajjhussein and O'Donnell, 2008).

1.2.2. Second Generation Antipsychotics

Second Generation Antipsychotics (SGAs) are also described as atypical antipsychotics, due to the drug clozapine, the first SGA to be introduced (Duncan *et al.*, 2000). Clozapine seemed atypical in the sense that it did not cause extra-pyramidal side effects in patients, in contrast to the FGAs (Kapur and Remington, 2001).

Imaging studies suggest that while FGAs require striatal D2 occupancy of ~75% for efficacy (and EPS occur at ~80% occupancy), SGAs display <60% occupancy of striatal D2 receptors (Wenthur and Lindsley, 2013).

The atypical antipsychotics are classified according to their pharmacological properties (Park, E. J. *et al.*, 2013), and the development of other SGAs like risperidone, olanzapine, quetiapine, ziprasidone, amisulpiride, sertindole, and zotepine have also gained atypical status (Kapur and Remington, 2001).

The efficacy of second-generation antipsychotics on cognitive and social functioning, as well as other longer-term effects such as mortality and quality of life, are inconsistent (Chien *et al.*, 2013).

SGAs have similar effects to FGAs in terms of reduction of positive and disorganization symptoms. Although, neither of them has convincingly proven to be effective in reducing negative symptoms, SGAs have more advantages against these, for the reason perhaps that they don´t cause extra-pyramidal side effects which can even worsen the negative symptoms (Lieberman and Stroup, 2005).

The safety advantages of the atypical drugs have been questioned because of their propensity to induce weight gain, drowsiness, sexual dysfunction, and altered glucose and lipid metabolism (Ellenbroek, 2011; Lieberman and Stroup, 2005).

The atypical agents differ pharmacologically from previous antipsychotic agents in their lower affinity for dopamine D2 receptors, but they have affinities for other neuro-receptors, including other dopaminergic (D1, D3 or D4), serotonergic (especially 5-HT_{2A} and 5-HT_{2C}), adrenergic (mainly α1) and histaminergic (especially H1) (Ellenbroek, 2011; Lieberman and Stroup, 2005).

The discovery of clozapine, and similar drugs, also led to the dopamine hypothesis of schizophrenia, which had a high impact on the search for neurotransmitter functions. However, the pathophysiology of schizophrenic symptoms and the related mechanism of action of antipsychotics could not be fully explained (Ackenheil and Weber, 2002).

Clozapine

Clozapine, which structure is represented in Figure 1.2, is a generic name for the brand Clozaril, manufactured by Novartis (Wenthur and Lindsley, 2013). It was the first second generation antipsychotic to be introduced in Europe in 1971 (Park, J. *et al.*, 2012b; Wenthur and Lindsley, 2013)

This drug was also the first antipsychotic agent that demonstrated clinical efficacy for positive symptoms without the risk of developing EPS (Abi-Dargham and Laruelle, 2005; Duncan *et al.*, 2000), and until today clozapine remains one of the most clinically effective antipsychotics available (Wenthur and Lindsley, 2013).

This unique feature of clozapine significantly broadened understanding of the mode of action of antipsychotics, and created new hypotheses for schizophrenia (Ackenheil and Weber, 2002).

The common adverse effects of the SGAs have also been associated with clozapine (Wenthur and Lindsley, 2013), such as metabolic syndrome, specially weight gain (Chien *et al.*, 2013). Nonetheless, other serious effects have been reported, in fact, clozapine was removed

from the market in 1975 because of its risk for agranulocytosis, an acute condition resulting in lowered white blood cell count (commonly neutrophils), placing patients at high risk of infections due to suppressed immune system (Abi-Dargham and Laruelle, 2005; Park, J. *et al.*, 2012b; Wenthur and Lindsley, 2013).
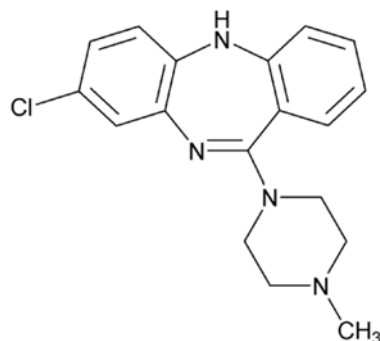
Figure 1.2 - Chemical structure of Clozapine (Seeman, 2014). The chemical designation is 8-Chloro-11-(4-methyl-1-piperazinyl)-5H-dibenzo[b,e][1,4]diazepine and it has the following molecular formula: $C_{18}H_{19}ClN_4$ and molecular weight: 326.82326g/mL.

Clozapine was then reintroduced in 1989, since patients who are resistant to treatment with typical antipsychotics remain a major therapeutic challenge in schizophrenia, and clozapine was shown to be the gold standard treatment for this patient group (Abi-Dargham and Laruelle, 2005; Cacabelos, Hashimoto and Takeda, 2011; Chandrappa and Ho, 2012; Duncan *et al.*, 2000).

Clozapine is a tricyclic benzodiazepine and an example of polypharmacology, once this drug and its active metabolite norclozapine (N-desmethylclozapine) has affinity for several receptors (Wenthur and Lindsley, 2013). It has low affinity, with only 40−60% occupancy, and a fast dissociation from dopamine D2 receptors, in contrast with >80% occupancy by FGAs, which may account for the lack of extrapyramidal side effects (Kapur and Seeman, 2000). The chemical structure of clozapine facilitates a relatively rapid dissociation from D2 receptors (Seeman, 2014). It shows high affinity for serotonin receptors, specially 5-HT$_{2A}$ receptor, but also muscarinic, cholinergic, histamine and preference for others dopaminergic receptors, such as D1 and D4 over D2 (Ellenbroek, 2011).

The high affinity of clozapine, which occupies almost all (actually 96%) of the 5HT$_{2A}$ receptors (Seeman, 2014), was suggested to contribute to its reduced side-effect liability, greater efficacy and its activity in therapy-resistant schizophrenia (Schmidt *et al.*, 1995). However new studies propose that the great difference between the serotonin 5HT$_{2A}$ and D2

affinities in atypical antipsychotics was not due to higher 5HT$_{2A}$ affinities but to lower D2 affinities (Seeman, 2014).

Thus, the observed clinical efficacy of clozapine can be accounted for almost all of the prevailing hypotheses used to explain the etiology of schizophrenia (Wenthur and Lindsley, 2013). Despite of these intense studies, the precise molecular underpinnings that account for clozapine's unique efficacy remain elusive (Wenthur and Lindsley, 2013).

1.2.3. Antidepressants

Depressive symptoms occur in a large set of patients with schizophrenia and may be present throughout all phases of this disease (Lako *et al.*, 2012).

Negative and cognitive symptoms in schizophrenia are generally poorly responsive to antipsychotic drug treatment (Dawes *et al.*, 2012; Iancu *et al.*, 2010). Therefore various augmentation strategies are used, among them the combination of the antipsychotic with an antidepressant (Rummel, Kissling and Leucht, 2005).

Antidepressants can be distributed according to their mechanism of action into several groups (Lôo *et al.*, 2004) such as monoamine re-uptake inhibitors (which comprises tricyclic antidepressants, and selective serotonin re-uptake inhibitors (SSRIs)), psychostimulant antidepressants, receptor antagonists, and monoamine oxidase inhibitors (Howard *et al.*, 2012).

All antidepressants enhance transmission of one or more monoamines, either by reuptake inhibition, enzyme inhibition or activity at pre- or postsynaptic receptors (Howard *et al.*, 2012). Although increased monoamine transmission occurs within hours, the antidepressant effect is slower to appear because this requires normalization of receptor sensitivity and neuroplasticity (Howard *et al.*, 2012).

Several studies suggest that selective SSRIs, which citalopram belongs to, have the potential for ameliorating the negative symptomatology of schizophrenia patients (Dawes *et al.*, 2012; Iancu *et al.*, 2010).

The tricyclic antidepressants (TCA) were the first drugs to be considered antidepressants. The SSRIs are newer and largely replaced the TCA because they show a similar efficacy with less significant side effects (Ables and Baughman, 2003; Fitzgerald and Bronstein, 2013; Helmut Buschmann, Jörg Holenz and Vela, 2007). Common side effects of SSRIs include transient nausea, diarrhea, insomnia, somnolence, dizziness, akathisia, and long-term orgasmic dysfunction (Ables and Baughman, 2003; Gordon, 2013).

SSRIs block the reuptake of serotonin (5-HT$_{1A}$, 5-HT$_{2C}$, 5-HT$_{2C}$, and 5-HT$_{3C}$) into the presynaptic nerve terminal, thereby enhancing serotonin neurotransmission (Ables and Baughman, 2003; Gordon, 2013; Nutt *et al.*, 1999). Atypical antipsychotics antagonize both serotonin and dopamine receptors, so this antagonism is, however, often confounded by co-administration of antidepressants (Sheremata and Chen, 2004).

The developments in the future are likely to remain focused on monoamine neurotransmitters, with the aim of finding agents that are either more effective, better tolerated or that have a faster onset of action than the existing options (Nash and Nutt, 2007).

Citalopram

Citalopram, which structure is represented in Figure 1.3, marketed as Celexa, was originally created in 1989, by the pharmaceutical company Lundbeck.
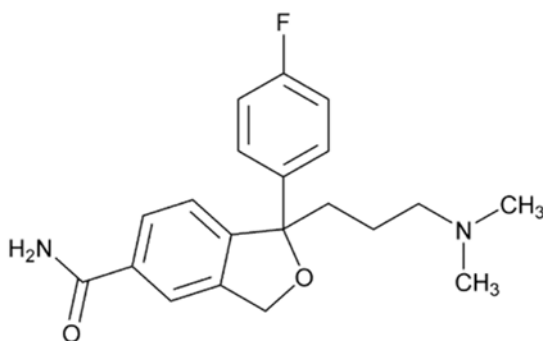
Figure 1.3 - Chemical structure of Citalopram (Moltke, von *et al.*, 1999). The chemical designation is 1-[3-(dimethylamino)propyl]-1-(4-fluorophenyl)-3H-2-benzofuran-5-carbonitrile and it has the following molecular formula: $C_{20}H_{21}FN_2O$ and molecular weight: 324.391943g/mL.

It is a selective serotonin reuptake inhibitor, and was approved to treat depression becoming available in the United States in 1998 (Vieweg *et al.*, 2012).

The use of antipsychotic treatment with this antidepressant drug results in a significant reduction of the severity of subsyndromal depressive symptoms in patients with schizophrenia (Dawes *et al.*, 2012).

As a SSRI, citalopram acts by inhibiting the neuronal uptake of serotonin with minimal effect on norepinephrine and dopamine (Cuenca, Holt and Hoefle, 2004), therefore it is the most selective of the SSRIs (Barak *et al.*, 2003).

In addition to its ability to inhibit serotonin reuptake, citalopram has some affinity to α1-adrenoceptors and a slight histamine H1-receptor blocking potency (Hiemke and Härtter, 2000).

Hepatic biotransformation of citalopram is mediated mainly by cytochrome P450 family of enzymes (Moltke, von *et al.*, 1999; Vieweg *et al.*, 2012), to form a principal metabolite, N-desmethylcitalopram (Moltke, von *et al.*, 1999; Unceta *et al.*, 2013) which can be measured in plasma (Hiemke and Härtter, 2000).

Side effects from citalopram include dizziness, sweating, nausea, vomiting, tremor, somnolence, and sinus tachycardia (Ables and Baughman, 2003; Cuenca *et al.*, 2004).

Nevertheless citalopram has a wide margin of safety (Brøsen and Naranjo, 2001), and although many of the SSRIs are reported as having many drug-drug interactions, this drug has low potential for drug interactions and may be appropriate in patients taking multiple medication and in elderly patients because of its tolerability (Ables and Baughman, 2003).

1.3. Proteomic Studies

Schizophrenia is the result of DNA alterations and environmental factors, which together lead to differential protein expression and ultimately to the development of the illness (Martins-de-Souza, Maccarrone, *et al.*, 2010). While genomic investigations continue to contribute with important insights (Föcking *et al.*, 2011), they have not answered elementary questions on the pathophysiology of the disease, nor have they resulted in the identification of biomarkers with predictive value for disease risk or therapeutic response (Martins-de-Souza *et al.*, 2012).

Thus several proteomic studies of postmortem brain tissue from subjects with schizophrenia and model animals of this disease have been made (English *et al.*, 2011; Föcking *et al.*, 2011; Martins-de-Souza, 2012; Martins-de-Souza, Maccarrone, *et al.*, 2010; Martins-de-Souza *et al.*, 2012; Rao *et al.*, 2012). They have demonstrated changes in cytoskeletal, synaptic, metabolic, and mitochondrial proteins (English *et al.*, 2011; Föcking *et al.*, 2011; Martins-de-Souza, 2012; Martins-de-Souza, Harris, *et al.*, 2010; Martins-de-Souza, Maccarrone, *et al.*, 2010).

However, confounding factors such as the effects of chronic medication and sample heterogeneity have resulted in difficulties in interpreting the results (Martins-de-Souza *et al.*, 2012). This has led to the need for studies that reveal proteomic alterations induced by the medication usually prescribed to SCZ patients (Konopaske *et al.*, 2013; Ma *et al.*, 2009).

One of these studies allowed the identification of 30 proteins, which functions are related with metabolic, signaling, transport, protein metabolism, chaperone, DNA binding and cell cycle categories, that are differently expressed in rats after chronic treatment with risperidone (O'Brien *et al.*, 2006).

Another study concluded that olanzapine and haloperidol alters protein expression associated with presynaptic function and nervous system development in rats (Ma *et al.*, 2009).

Haloperidol induced expression of proteins linked to oxidative stress and apoptosis while risperidone activated growth regulating metabolic pathways were the conclusion of a study in neural stem cells treated with these drugs (Ahmed *et al.*, 2012).

Another proteomic study proved that MK-801, a glutamergic antagonist, induced changes in the levels of three proteins in both cortex and thalamus and clozapine reversed all these protein changes whereas haloperidol reversed only two. Furthermore both antipsychotics induced new protein changes in both cortex and thalamus not seen after MK-801-treatment alone (Paulson *et al.*, 2007). Also haloperidol increased both c-fos and zif268 mRNA level in the caudate-putamen but clozapine only altered zif268 mRNA levels in the same region (Nguyen *et al.*, 1992).

Another study concluded that chronic treatment with escitalopram (a (S)-stereoisomer (enantiomer) of the drug citalopram) only affects the expression of a few of the proteins that were altered in rats that were separated from the progenitor at birth (which serve as depression model) and it targets another group of cytosolic proteins to achieve its therapeutic effect (Marais *et al.*, 2009).

These studies are essential to distinguish possible confounding factors as proteomic alterations due to chronic drug medication from disease alterations (Martins-de-Souza, Maccarrone, *et al.*, 2010). They can also help to reveal the mechanisms of action of these drugs, what could explain some adverse effects caused by them and giving clues about the pathogenesis of the disease (Critchlow *et al.*, 2006). Finding new targets and more effective and safe drugs could also be possible.

2. NEUROPROTEOMICS TECHNIQUES

Neuroproteomics is a subset of the proteomics field concerned with increasing basic biological mechanisms understanding and finding biomarkers of central nervous system diseases or drug response to improve understanding of the pathophysiology of brain disease (English *et al.*, 2011).

While other methods such as two-dimensional polyacrylamide gel electrophoresis (2DE) continue to be used, a variety of more in-depth mass spectrometry-based approaches including both label (ICAT, iTRAQ, TMT, SILAC, SILAM), label-free (MRM, SWATH®) and absolute quantification methods, are rapidly being applied to neurobiological investigations (Craft, Chen and Nairn, 2013).

2DE has some disadvantages such as its lack of ability to widen the protein dynamic range as well as the inability to analyze hydrophobic or very high or low molecular weight proteins (Martins-de-Souza, Maccarrone, *et al.*, 2010). One alternative to 2DE is the non-gel "bottom-up" liquid chromatography-coupled mass spectrometry-based shot-gun proteomics (Wang *et al.*, 2008). This methodology consists of the digestion of a given proteome, using a proteolytic enzyme (typically trypsin that cleaves at the C-terminal of arginine and lysine) (Kicman, Parkin and Iles, 2007), followed by multi-dimensional separation of the resultant peptides, generally using high-performance liquid chromatography (HPLC) coupled to tandem mass spectrometry (MS/MS) (Martins-de-Souza *et al.*, 2012). Protein digestion has the advantage of reducing proteins to peptides, more amenable to be identified in bottom-up LC-MS analysis (Meent, van de and Jong, de, 2011).

Although some successes using stable isotopic labeling technology for protein quantification have been reported, it remains technically difficult to comprehensively characterize the global proteome due to the high costs of the labeling reagents and the nature of the methodology (Wang *et al.*, 2008). Recently, label-free approaches have emerged as high-throughput methods for proteomics studies (Megger *et al.*, 2013). This provides a powerful tool to resolve and identify thousands of proteins from a complex biological sample (Wang *et al.*, 2008). Furthermore, this technique is apparently the easiest way of comparing proteomes, not only because labeling is not required but also because there are no limits regarding the number of samples that can be compared, which is an advantage for large clinical studies (Martins-de-Souza *et al.*, 2012).

Of the distinct label-free proteomics approaches that can be used, the one that has been used most in SCZ studies is data-independent analysis (Martins-de-Souza *et al.*, 2012). The data-independent mode of acquisition has been demonstrated to be the most-accurate label-free approach for estimating absolute/relative protein abundance (Craft *et al.*, 2013).

Independently of the proteomic screening method chosen, sample preparation is a decisive step of any proteomic analysis as this step determines the number and type of proteins in the final proteome. The loss of particular classes of proteins during sample preparation will lead to the underrepresentation of potential biomarkers that can be pivotal to the studied

proteome. Considering the high proteome complexity of some tissues, the use of methodologies leading to generation of subproteomes may be advisable in order to obtain the most complete proteome possible for a given sample (Martins-de-Souza *et al.*, 2012).

## 2.1. LIQUID CHROMATOGRAPHY COUPLED TO TANDEM MASS SPECTROMETRY (LC-MS/MS)

Liquid chromatography (LC) coupled with mass spectrometry is the predominant platform used to analyze proteomic samples because of its sensitivity, selectivity, accuracy, speed and throughput (Chen, G. and Pramanik, 2009; Meent, van de and Jong, de, 2011; Xie, Smith and Shen, 2012).

A single-dimension LC separation is one of the basic elements in LC–MS-based proteomics. High-performance liquid chromatography (HPLC) is the term used to describe LC in which the liquid mobile phase is mechanically pumped at high pressure through a column that contains the stationary phase (Weston and Brown, 1997).

Reversed phase (RP) is the most common LC format for separation of peptides (Xie *et al.*, 2012). The separation principle of RP is based on the polarity of the analytes under conditions where the stationary phase (silica derivatized C18 resins, are the most often used) is more hydrophobic than the mobile phase (usually a mixture of acetonitrile and water with an acidic ion-pairing reagent that should have an excellent compatibility with mass spectrometry (MS)) (Božović and Kulasingam, 2013; Palma, Di *et al.*, 2012). As a result, a decrease in the polarity of the mobile phase results in a decrease in solute retention (Weston and Brown, 1997).

Essentially, MS measures the mass-to-charge ratio (m/z) of gas-phase ions. Mass spectrometers consist of an ion source that converts analyte molecules into gas-phase ions, a mass analyzer that separates ionized analytes on the basis of m/z ratio, and a detector that records the number of ions at each m/z value (Figure 2.1) (Han, X., Aslanian and Yates, 2008).
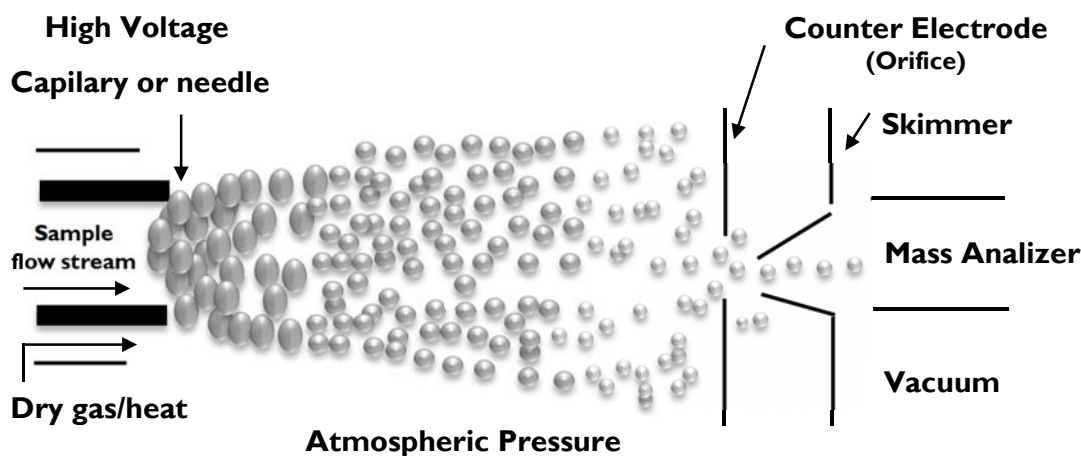
The development of electrospray ionization (ESI) and matrix-assisted laser desorption/ionization, the two soft ionization techniques capable of ionizing peptides or proteins, revolutionized protein analysis using MS (Chen, G. and Pramanik, 2009; Han, X. *et al.*, 2008).
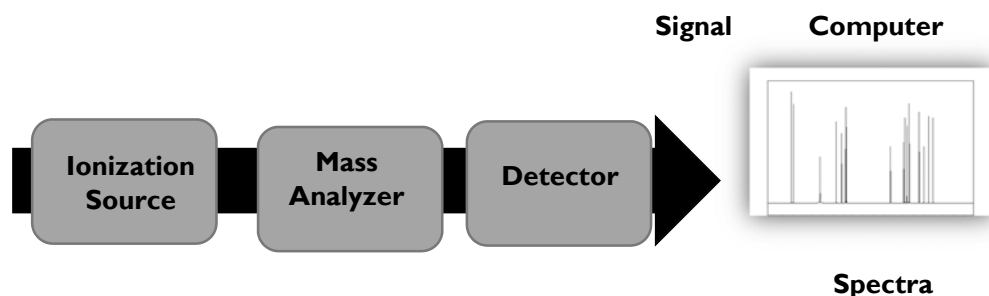
Figure 2.1 - The principle components of a mass spectrometer. Consisting of the ionization source followed by the mass analyzer, detector, and a data interrogation system. Adapted from (Kicman *et al.*, 2007).

ESI is often coupled with a chromatographic system, typically reverse phase chromatography, allowing the analysis of very complex samples (Wysocki *et al.*, 2005). ESI is set between a HPLC and the inlet of a mass spectrometer and uses an electric field to yield a spray of fine droplets (Lin, Tabb and Yates, 2003). In ESI, a dilute solution is sprayed from a fine needle, which carries a high potential, thus the droplets will have an excess of positive charges. At the tip of the needle the charged droplets spray assumes a conical shape referred to as the Taylor cone. The smaller droplets are repelled from the needle towards the sampling cone on the counter electrode at the orifice of the instrument (Kicman *et al.*, 2007). Evaporation of the volatile solvent results in increased Coulombic repulsion between the positive charges, which causes fragmentation of the droplet, generating smaller droplets (Figure 2.2) (Bakhtiar and Nelson, 2000). When operating at high solvent flow rates, a nebulization gas (or sheath gas) is needed to assist the solvent dispersion (Lin *et al.*, 2003).

As ions exit the ion source, they pass into a mass analyzer (Lin *et al.*, 2003). There are four major types of mass analyzers commonly used: quadrupole (Q), ion trap, time-of-flight (TOF), and Fourier-transform ion cyclotron resonance (Han, X. *et al.*, 2008).

High Voltage

Capilary or needle

Counter Electrode
(Orifice)

Skimmer

Sample
flow stream

Mass Analizer

Vacuum

**Dry gas/heat**

Atmospheric Pressure

Figure 2.2 - Electrospray ionization process. A fine mist of analyte is formed from the sample stream as droplets are formed from the Taylor cone. The charged droplets desolvate by Coulombic explosions and ions free from solvent can then enter the mass spectrometer via an intermediate vacuum region (Kicman *et al.*, 2007)

'Hybrid' instruments have been designed to combine the capabilities of different mass analyzers (Gygi and Aebersold, 2000; Han, X. *et al.*, 2008; Lin *et al.*, 2003). For example, quadrupole-TOFs are instruments that combine a quadrupole mass analyzer for ion selection in a tandem mass spectrometer mode and TOF analyzers to record m/z values with high resolution (Lin *et al.*, 2003). The combination of a quadrupole and a TOF analyzer provides high sensitivity and excellent mass accuracy (Kicman *et al.*, 2007).

The quadrupole analyzer is a device which uses the stability of the trajectories in oscillating electric fields to separate ions according to their m/z ratios (Hoffmann and Stroobant, 2007). It consists of four mutually parallel circular metal rods such that the electric field between them is hyperbolic (Figure 2.3) (Kicman *et al.*, 2007). A combination of radio frequency and direct current voltages are applied to each pair of rods to produce a complex, oscillating movement of the ions as they move from the beginning of the mass filter to the end (Kinter and Sherman, 2000).

The electrical field created in the mass analyzer could act as a filter in that it only allows ions of certain masses ('resonant ions') to pass down the gap between the four rods. Ions with different mass to charge ratios (non-resonant ions) will collide with the rods and become neutralized (Hoffmann and Stroobant, 2007; Kicman *et al.*, 2007).
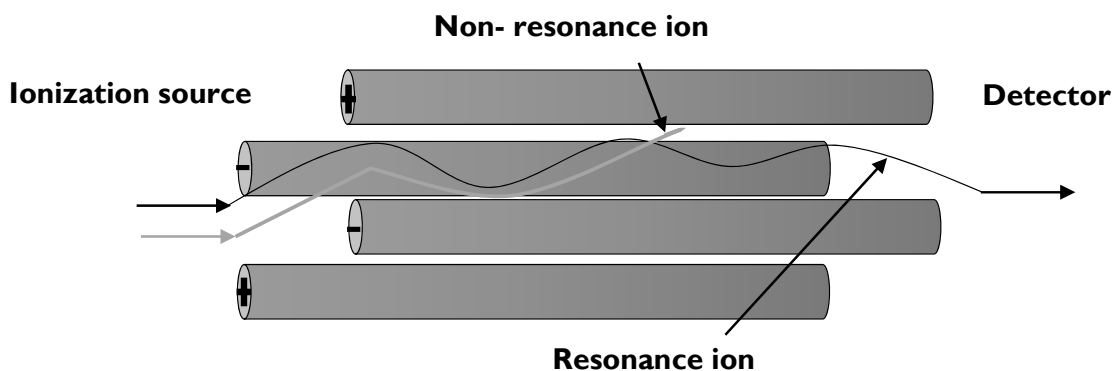
Figure 2.3 - Schematic diagram of a quadrupole mass filter. One pair of rods receives a superimposed positive direct current (DC) potential and a radio-frequency potential. The other adjacent pair of rods receives a negative DC potential and a radio-frequency potential of the same magnitude. Adapted from (Kicman *et al.*, 2007).

In time-of-flight mass analyzers (Figure 2.4) an ion is given a fixed amount of kinetic energy by acceleration in an electric field that is generated by the application of a high voltage, and the ion enters a field-free region where it travels at a velocity that is inversely proportional to its m/z. Because of this inverse relationship, ions with lower m/z travel more rapidly than ions with higher m/z. The time required for the ion to travel the length of the field-free region is measured and used to calculate the velocity and ultimately the m/z of the ion (Kinter and Sherman, 2000). The most significant limit on m/z resolution in a TOF is the range of initial velocities of the ions as they are accelerated. A method to correct for the deleterious effects of initial kinetic-energy spreads is to use an ion reflector, (also referred to as a "reflectron"). The reflectron is an ion mirror, created by an electric field that reverses the flight path of the ion (Takahashi and Isobe, 2007).
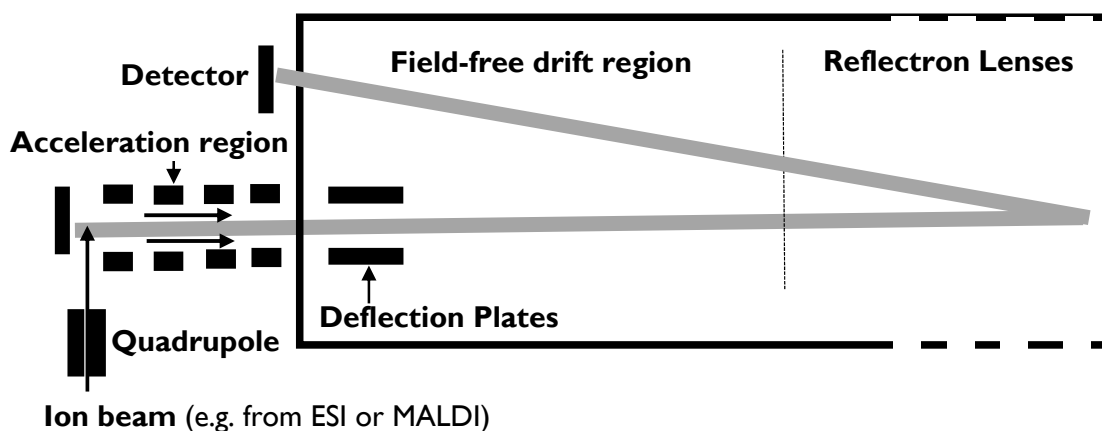
Figure 2.4 - Principle of a time-of-flight mass analyzer. A beam of ions from a continuous ionization source, such as ESI, are transmitted between the orthogonal ion extraction plate and grid. A segment of the beam is then pushed into the field-free region by a pulse in the orthogonal direction. Adapted from (Dass, [s.d.]).

The use of tandem mass spectrometry is the most popular approach to protein identification (Wysocki *et al.*, 2005). In the case of using a hybrid instrument Q-TOF the tandem mass spectrometry is designed "in space" once it has two mass analyzers (Hoffmann and Stroobant, 2007). In this case the quadrupole performs the mass selection of a desired target ion from a stream of ions produced in the ion source, then it is fragmented in a second quadrupole by collision induced dissociation (CID) (Chen, G. and Pramanik, 2009), and the TOF performs the analysis of the mass of the product ions (Kinter and Sherman, 2000). The term "tandem mass spectrometry" reflects the fact that two stages of mass analysis are used in a single experiment (Kinter and Sherman, 2000).

CID is based on the collision between a selected molecular ion with an inert gas (rare gas atoms or nitrogen molecules) (Han, X. *et al.*, 2008). In peptides this leads to backbone fragmentation of the C–N bond resulting in a series of b- and y-fragment ions (Chen, G. and Pramanik, 2009; Han, X. *et al.*, 2008). The mass difference between consecutive ions in the same series can be used to determine the identity of the consecutive amino acids except leucine and isoleucine, since they are isobaric (Chen, C.-H. W., 2008).

The information produced by the mass spectrometer, lists of mass-to-charge (m/z) values and their intensities, can be processed and compared with lists generated from "theoretical" fragmentation of a peptide (Wysocki *et al.*, 2005; Yates, 2000).

Shotgun proteomics, also known as discovery proteomics, is a universally and successfully used proteomic method for identifying proteins in complex mixtures. In this

method, the enzymatically digested protein sample is analyzed by LC–MS/MS operated in data-dependent acquisition or information dependent acquisition (IDA) mode (Liu, Hüttenhain, Collins, *et al.*, 2013). In this mode, peptide fragmentation in the mass spectrometers is guided by the abundance of peptide ions or so-called precursor ions detected in a survey scan (Liu, Hüttenhain, Collins, *et al.*, 2013). Experimentally, the IDA function will acquire a TOF-MS survey scan and search for the most intense ions in the spectrum. Ions which intensities exceed the threshold level are selected by the first mass analyzer and subjected to collision-induced dissociation. A high-resolution mass spectrum of the fragment ions is collected with the TOF analyzer (Figure 2.5) (Aguilar, 2004). The fragment ion spectra along with the mass of the precursor ion are then searched against isolation protein database to infer the peptide sequence and protein identity (Liu, Hüttenhain, Collins, *et al.*, 2013).

The confidence in protein identification is increased with the number of distinct amino acid sequences identified. Therefore, proteins are normally categorized into different priority group depending on whether they have only one or multiple unique sequences of the required peptide identification confidence (Wang *et al.*, 2008).
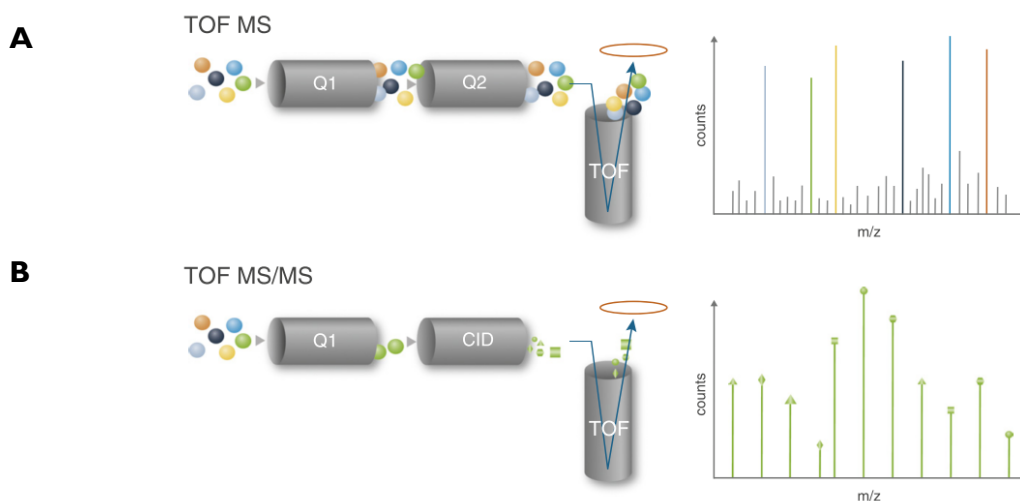
Figure 2.5 - Schematic description of a typical "shotgun" experiment in a Q-TOF instrument. The instrument cycles between 2 different scan modes. (A) In the first mode all ions are transmitted through the instrument and detected after the TOF analyzer, the detector can be subsequently used for parent ion determinations. The derived MS spectrum is analyzed using simple rules (intensity, charge state and whether the ion has been fragmented before). Ions which pass these simple rules are then isolated and fragmented. (B) In MS/MS mode, specific masses are isolated in the first quadrupole and fragmented in the second quadrupole. All of the fragment ions are recorded in the analyzer and a MS/MS spectrum is generated, which can be used for peptide identification (Tate *et al.*, 2013).

Some strategies have been developed that rely on neither detection nor knowledge of the precursor ions to trigger acquisition of fragment ion spectra (Gillet *et al.*, 2012). These include data independent acquisition (DIA) which does not select ions to be fragmented based on information in the precursor ion scan. The aim of this approach is to fragment the entire set of precursor ions in the visible range of the mass spectrometer (Tate *et al.*, 2013).

DIA provides a unique feature, namely a complete digital MS/MS record of all compounds that are detectable within the sample. This record allows a hypothesis to change during a biological study, and hence data from libraries can be used to probe samples for proteins which were not originally targeted or identified within a sample (Tate *et al.*, 2013).

Improvements in MS instrument design allowed the introduction of more robust quantitative MS-based techniques for handling the relatively low amount of protein available for neuroproteomic studies (Craft *et al.*, 2013).

In this project a label free quantitative mass spectrometry approach will be used, specifically, a SWATH-MS analysis (Figure 2.6), a data-independent acquisition technique.
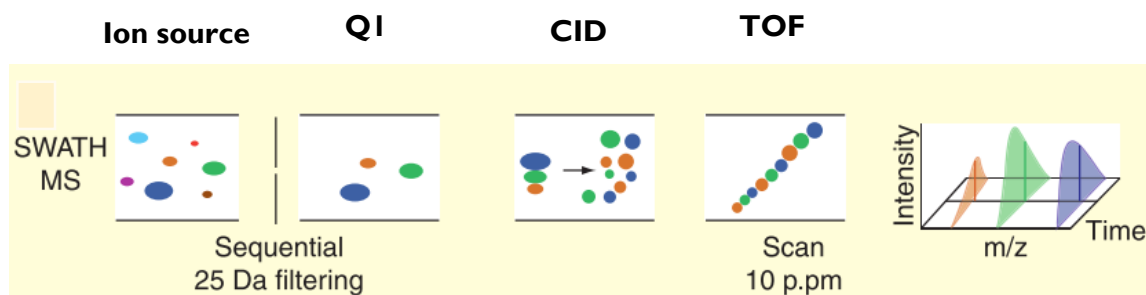
Figure 2.6 - Schematic representation of SWATH DIA. Here, the first mass selection quadrupole isolates and transmits ions in a defined window (25 Da, swaths) which will contain a number of different parent ions. This mixture of ions is fragmented in a collision cell by collision induced fragmentation and transmitted to the TOF analyzer where all product ions are measured at resolution 10 p.p.m. The high resolution of MS spectra ensures the specificity of peptide identification (adapted from (Ong, Foster and Mann, 2003)).

In a label-free experiment, quantification is achieved through comparison of peak areas obtained for an analyte under two or more biological conditions (Vowinckel *et al.*, 2013).

SWATH (sequential window acquisition of all theoretical fragmentation spectra) allows both relative and absolute protein levels to be measured in a biological sample (Craft *et al.*, 2013). It is a method in which data are acquired on a fast, high resolution Q-TOF instrument (Liu, Hüttenhain, Surinova, *et al.*, 2013). SWATH acquisition consists of the sequential selection of sequential precursor ion mass windows (normally repeatedly cycle through 32 consecutive

25 Da precursor isolation windows (swaths)) (Zhang, Fanglin *et al.*, 2014), fragmentation of all precursor ions selected in each window within the 400 to 1200 m/z precursor range and recording of the resulting composite fragment ion spectra (Gillet *et al.*, 2012; Liu, Hüttenhain, Collins, *et al.*, 2013; Tate *et al.*, 2013; Vowinckel *et al.*, 2013).

Using such scans, the link between the fragment ions and the precursors from which they originate is lost, increasing the complexity of the analysis of the acquired data sets. Consequently, the composite spectra generated by DIA methods have been mainly analyzed with the standard database searching tools developed for IDA, either by searching the composite fragment ion spectra directly or by searching pseudo fragment ion spectra reconstituted post acquisition based on the co-elution profiles of precursor ions (from the survey scans) and of their potentially corresponding fragment ions (Gillet *et al.*, 2012).

This acquisition mode essentially converts the peptides in a physical sample into a high-resolution digital map consisting of fragment ions spectra derived from the fragmentation of all precursor ions present in the sample in a predetermined mass to charge window and at a certain time (Liu, Hüttenhain, Collins, *et al.*, 2013). Quantification is conducted based on the peak areas of extracted ion chromatograms (XIC), which are computationally reconstituted from the merged spectra on the basis of both experimental and *in silico* generated spectral information (Vowinckel *et al.*, 2013).

OBJECTIVES

3. OBJECTIVES

Psychotic medication is the main treatment for schizophrenia patients, however their long-term mechanisms of action are not completely understood. Thus, the proteomic alterations observed in SCZ patients subjected to chronic medication act as a confounding factor with alterations from the disease alone. This distinction between pharmacological and disease related changes is crucial to reveal the etiology and pathophysiological mechanisms of the disease.

Therefore, the aim of the present study was the identification of proteomic changes in prefrontal cortex tissue from mice chronically treated with three commonly prescribed psychotropic drugs namely, haloperidol, clozapine and citalopram.

The identification of the proteomic alterations of these drugs will help to provide a better understanding of drug action, leading to a better comprehension of their efficacy and adverse effects, as well as, to gain new insights into the protein signaling pathways that they influence, in order to better combine and potentiate the outcomes of the therapies or even to discover new therapeutic targets.

To accomplish this goal, the following tasks were proposed:

1) Optimization and evaluation of the subproteome fractionation procedure;
2) Subproteome fractionation of the prefrontal cortex tissue from mice treated with the psychotropic drugs mentioned above;
3) Proteomic identification of medication-associated changes using a label free quantitative mass spectrometry approach (SWATH analysis).

EXPERIMENTAL PROCEDURES

4. EXPERIMENTAL PROCEDURES

4.1. ANIMALS AND DRUGS ADMINSTRATION

Animals' samples were kindly prepared in Dra. Graça Baltazar's lab with the help of Sandra Rocha (University of Beira Interior, Covilhã).

Young black male C57BL/6J mice were purchased from Charles River, Laboratories International, Inc. (Spain). They were divided into four groups, 6 animals per group. Each animal weighed around 20-25 g with access to food and water *ad libitum*.

After a habituation phase in which animals got used to the injection needle they were chronically treated for four weeks. The animals were injected, via intraperitoneal with clozapine, citalopram and haloperidol at a dose of 20 mg/Kg, 10 mg/Kg and 1 mg/Kg, respectively. All drugs were dissolved by diluting of stock on 0.13% HCl 5M with 0.9% NaCl. An additional group was treated with vehicle only (saline solution) and represent the control. The age of animals at start of the habituation phase was 10 weeks and mice were injected daily for 30 days.

After the drug treatment, animals were weighed and anesthetized with a mixture of ketamine (100 mg/Kg) and xylazine (10 mg/Kg) 24 hours after the final injection.

Animals were sacrificed and their brains were removed and dissected. Tissue was dissected bilaterally and prefrontal cortex was collected. TEAB 0.5 M (triethylammonium bicarbonate buffer) with phosphatases and proteases inhibitors (Roche) was added to each tube. All samples were stored at -80°C until use.

4.2. SUBPROTEOME FRACTIONATION (Membrane Protein Enrichment)

To each microcentrifuge tube containing the prefrontal cortex, 1 mL of Tris 0.05 M (tris(hydroxymethyl)aminomethane) with phosphatases and proteases inhibitors was added. The brain tissues were homogenized with ultrasonication (Vibra Cell 130 watts, Sonics) with the 3 mm probe for 30 seconds at 40% amplitude with 1 second cycles and for 15 seconds at 50% with 1 second cycles. Afterwards the samples were centrifuged (Centrifuge 5417R, Eppendorf) at 5,000×*g* for 5 minutes at 4°C. The supernatants were saved in a new microcentrifuge tube and 500 µL of Tris 0.05 M with phosphatases and proteases inhibitors were added to the pellets. Pellets were homogenized with the 3 mm probe for 30 seconds at

40% with 1 second cycles, and centrifuged as mentioned before. The supernatants were saved with the rest of the samples and the volume was adjusted to 2 mL with Tris-buffer. The new pellets (tissue debris) were discarded.

Then the volume corresponding to 30 mg of brain tissue were transferred to ultracentrifuge tubes and the volume was adjust at 2 mL with Tris-buffer. The rest of the sample was kept at -80°C.

An ultracentrifugation (Optimal^{TM} L-100 XP, Beckman Coulter) at 144,000×*g* for 1hour at 4°C was performed and the supernatant (soluble fraction) was taken to a centrifuge tube. To the pellet samples (membrane enriched fraction) 750 μL of TEAB 0.5 M were added and the pellet was dissolved using the sonicator with the 3 mm probe for 15 seconds at 40%, once, after this the pellet was unstacked from the ultracentrifuge tube and homogenized again, 30 seconds at 40% amplitude with 1 second cycles and 30 seconds at 50% amplitude with 1 second cycles, this step was repeated until total dissolution.

4.3. PROTEIN PRECIPITATION

Cold acetone (-20 °C) in a volume ratio of 1:6 (sample:acetone) was added to each soluble samples and methanol 1:4 (sample:methanol) was added to each membrane samples. The sample tubes were inverted several times to mix and incubated at -80°C overnight. All samples were centrifuged (Centrifuge 5810 R, Eppendorf) at 3,220×*g* at 4°C during 20 minutes and 150 μL of TEAB 0.5 M were added to the samples pellet, further dissolved using the 3 mm probe for 10 seconds at 20% amplitude with 1 second cycles twice. The homogenized samples were transferred to a microcentrifuge tube and the volume was adjusted at 200 μL. All samples were stored at -80°C until posterior use.

4.4. PROTEIN QUANTIFICATION (2-D Quant Kit)

The 2-D Quant Kit (GE Healthcare) was used to determine the protein concentration in samples. Bovine serum albumin (BSA) was used as standard and the assay was performed following the manufacturer protocol. Shortly, the standards and the samples were first precipitated and then resuspended in a copper solution. The copper binds to the protein and the unbound copper is measured with a colorimetric agent. Samples were incubated at room temperature for 15 minutes. The samples' absorbance was measured at 480 nm on a

Microplate Spectrophotometer (PowerWave XS, BioTek). Using the results, a calibration curve was obtained and the protein concentration was interpolated from it.

4.5. EVALUATION OF THE SUBPROTEOME FRACTIONATION

4.5.1. SDS-PAGE (Sodium Dodecyl Sulfate PolyAcrylamide Gel Electrophoresis)

Three soluble pools and three membrane pools were made using eight samples by pool (5 µg of protein of each sample). The eight samples were obtained from each subproteome fractionation procedure that was performed 3 times. For this procedure 30 µg of protein of each pool were denatured with the addition of Laemmli Sample Buffer 6× [0.35 M Tris-HCl, pH 6.8 with 0.4% SDS (v/v), 30% glycerol (v/v), 12% SDS (w/v), 9.3% DTT (w/v), 0.01% bromophenol blue (w/v) and 4 M NaCl] to a 1× final concentration and boiled at 60°C for 10 minutes.

Green Fluorescence Protein (GFP) was denatured with the addition of Laemmli Sample Buffer 6× [0.35M Tris-HCl, pH 6.8 with 0.4% SDS (v/v), 30% glycerol (v/v), 10% SDS (w/v), 9.3% DTT (w/v) and 0.01% bromophenol blue (w/v)] to a 1× final concentration and boiled at 95°C for 5 minutes. To each sample 0.84 ng of GFP were added and used to normalize the western blot procedure.

The samples were electrophoretically separated in a pre-cast stain-free 4-20% SDS-polyacrylamide gel (Bio-Rad) using a Mini-PROTEAN Tetra Electrophoresis System (Bio-Rad). The profile of the gel was then visualized by ultraviolet light (GelDoc XR, BioRad).

The rest of each pool (10 µg) were added to made a new soluble pool and membrane pool, thus 30 µg of protein of each pool were denatured in the same conditions described above for GFP and were electrophoretically separated on a 12.5% SDS-polyacrylamide gel (Bio-Rad) using a Mini-PROTEAN Tetra Electrophoresis System.

4.5.2. Immunoblot Detection

Proteins were transferred to Trans-Blot® Turbo™ Midi-size polyvinylidene fluoride (PVDF) membranes (Bio-Rad) using a Trans-Blot® Transfer System (Bio-Rad). The following programs were used to transfer the pre-cast stain-free 4-20% and 12.5% SDS-polyacrylamide gels: 2.5 A constant; up to 25 V during 10 min and up to 1.0 A; 25 v constant during 30 min, respectively. After the transference, the membranes were blocked for 1 hour at room

temperature (RT) with 5% (w/v) skimmed milk powder dissolved in PBS with 0.1% (v/v) Tween-20 (PBS-T) (Bio-Rad).

Membranes were then incubated with primary antibodies against NMDA C-20 (1:500) (115 kDa), DJ1 C-16 (1:200) (25 kDa) [Santa Cruz Biotechnology, Inc. (sc-1467)] and GFP (1:500) (27 kDa) (SicGen AB0020-500) in 5% (w/v) skimmed milk powder dissolved in PBS-T, overnight at 4°C followed by 1 hour at RT. Primary antibodies are removed and membranes were washed with PBS-T (3 times for 15 min under agitation). Subsequently, the membranes were incubated 1 hour at RT with the secondary antibody conjugated with alkaline phosphatase (anti-goat (1:6000), from Jackson ImmunoResearch Laboratories), in 5% (w/v) skimmed milk powder dissolved in PBS-T, followed by three washes as above. Each membrane was incubated for a maximum period 5 minutes, to observe protein-immunoreactive bands, with "Enhanced Chemifluorescence (ECF) detection system" (GE Healthcare) and visualized in a Molecular Imager FX System (Bio-Rad) (filter A – 530 nm; laser- 488 nm). The Quantity One® software (Bio-Rad version 4.6) was used to adjust the volumes (total intensities in a given area with global and local background subtraction for each band and with global background subtraction for each lane).

Thereafter, the membranes incubated with NMDA antibodies were incubated for 15 min with a stripping solution [0.2 M Glycine, 0.1% SDS and 1% Tween-20] to remove the labeling of the antibodies and the procedure was repeated with new antibodies Anti-VDAC-1 N-18 (1:500) (33 kDa) [Santa Cruz Biotechnology, Inc. (sc-8828)].

4.6. SAMPLE PREPARATION FOR LC-MS

For each sample group (control, haloperidol, citalopram and clozapine), 20 µg of protein were pooled together for the library identification (total of mg of proteins from the 6 animals). These pools (120 µg of protein with 2.1 µg of GFP) and 80 µg of each sample (with 2.1 µg of GFP), for the SWATH analysis, were denatured with Laemmli Sample Buffer 6× to a 1× final concentration and boiled at 95°C during 5 minutes. In order to promote the cysteine alkylation, acrylamide [40% acrylamide/bis solution (Bio-Rad)] was added to the samples (2 µL of acrylamide per 30 µL of sample). The samples were loaded in a pre-cast 4-20% SDS-polyacrylamide gel and electrophoretically resolved during 15 minutes at 110 v using a Mini-PROTEAN Tetra Electrophoresis System. The pools were separated in 3 different wells in the gel while individual samples were separated into two wells.

The gel was then stained with Coolloidal Coomassie Blue. Briefly, after electrophoresis, the gel was washed with deionized water and immersed in staining solution [10% (v/v) of 85% solution of phosphoric acid, 10% (w/v) ammonium sulphate, 20% (v/v) methanol]. The Coomassie powder was added to the solution with a strainer to allow the formation of colloidal particles under agitation and allowed to stain. After that, successive washes were made and the gel was maintained in water.

The top of each gel lanes was sliced into 9 bands of equal size using a disposable GridCutter (2 mm × 7 mm lanes, 25 rows, 1 column). Then the bands were grouped three by three, sliced into smaller pieces, and transferred to microcentrifuge tubes with 600 μL of ultra-pure water (VWR) to prevent band pieces to dry. To destain the gel pieces the water was removed and 1 mL of the destaining solution (50 mM ammonium bicarbonate and 30% acetonitrile) was added. The tubes were placed in a thermomixer (Comfort, Eppendorf) at 850 rpm for 15 minutes at 25°C. The solution was removed and 1mL of water was added and tubes were shaken in the thermomixer at 850 rpm for 10 minutes at 25°C. If the gels pieces remained blue this destaining step was repeated. Afterwards, the water was removed and the gel pieces were dehydrated on the Concentrador Plus (Eppendorf) for 1 hour at 60°C. When the gel pieces were dehydrated, sufficient volume of trypsin (Roche) (15 ng/μL in 10 mM ammonium bicarbonate) was added until all dried gel pieces were covered and incubated during 15 minutes, on ice, to rehydrate the gel. After this period, 10 mM ammonium bicarbonate (final concentration of trypsin 10 ng/μL) was added to cover gel pieces again, and incubated overnight (16 hours) at room temperature in the dark to perform the in-gel digestion. After digestion, the tryptic solution (containing trypsin and some peptides) was collected to Lobinding® microcentrifuge tubes (Eppendorf). The pool samples were collected to three different tubes to separate the top, middle and bottom of the gel and the other samples were collected each for individual tubes. The remaining peptides were extracted by adding solutions with an increase concentration of acetonitrile (ACN), thus 100 μL of 30%, 50%, and 98% of ACN in 1% formic acid (FA) were added. After the addition of each extract solution the tubes were placed in the thermomixer at 1050 rpm for 15 minutes at 25°C and each solution was collected to the tube containing the initial tryptic solution. The peptide mixtures were concentrated on the Concentrador Plus (Eppendorf) at 60°C, resuspended to a final volume of 100 μL in a solution of 2% ACN and 1% FA, and sonicated on a Sonics 750 W using a cup-horn (2 min with 1 sec on 1 sec off cycles at 20% of amplitude). At this point the peptide extraction was complete and the peptides were prepared to be desalted.

4.7. C18 PEPTIDE CLEAN UP

Peptides were cleaned/desalted using C18 Bond Elut OMIX solid phase extraction pipette tips (Agilent technology). Briefly, 200 µL of 50% ACN were used to hydrate the tip columns, to equilibrate them 300 µL of 2% ACN with 1% FA solution were added. The peptides were loaded into the column and this step was repeated five times followed a wash step with 100 µL of 2% ACN with 1% FA solution (this wash is saved until the analysis of the peptides is performed). Peptides were eluted to new tubes with 400 µL of 70% ACN and 0.1% FA and eluates were concentrated using the Concentrator Plus at 60 °C. Individual sample volume was adjusted to 30 µL and pool samples to 20 µL in a solution of 2% ACN and 0.1% FA with Indexed Retention Time (iRTs) (BIOGNOSYS) and sonicated at 20% of amplitude for 2 minutes (1 second on 1 second off cycle), centrifuged at 14,000×g for 5 minutes and the supernatants were transferred into vials for posterior LC-MS/MS analysis.

4.8. PROTEIN IDENTIFICATION AND QUANTIFICATION

Digested proteins were analyzed on a hybrid quadrupole time-of-flight mass spectrometer (Triple TOF™ 5600 System; ABSciex). Firstly, peptides were separated by liquid chromatography (NanoLC Ultra 2D, Eksigent) on a ChromXP™ C18 reverse phase column (300 µm ID × 15 cm length, 3 µm particles, 120 Å pore size, Eksigent) at 5 µL/min. Peptides were eluted into the mass spectrometer in a linear gradient for 45 min with an acetonitrile gradient in 0.1% FA (from 2% to 30%), using an electrospray ionization source (DuoSpray™ Source, ABSciex) in positive mode. Using the same chromatographic conditions, the pool samples were analyzed by information dependent acquisition to create the library identification and the rest of the soluble samples by information independent acquisition. Rolling collision was used with a collision energy spread of 5. The volume of each poll sample (5 µL) was analyzed using classical shotgun data acquisition. The mass spectrometer was set for information dependent acquisition scanning full spectra (350-1250 m/z) for 250 ms, only for the 30 most intense ions. Candidate ions with a charge state between +2 and +5 and counts above a minimum threshold of 70 counts per second were isolated for fragmentation and performed one MS/MS (100-1500 m/z for 100 ms) before adding those ions to the exclusion list for 15 seconds (mass spectrometer operated by Analyst® TF 1.6, ABSciex). In quantitative analysis by acquisition in SWATH mode, 5 µL of the volume of each soluble sample were used. In the SWATH analysis the same chromatographic conditions as in the IDA run described

above were used. For SWATH-MS–based experiments, the mass spectrometer was operated in a looped product ion mode. The instrument was specifically tuned to allow a quadrupole resolution of 25-m/z mass selection. Using an isolation width of 26 m/z (containing one m/z for the window overlap), a set of 29 overlapping windows was constructed covering the precursor mass range of 350–1100 m/z. A 50 ms survey scan was acquired at the beginning of each cycle for instrument calibration and SWATH MS/MS spectra were collected from 100–1500 m/z for 100 ms resulting in a cycle time of 3.15 s from the precursors ranging from 350 to 1100 m/z. The collision energy for each window was determined according to the calculation for a charge 2+ ion centered upon the window with a collision energy spread of 15.

4.9. IDA AND SWATH DATA FILE ANALYSIS

To the IDA analysis the pools' files were combining by condition (control, haloperidol, citalopram and clozapine) and peptide identification was performed using Protein Pilot software v5 (ABSciex). The parameters for search were the following: Uniprot_SwissProt database for mouse (last update in July 2014); trypsin digestion, acrylamide as cysteine alkylating reagent, thorough ID search effort, and 0.05 unused ProtScore (10% confidence score) as detected protein threshold. Data analysis was based on an independent False Discovery Rate analysis (FDR) using the target-decoy approach. Positive identifications were considered when proteins present 95% confidence (5% local FDR) with more than one peptide hit with individual confidence above 95%. When a protein was identified with a single peptide, an Unused above 1.3 was considered as positive identification or the peptide has to present an individual confidence above 95% and a minimum sequence tag of 3 amino acids (4 consecutive peaks in the MS/MS spectrum). The reverse proteins and peptides, as well as, the peptides with zero contribution were removed.

Combining all files from the IDA experiments led to the creation of a library of precursor masses and fragment ions, that was used for subsequent SWATH processing. Search parameters used were the same for the pools' IDA with the addition of GFP protein and iRTs peptides to the database.

The protein quantification was performed using Peak View Software v2.1 (ABSciex). The IDA library was imported to the software along with the swath files. Peptides were selected automatically from the library using the following criteria: (i) the unique peptides for a specific targeted protein were ranked by the intensity of the precursor ion from the IDA analysis as estimated by the ProteinPilot software, and (ii) Peptides that were shared between different

protein entries/isoforms were excluded from selection. Up to 15 peptides were chosen per protein, and SWATH quantitation was attempted for all proteins in library files that were identified below 5% local FDR from ProteinPilot searches.

According to the criteria described in (Lambert *et al*, 2013) target fragment ions, up to 5, were automatically selected and peak groups were scored. For the latter the criteria are the following: each target fragment ion was scored based on the retention time adjustment, peak width overlap, peak intensity ratio, correct isotopic state, m/z error and MS/MS score. The individual peak group scores were combination of all subscores (scores from fragment ions) and the peak group with the best score was taken forward. Peak group confidence threshold was determined based on a FDR analysis using the target-decoy approach and 1% extraction FDR threshold was used for all the analyses.

The peak areas of the target fragment ions of peptides were extracted across the experiments using an extracted-ion chromatogram (XIC) window of 5 minutes with a 0.02 Da width.

Peptide features (i.e., peptides in a given charge state) that met the 1% FDR threshold at least in 3 replicates for a given condition were retained, as well as, peptides that have contribution for all the experiments. In order to estimate the protein levels, all the transitions from all the peptides for a given protein were summed. Protein levels were normalized using GFP protein as internal standard.

4.10.   SOFTWARE TOOLS FOR PROTEINS ANALYSIS

Venn diagrams were used to compare the number of proteins that are shared or unique among the four groups.

The Venn diagram tool (http://bioinformatics.psb.ugent.be/webtools/Venn/) from Bioinformatics & Evolutionary Genomics was used. The lists containing the proteins from the desired conditions to be compared were uploaded and the selected output was symmetric Venn diagrams. The tool generates a Venn diagram of the inserted conditions and a text file containing the accession numbers of the analyzed proteins and the distribution of these proteins within the different conditions compared.

GO enrichment analysis was performed for each list of proteins identified in each condition, using the web-based application Gene Ontology enRIchment anaLysis and visuaLizAtion tool – GOrilla (http://cbl-gorilla.cs.technion.ac.il/). GOrilla helps to identify and visualize enriched GO terms in genes or proteins lists. The output of this analysis is visualized

as a hierarchical structure, using a representation with color-coding that reflects the enrichment degree based on the p-value. All the analyses were done for the *Mus musculus*, in the single ranked list of genes running mode and based on cellular component, molecular function and biological process. Diagrams were exported and presented as results.

PANTHER Classification System (http://www.pantherdb.org/tools/) was performed for each list of proteins that were considered altered. This tool creates map lists of molecular function and biological process categories, as well as cell component. All the analyses were done for the *Mus musculus*, and the results were viewed in pie chart based in their functional classification - biological process.

UniProt (http://www.uniprot.org/) is the universal protein resource, a central repository of protein data created by combining the Swiss-Prot, TrEMBL and PIR-PSD databases. This software was used to identify and to provide information about the proteins that were found changed comparing with the control condition, using the accession number of them.

4.11. STATISTICAL ANALYSIS

Statistical analysis of results from western blot procedure was performed using GraphPad PRISM® v5, data normality was tested using Mann-Whitney Test and statistical evaluation was performed with a one-way ANOVA analysis. The results were reported as statistically significant when $p < 0.05$. Data were expressed as mean ± standard error of the mean (S.E.M.).

SPSS (Statistical Package for the Social Sciences) version 18 (IBM®) was used to identify the proteins that were altered by the drugs. An outlier analysis was performed and the control data were compared with each drug group (haloperidol, clozapine and citalopram). The results were reported as statistically significant when $p < 0.05$ and/or proteins which are outside a 1.5 fold factor were considered as being changed between the control and the drug group.

RESULTS AND DISCUSSION

5. RESULTS AND DISCUSSION

Schizophrenia is likely to be a multifactorial disorder, consequence of alterations in gene and protein expression, since the neuro-development together with environmental factors will trigger the establishment of the disease (Martins-de-Souza, 2011). In the post-genomic era, proteomics has emerged as a promising strategy for revealing disease and treatment biomarkers as well as a tool for understanding the mechanisms of schizophrenia pathobiology (Martins-de-Souza, 2011).

The analysis of the pharmacological profile of antipsychotic drugs or neurochemical consequences of antipsychotic treatment has been widely used to understand the pathophysiology of schizophrenia (Park, J. *et al.*, 2012b). Considering that SCZ is a brain disorder, the study of brain tissue seems a natural path to follow for the understanding of its pathobiology. The prefrontal cortex is one of the brain regions that have been strongly correlated with SCZ (Martins-de-Souza, 2011), and for this reason it was the tissue studied in this project.

In this project four animals groups were studied: control, haloperidol, citalopram and clozapine. The control group represents the mice that were not injected with the drugs and the haloperidol, citalopram and clozapine groups, the mice that were injected with the respective drugs (see Experimental procedure 4.1). In each group there are six mice that were the biological replicates, the samples CT1, CT2, CT3, CT4, CT5, CT6 are mice from the control group; the samples HA1, HA2, HA3, HA4, HA5, HA6 are from the haloperidol group; the samples CI1, CI2, CI3, CI4, CI5 and CI6 are from the citalopram group; and the samples CL1, CL2, CL3, CL4, CL5 and CL6 are from the clozapine group.

A major difficulty with proteomic approaches is the extraordinarily high protein complexity of biological samples. Likely more than 100,000 different protein isoforms exist in a cell. This complexity requires the prefractionation of samples prior to protein analysis in order to make low-to-medium abundant proteins detectable (Schindler *et al.*, 2006). In order to simplify the prefrontal cortex samples, a membrane protein enrichment was performed (see Experimental Procedure 4.2). In this procedure, an ultracentrifugation step was sufficient to separate membrane from soluble proteins (see Supplementary Subchapter 8.1). Only the soluble fractions were analyzed by mass spectrometry in this project.

After the subproteome fractionation procedure the proteins in the soluble fraction were precipitated with acetone and the proteins in membrane samples were precipitated with

methanol (see Experimental Procedure 4.3), once these two solvents proved to be most appropriate for the precipitation of the different fractions (see Supplementary Subchapter 8.2).

5.1. PROTEIN QUANTIFICATION

The quantification of the protein in each sample was performed using the 2D-Quant Kit (see Experimental Procedure 4.4). The quantification of protein was essential to determine the volumes that were used in subsequent analysis, so that the amount of protein in each well was the same. The table 5.1 showed the protein concentration (mg/mL) and the total amount of protein (mg) of each sample.

Table 5.1: Protein concentration of samples obtained by 2-D Quant Kit. Protein concentration and the total amount of each sample was calculated. [] - concentration of proteins. CT1/CT2/CT3/CT4/CT5/CT6- soluble and membrane protein fraction from Control group obtained after the subproteome fractionation; HA1/HA2/HA3/HA4/HA5/HA6- soluble and membrane protein fraction from Haloperidol group obtained after the subproteome fractionation; CI1/CI2/CI3/CI4/CI5/CI6- soluble and membrane protein fraction from Citalopram group obtained after the subproteome fractionation; CL1/CL2/CL3/CL4/CL5/CL6- soluble and membrane protein fraction from Clozapine group obtained after the subproteome fraction.

Soluble Samples	[] (mg/mL)	Total amount (mg)	Soluble Sample	[] (mg/mL)	Total amount (mg)	Membrane Samples	[] (mg/mL)	Total amount (mg)	Membrane Samples	[] (mg/mL)	Total amount (mg)
CT1	2.91	0.58	CI1	2.6	0.52	CT1	5.09	1.02	CI1	4.28	0.86
CT2	2.24	0.45	CI2	3.42	0.69	CT2	3.99	0.8	CI2	4.3	0.86
CT3	3.22	0.64	CI3	4.29	0.86	CT3	4.63	0.93	CI3	5.51	1.1
CT4	3.07	0.61	CI4	4.02	0.8	CT4	3.95	0.79	CI4	5.02	1
CT5	1.97	0.39	CI5	1.98	0.4	CT5	3.88	0.78	CI5	3.64	0.73
CT6	1.97	0.39	CI6	2.03	0.41	CT6	3.79	0.76	CI6	3.59	0.72
HA1	2.77	0.55	CL1	2.19	0.44	HA1	4.81	0.96	CL1	3.84	0.77
HA2	3.21	0.64	CL2	2.77	0.55	HA2	4.88	0.98	CL2	4.56	0.91
HA3	3.15	0.63	CL3	3.29	0.66	HA3	5.26	1.05	CL3	5.14	1.03
HA4	3.71	0.74	CL4	3.64	0.73	HA4	4.9	0.98	CL4	5.07	1.01
HA5	2.91	0.58	CL5	2.13	0.43	HA5	5.31	1.06	CL5	3.73	0.75
HA6	2.6	0.52	CL6	2.47	0.49	HA6	4.97	0.99	CL6	3.85	0.77

The total amount of protein in the soluble and membrane samples range between 0.39-0.86 mg and 0.72-1.13 mg, respectively. According (Schindler *et al.*, 2006) the class of membrane protein are less abundant in a cell, they are assumed to constitute about 20–30% of cellular proteins. Nevertheless, the amount of protein in membrane samples were higher than the soluble samples, this is due to the fact that during the membrane enrichment procedure there is the accumulation of membrane proteins but also cytoskeletal proteins in

the membrane fraction, making the amount of protein content greater in the membrane fraction than in the soluble fraction.

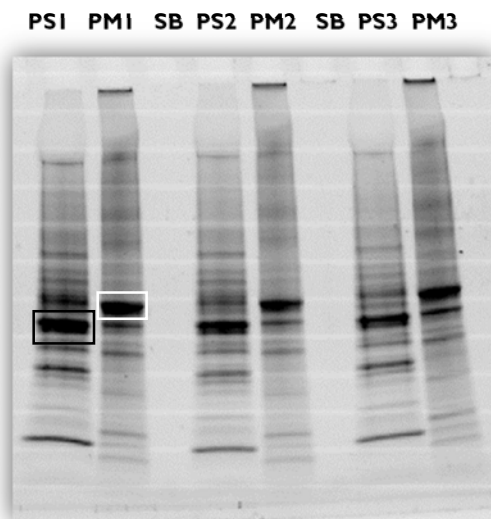## 5.2. EVALUATION OF THE SUBPROTEOME FRACTIONATION PROCEDURE

In order to evaluate the subproteome fractionation procedure, the samples were pooled and resolved in a pre-cast stain-free 4-20% SDS-polyacrylamide gel, and the profile of the gel was visualized by ultraviolet light (figure 5.1). The soluble pools (PS1, PS2 and PS3) and membrane pools (PM1, PM2 and PM3) were prepared adding the soluble and membrane samples that were processed in the same ultracentrifugation step, respectively (see Experimental Procedure 4.5.1).

As it can be observed in figure 5.1, the pooled samples of the soluble fractions present a similar profile among themselves. The pooled samples of the membrane fractions also present a similar profile among themselves but different comparing with the soluble samples. For instance, the first intense band in the soluble samples (black box) corresponds to a less intense band in the membrane samples, as well as, the first intense band in the membrane samples (white box) corresponds to a less intense band in the soluble samples. In the upper part of the gel a band with high intensity can be noted in the membrane samples, which represents proteins with higher molecular weight (which are usually associated to membrane proteins), while in the soluble samples the most intense bands are observed in the bottom of the gel, which correspond to proteins with low molecular weight (possibly soluble proteins).

Accordingly, it is possible to conclude that there was a separation of certain subsets of proteins during the subproteome fractionation procedure which cause the different profiles between the membrane and soluble samples.

To accomplish the same goal described above, pooled samples were analyzed by western blot (see Experimental Procedure 4.5.2), thus, some proteins were used as potential membrane and soluble markers to confirm the subproteome fractionation procedure.

Primarily, the PSD-95 (postsynaptic density protein 95) and GAPDH (Glyceraldehyde 3-phosphate dehydrogenase) proteins were used as membrane and soluble markers, (as widely referred in the literature) respectively, but as the PSD-95 is not a transmembrane protein and GAPDH was observed in all cellular compartments the results were not conclusive (see Supplementary subchapter 8.3.1), consequently other proteins were chosen as fractionation on enrichment markers.

Figure 5.1: Evaluation of the subproteome fractionation procedure. PS1/PS2/PS3- pool of the soluble samples that were performed in the first, second and third days of ultracentrifugation, respectively; PM1/PM2/PM3- pool of the membrane samples that were performed in the first, second and third days of ultracentrifugation, respectively; SB- sample buffer.

NMDA (N-methyl-D-aspartate) receptor is a specific type of ionotropic glutamate receptor involved in synaptic plasticity and memory (Marti *et al.*, 1993). During excitatory neurotransmission, presynaptic release of glutamate activates glutamate receptors in the postsynaptic membrane, resulting in the generation of an excitatory postsynaptic potential (Conti, 1997; Zito, 2009). The receptor forms a heterotetramer between several subunits, primarily comprised of NR1, NR2 and NR3 subunits (Marti *et al.*, 1993). In this project NMDA receptor was used as a membrane marker. The denaturation of the NMDA protein in samples with Laemmli Sample Buffer 6× to a 1× final concentration and at 95°C for 5 minutes was insufficient, once the protein did not enter in the gel completely. Which led to the need for a protocol optimization (see Supplementary Subchapter 8.3.2). The following denaturation condition showed better results for NMDAR detection: addition of Laemmli Sample Buffer 6× (with 12% SDS and 4M NaCl) to a 1× final concentration and boiled at 60°C for 10 minutes (see Experimental Procedure 4.5). On the other hand, the GFP protein that was added to the samples for data normalization, did not show a good profile with the new denaturation condition (see Supplementary Subchapter 8.3.2, supplementary figure 8.9). Therefore, the GFP protein had to be denatured separately with the Laemmli Sample Buffer 6× to a 1× final

concentration, at 95°C for 5 minutes and added afterwards to the final samples (see Experimental Procedure 4.5).

The results obtained from western blot (figure 5.2) showed intense bands with a molecular weight corresponding to the NMDAR detection (115 kDa) only in the pools of membrane samples, as expected. As previously stated NMDAR is a complex protein and although the denaturation conditions were changed and the majority of the protein entered into the running gel, an intense smearing in the lane continues to be observed. Therefore, both the bands and the lanes were analyzed in Quantity One® software with local subtraction background, in order to confirm the results.

Although the standard deviation (SD) was higher in the analysis of the lanes than in the bands, the results were as expected, both analysis (bands and lanes) showed a higher detection of NMDAR for the pools of membrane samples (black bars) comparing with the pools of soluble samples (white bars), meaning that the NMDAR was found in greater amount in the membrane fractions. The same was observed with lower standard deviation using a dot blot analysis, and showed a % of coefficient of variation (CV) below 30% in the samples where NMDA is supposed to be present (see Supplementary table 8.2).

Once the NMDA detection always presents an intense smearing throughout the lane, to remove any doubt relatively to the previous results, the same procedure was performed using VDAC-1 protein as a membrane marker.
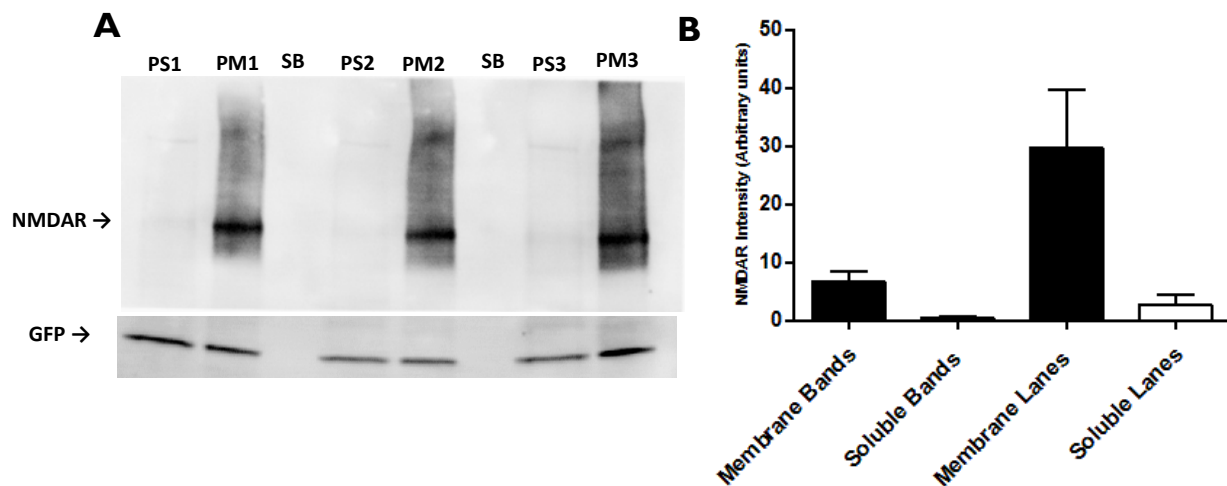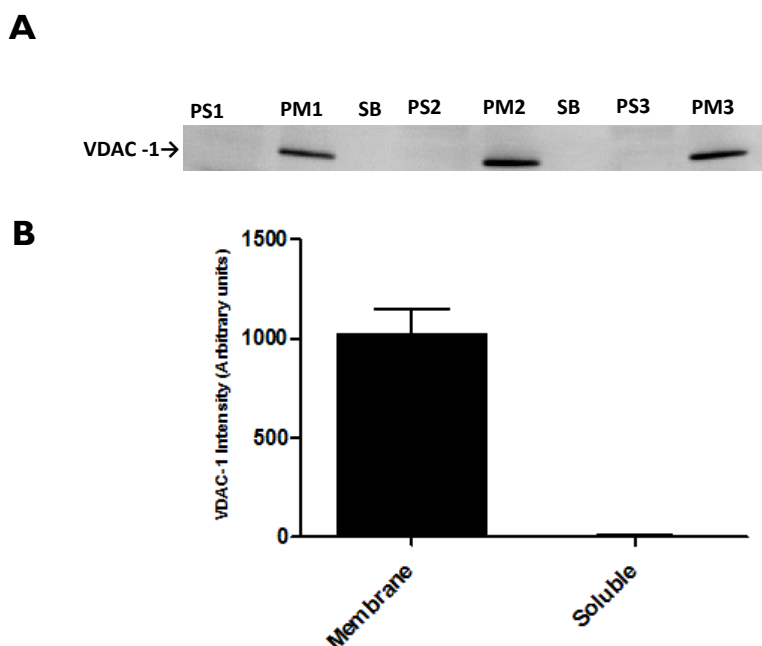

Figure 5.2: Evaluation of the subproteome fractionation procedure. Imunodetection of NMDAR as a membrane marker. A- imonodetection of NMDAR as a membrane marker, the GFP protein was used

to the normalization of western blot. **B-** The bands and the lanes of the membrane (A) were analyzed using Quantity One® software with local subtraction background and the results represent mean values ± SEM.

The voltage-dependent anion channel (VDAC-1), also known as mitochondrial porin, is located in the mitochondrial outer membrane. It functions as a gatekeeper for the entry and exit of mitochondrial metabolites, thereby controlling cross-talk between mitochondria and the rest of the cell. VDAC-1 is also a key player in mitochondria-mediated apoptosis (Shoshan-Barmatz *et al.*, 2010).

After the detection of NMDAR the same blot membrane was used for the detection of VDAC-1 protein (see Experimental Procedure 4.5).

Figure 5.3: Evaluation of the subproteome fractionation procedure. Imunodetection of VDAC as a membrane marker. The bands of the membrane (A) were analyzed (B) using Quantity One® software with local subtraction background and the results represent mean values ± SEM.

As expected, intense bands with a molecular weight corresponding to VDAC-1 protein (33 kDa) were observed only in the pool of membrane samples (figure 5.3). The results showed higher value of intensity in the membrane samples (black bar) than in the soluble samples, as expected, this indicates that, as for NMDAR, the VDAC-1 protein was found in higher amount in the membrane fractions.

In this project the protein DJ-1 protein was used as a soluble marker. DJ-1 is a multifunctional protein with anti-oxidant and transcription modulatory activity. It localizes in

the cytoplasm, mitochondria and nucleus (Junn, 2010). The DJ-1 protein was previous quantified by SWATH analysis using the samples that were prepared in Supplementary Subchapter 8.1. This protein, although has different localization in the cell, showed a higher amount in soluble samples in relation with the membrane samples (data not showed) and a western blot for detection of this protein were performed (see Experimental Procedure 4.5).

A

SB   PS   PM   MW
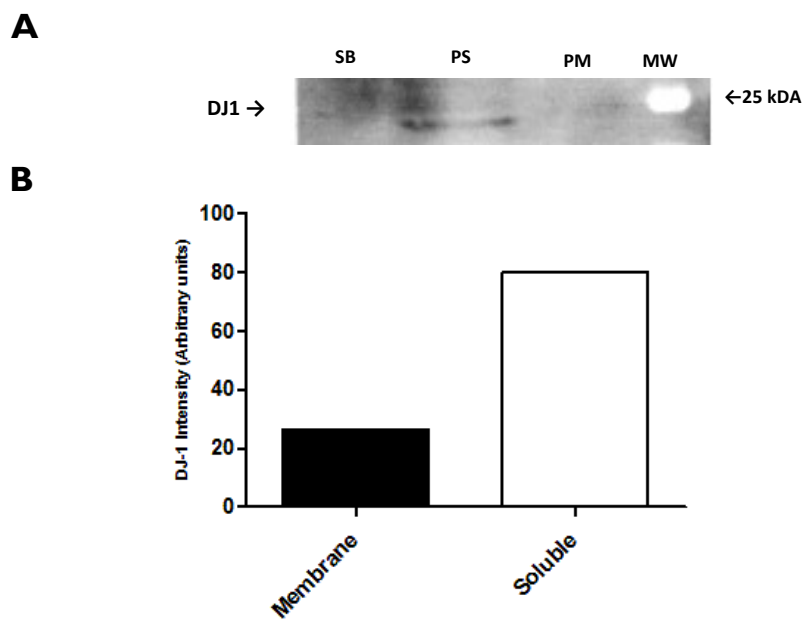
DJ1 →   ←25 kDA

B

Figure 5.4: Evaluation of the subproteome fractionation procedure. Imunodetection of DJ-1 as a soluble marker. The bands of the membrane (A) were analyzed (B) using Quantity One® software with local subtraction background.

The results (figure 5.4) show a higher intensity in the soluble fractions than the membrane fractions. Altogether, these results show that the ultracentrifugation results in an enrichment of membrane proteins (demonstrated here by NMDAR and VDAC-1) in membrane fractions, while the soluble proteins (demonstrated here by DJ-1) were enriched in the soluble fractions.

5.3. PROTEIN IDENTIFICATION

In order to verify if the number of proteins in each condition was similar, the six replicates in each condition were joined and an identification of the proteins was performed by LC-MS/MS (see Experimental Procedure 4.9). The identification of high numbers of proteins

is essential to obtain a good IDA library to be used in SWATH analysis, thus a gel digestion was performed to the samples, followed by LC-MS/MS and protein identification (the digestion procedure was chosen based on the results from different approaches (see Supplementary Subchapter 8.4). The total number of proteins that were identified in each condition is very similar (figure 5.5).
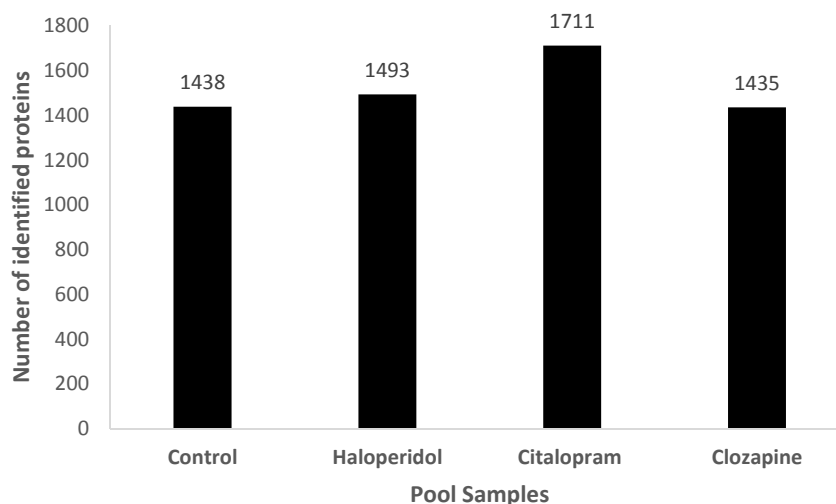
Figure 5.5: Total number of proteins identified by Mass Spectrometry for each condition. A gel digestion was performed to the samples of each condition.

Venn diagrams were used to help to visualize the number of shared and unique proteins among different conditions (see Experimental Procedures 4.10). The comparison between the pooled samples of control, haloperidol, citalopram and clozapine conditions (figure 5.6) revealed that 1190 proteins were shared by all the conditions and 45, 44, 160 and 52 were unique proteins identified in control, haloperidol, citalopram and clozapine, respectively.

Total Number: 1898
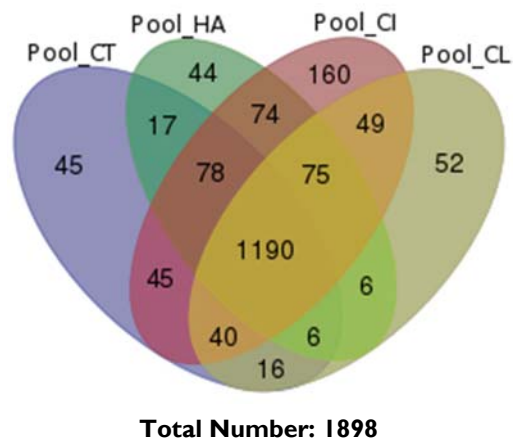
Figure 5.6: Venn Diagrams illustrating the number of shared or unique proteins identified by Mass spectrometry. There are 1190 common proteins and the combined protein number is 1898. Pool_CT- Pool

of control samples; Pool_HA- Pool of Haloperidol samples; Pool_CI- Pool of Citalopram samples; Pool Clozapine- Pool of Clozapine samples.

Worth to mention is that the number of unique proteins identified in control, haloperidol and clozapine were similar, while in citalopram condition was higher. This fact is explained by the increased number of proteins identified by LC-MS/MS (figure 5.5), Nevertheless the number of unique proteins identified in the other three conditions was similar.

5.3.1. GO Enrichment analysis

An important analysis was to evaluate whether the overall lists of proteins obtained were significantly enriched in any particular GO terms based on cellular component, molecular function and biological process. For that Gene Ontology enRIchment anaLysis and visualization tool (GOrilla) was used (see Experimental Procedures 4.10), which provides a clear view in the form of a tree diagram.

This type of analysis generates large amounts of results and information to be evaluated, so considering the enrichment values were formed groups for a simplified visualization of the results - "Extracellular Region part" and "Cytoplasmic part of the neuron" in the cellular component analysis; "Protein Binding" and "Catalytic activity" in molecular function analysis; and "Catalytic Process" and "Carbohydrate catabolic process" in biological process analysis (black boxes). For the three analysis (cellular component, molecular function and biological process) the diagrams formed for the four conditions (control, haloperidol, citalopram and clozapine) were exactly the same, so only the three diagrams for control condition are shown (figure 5.7).

A   **CT_cellular component**

Extracellular region part

Cytoplasmic part of neuron

B   **CT_molecular function**

Protein Binding

Catalytic activity

C   **CT_Biological Process**

Glycolytic Process

Carbohydrate
catabolic process
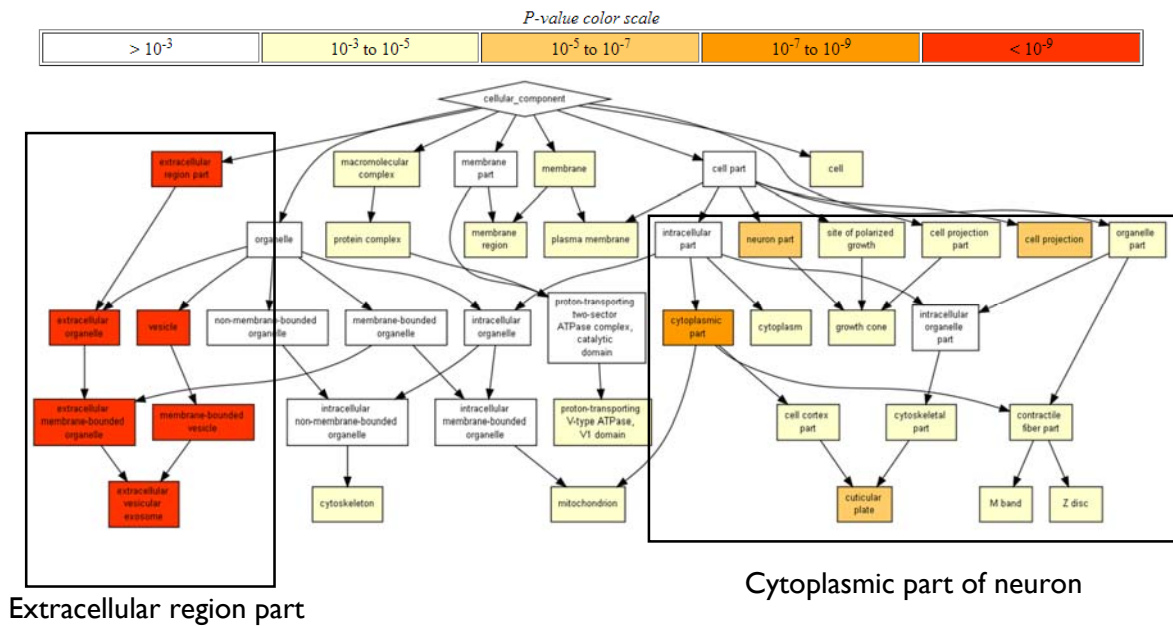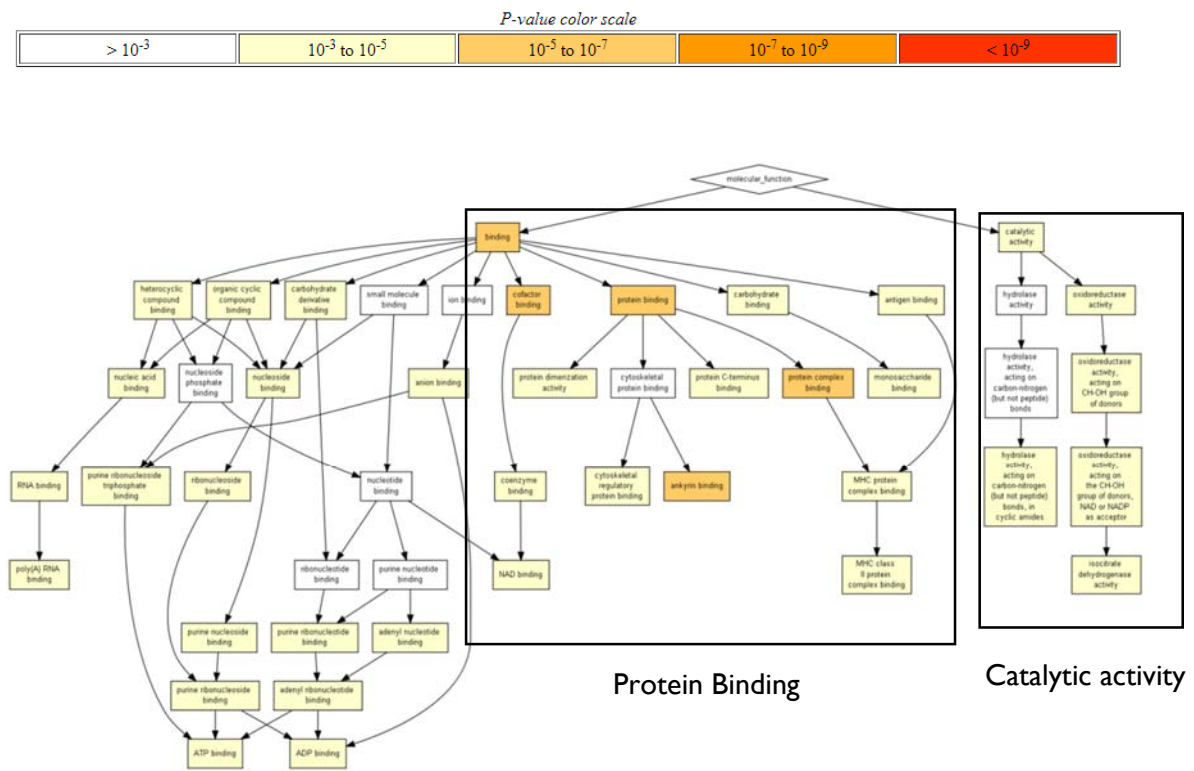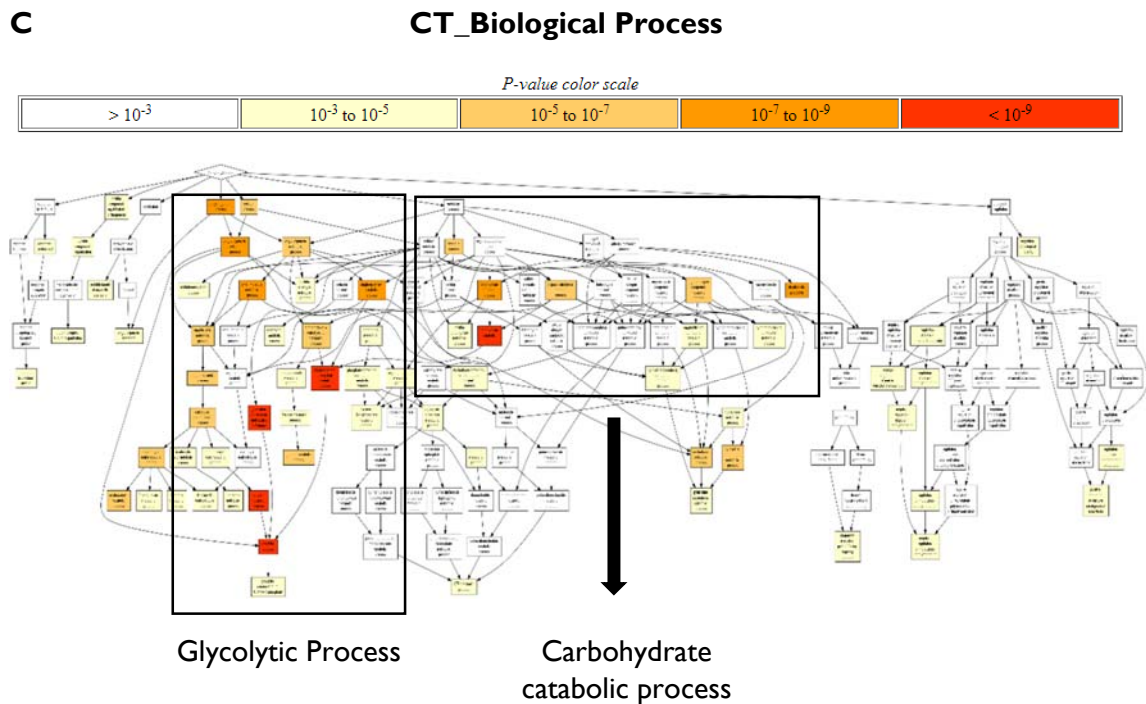
Figure 5.7: Gene Ontology (GO) Enrichment of the identified proteins in the different groups.
Analysis of the identified proteins in the control group based in cellular component (A) molecular function (B) and biological process (C).

Regarding the cellular component analysis these results indicate that there was an enrichment of proteins that belong to the extracellular region part and cytoplasmic part of the cell, as expected, once the samples were obtained from the soluble fraction (supernatant) of the subproteome fractionation procedure, corresponding to the soluble proteins of the cell. The results concerning to the molecular function of the proteins showed an enrichment of proteins which had biding and catalytic functions, although this enrichment was not so significant with a $p < 10^{-3}$ to 10^{-7}. In biological process analysis the proteins belong to the groups of glycolytic process and carbohydrate catabolic process were the ones with higher enrichment. The same results were obtained for the three other conditions and this suggests that the identified proteins in the four conditions were very similar.

5.4. SWATH ANALISIS

A SWATH-MS analysis was performed to determine which proteins were altered by the drugs. Briefly, this approach generates a complete recording of the fragment ion spectra of all the analytes in a sample within a determined m/z window and then acquired data from the chromatographic peak of each peptide is further used to determine the relative quantity of a certain protein. From a total of 1854 quantified proteins (GFP included), 489 proteins passed through the criteria mentioned in Experimental Procedure 4.9. The proteins were analyzed using SPSS (see Experimental Procedure 4.11), and in order to obtain more reliable results an outlier analysis was performed. Three of the replicates samples (CT4, HA1 and HA5) were eliminated, once the results for this samples were consistently considered outliers, which suggests that something could be wrong with each sample and not only with the proteins that were considered outliers. The rest of the proteins that were considered outliers were eliminated from the results and the p-values were determined, comparing the control data with each experimental group (haloperidol, clozapine and citalopram). Then, a fold increase analysis was performed comparing the same conditions (figure 5.8). The results were reported either if i) they were statistically significant when $p < 0.05$ and/or ii) proteins presented a ratio below than 0.66 or higher than 1.5 (figure 5.9).

The graphic A in figure 5.8 shows that in the haloperidol condition half of the proteins were found up-regulated (ratio > 1, $\log_{10}$ scale > 0) and the other half was down regulated (ratio < 1, $\log_{10}$ scale < 0) relative to control.

In the citalopram condition (graphic B) more than half of the proteins were up regulated (above zero) relative to the control. On the contrary, in the clozapine condition the majority of the proteins were down regulated (below zero) relative to the control.

In haloperidol condition (figure 5.9, graphic A) 19 proteins were differentially regulated by this drug, and the majority (15 proteins) being up regulated relatively to the control condition, while 9 of them were down regulated to the control. The proteins with $p < 0.05$ were 2, namely L-lactate dehydrogenase B chain, which was down regulated in relation with the control and UDP-N-acetylglucosamine--peptide N-acetylglucosaminyltransferase 110 kDa subunit that was up regulated relatively to the control.

A

Haloperidol

B

Citalopram

C
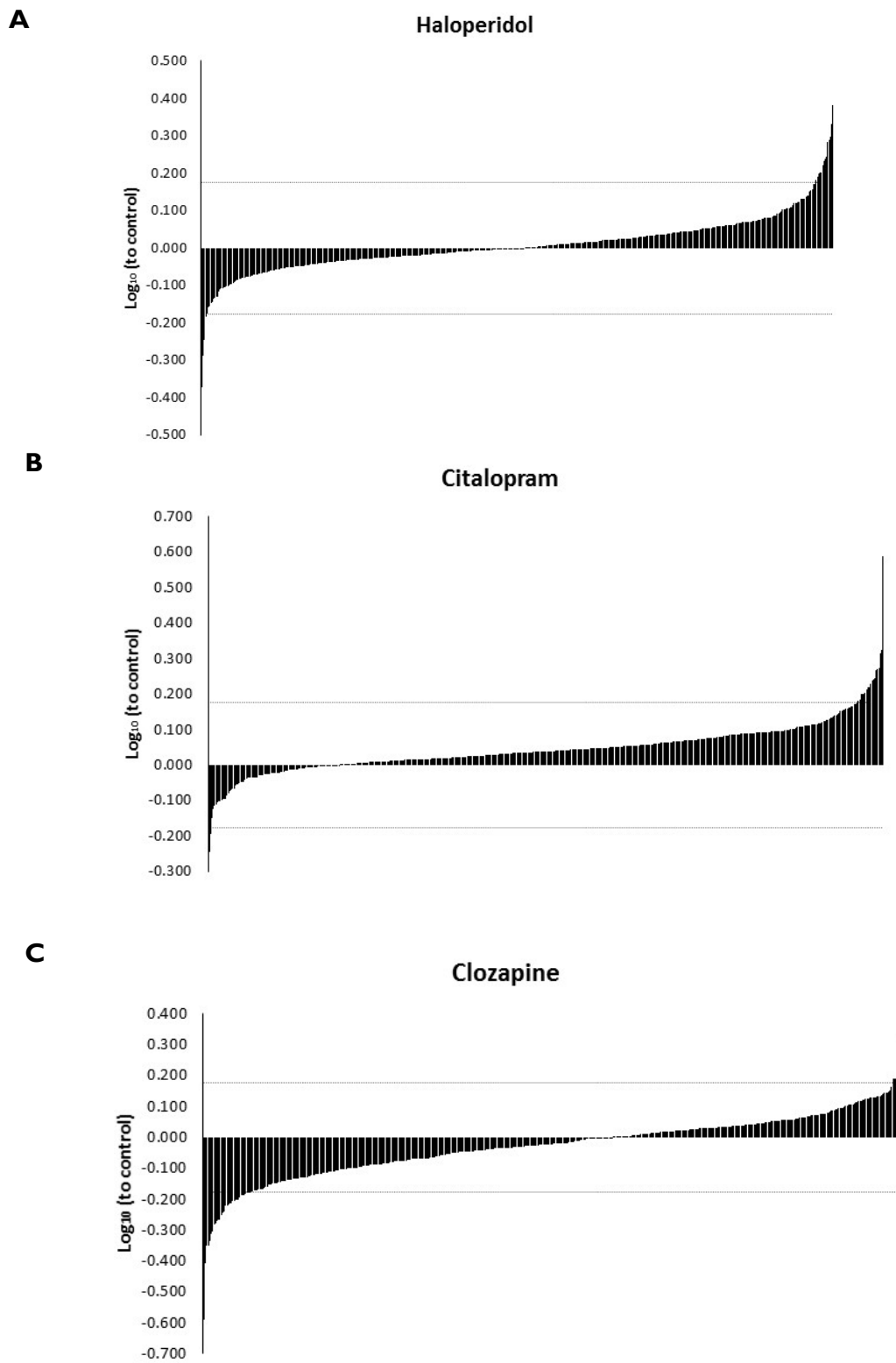
Clozapine

Figure 5.8: Differential protein expression analysis induced by psychotropic medication. Fold-increase of quantified proteins in a (A) Haloperidol, (B) Citalopram and (C) Clozapine. The relative quantitative

proteins are presented in a log scale and were normalized for the control. The dashed line represents the fold-increase and fold-decrease (0.66 and 1.5 in the log scale).

A

Haloperidol

B

Citalopram

C
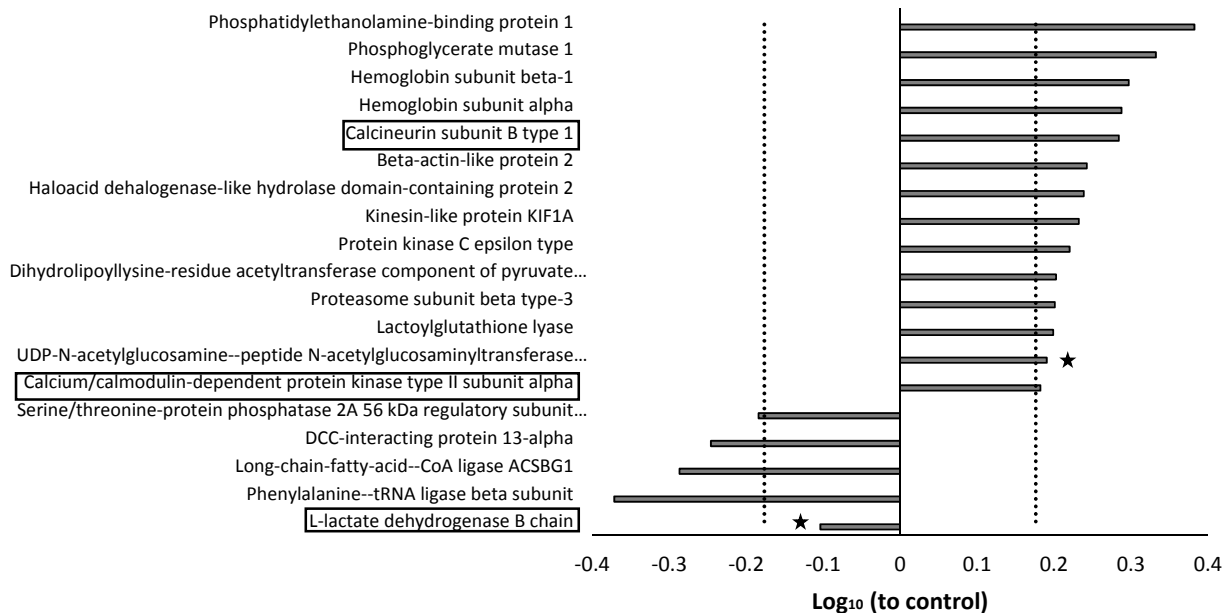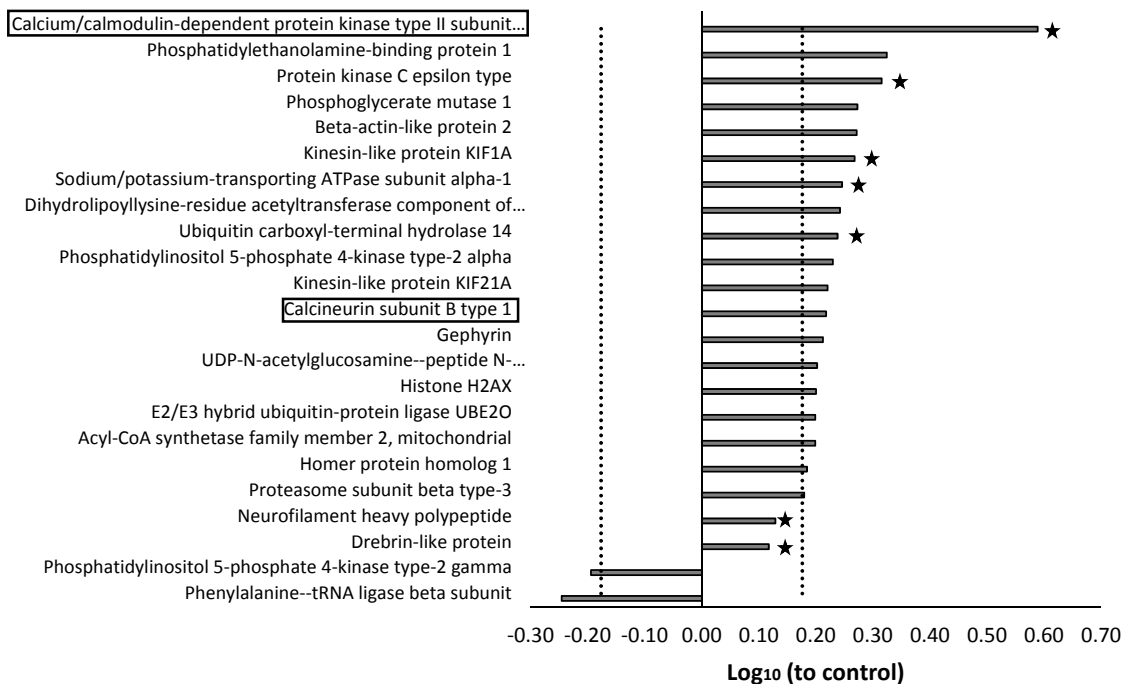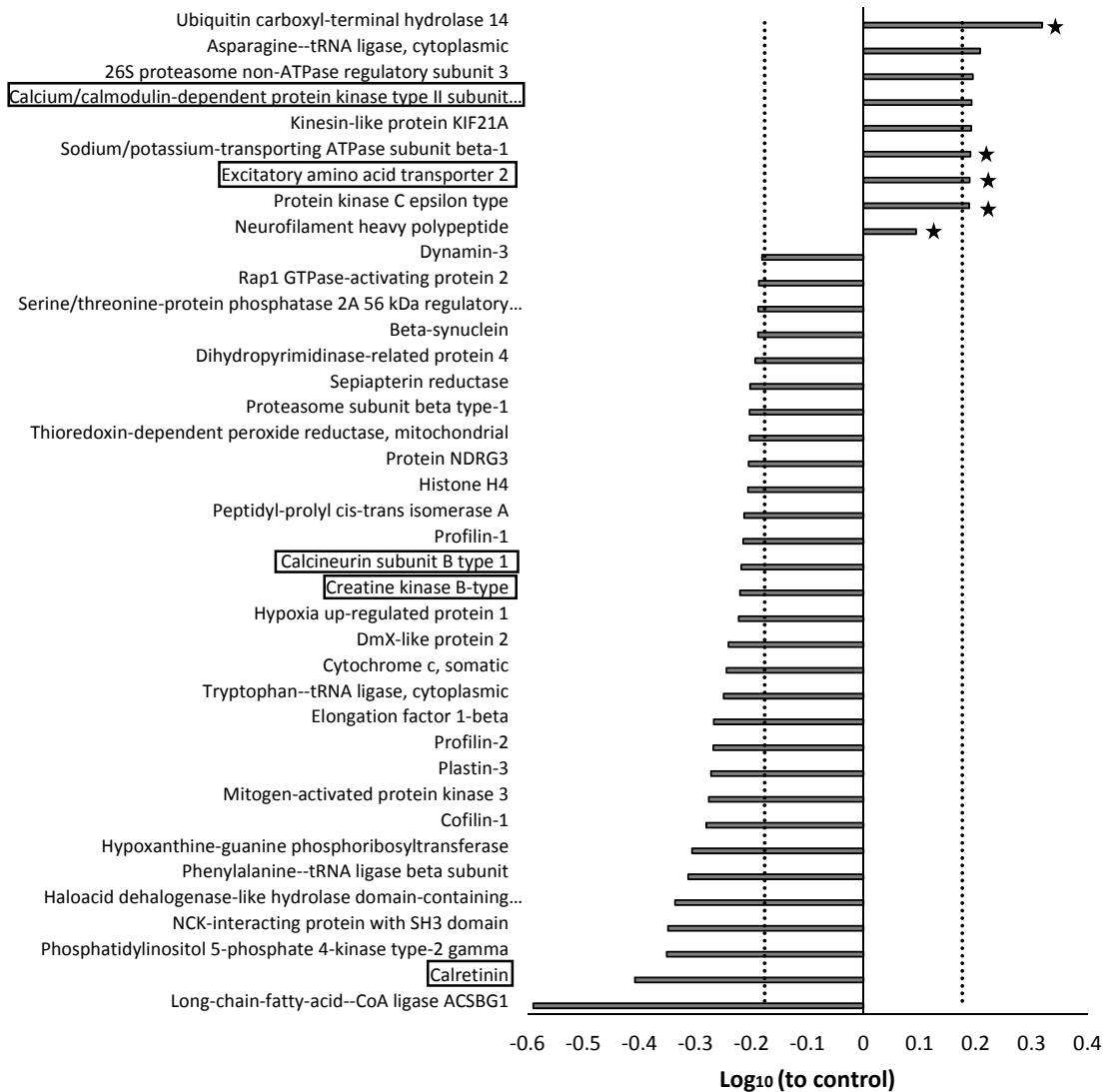
Clozapine

Figure 5.9: Differential protein expression analysis induced by psychotropic medication. Fold-increase of quantified proteins in a (A) Haloperidol, (B) Citalopram and (C) Clozapine. The relative quantitative proteins are presented in a log scale and were normalized for the control. The criteria for the selection of this proteins were the following: $p < 0.05$ and/or ratio below 0.66 or above 1.5 (dashed lines). The proteins with the signal (*) were statistically significant with a $p < 0.05$.

In the citalopram condition (figure 5.9, graphic B) 23 proteins were considered altered by the drug, 21 of them were up regulated in relation to the control and 2 of them were down regulated. In this condition the Drebrin-like protein, Neurofilament heavy polypeptide, Kinesin-like protein KIF21A, Ubiquitin carboxyl-terminal hydrolase 14, Sodium/potassium-transporting ATPase subunit alpha-1, Protein kinase C epsilon type and Calcium/calmodulin-dependent protein kinase type II subunit alpha, were the 7 proteins with $p < 0.05$ and all of them were up regulated in relation with the control.

A total number of 39 proteins were considered altered in the clozapine condition (figure 5.9, graphic C), 9 of them were up regulated and 30 of them were down regulated in relation with the control condition. The proteins with a $p < 0.05$ were Neurofilament heavy polypeptide, Excitatory amino acid transporter 2, Sodium/potassium-transporting ATPase subunit beta-1, Kinesin-like protein KIF21A and Ubiquitin carboxyl-terminal hydrolase 14 and although the majority of the proteins in this condition were down regulated, these proteins were up regulated in relation to the control condition.

Relatively to the proteins that were altered by the drugs, some of them are common regulated by the medications (table 5.2).

Table 5.2: Differential protein expression commonly regulated between the psychotropic medications. ↑ - up regulated protein; ↓ - down regulated protein.

Common Proteins	Haloperidol	Citalopram	Clozapine
Calcineurin subunit beta type 1	↑	↑	↓
Calcium/calmodulin-dependent protein kinase type II subunit alpha	↑	↑	↑
Phenylalanine--tRNA ligase beta subunit	↓	↓	↓
Protein kinase C epsilon type	↑	↑	↑
Beta-actin-like protein 2	↑	↑	
Dihydrolipoyllysine-residue acetyltransferase component of pyruvate dehydrogenase complex, mitochondrial	↑	↑	
Kinesin-like protein KIF1A	↑	↑	
Phosphatidylethanolamine-binding protein 1	↑	↑	
Proteasome subunit beta type-3	↑	↑	
UDP-N-acetylglucosamine--peptide N-acetylglucosaminyltransferase 110 kDa subunit	↑	↑	
Haloacid dehalogenase-like hydrolase domain-containing protein 2	↑		↓
Long-chain-fatty-acid--CoA ligase ACSBG1	↓		↓
Serine/threonine-protein phosphatase 2A 56 kDa regulatory subunit epsilon isoform	↓		↓
Kinesin-like protein KIF21A		↑	↑
Neurofilament heavy polypeptide		↑	↑
Phosphatidylinositol 5-phosphate 4-kinase type-2 gamma		↑	↓
Sodium/potassium-transporting ATPase subunit beta-1		↑	↑
Ubiquitin carboxyl-terminal hydrolase 14		↑	↑

The results above showed that clozapine (atypical antipsychotic) expressed more altered proteins than typical antipsychotic haloperidol, as well as, the majority of the proteins were down regulated by clozapine while with Haloperidol the majority of the altered proteins were up regulated. These results might explain the molecular mechanisms underlying the different effects of both drugs on the organism (described in the Introduction 1.2).

In order to determine which functional group the differentially regulated proteins belong an analysis using the software PANTHER and based in Biological Processes was performed (see Experimental Procedure 4.10) (figure 5.10).
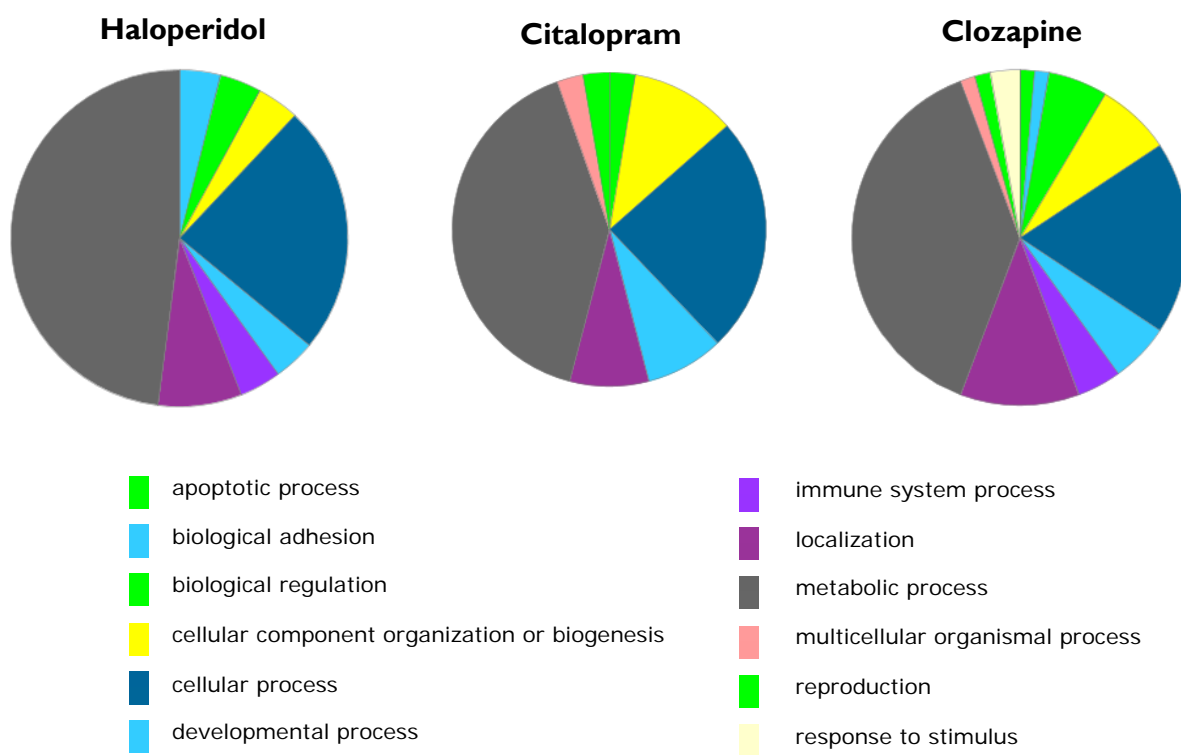
Figure 5.10: Pie charts illustrating the biological processes of the proteins differently regulated in the three drugs conditions. Proteins selected with a fold increase of 1.5 and fold decrease of 0.66 and/or p < 0.05 were used for this analysis.

Haloperidol **Citalopram** **Clozapine**

- biosynthetic process
- generation of precursor metabolites and energy
- nitrogen compound metabolic process
- phosphate-containing compound metabolic process
- primary metabolic process
- coenzyme metabolic process
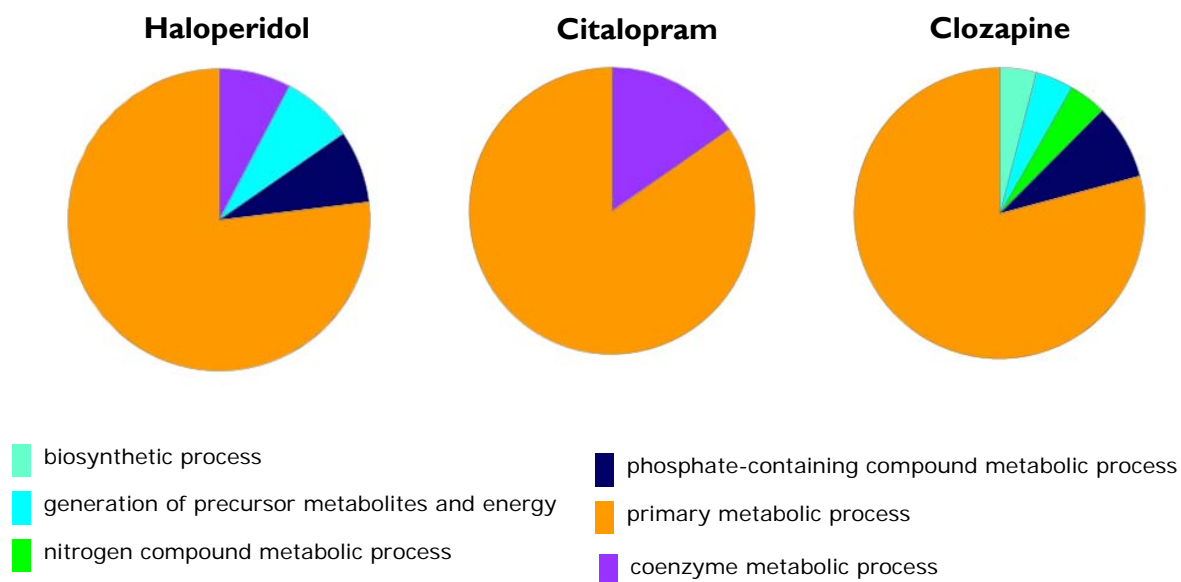
Figure 5.11: Pie charts illustrating the biological processes of the proteins differently regulated in the three drugs conditions. Proteins selected with a fold increase of 1.5 and fold decrease of 0.66 and/or p < 0.05 were used for this analysis. The pie chart section of metabolic process in the previous figure (5.10) was selected to each condition.

Haloperidol **Citalopram** **Clozapine**

- carbohydrate metabolic process
- lipid metabolic process
- protein metabolic process
- tricarboxylic acid cycle
- nucleobase-containing compound metabolic process
- cellular amino acid metabolic process
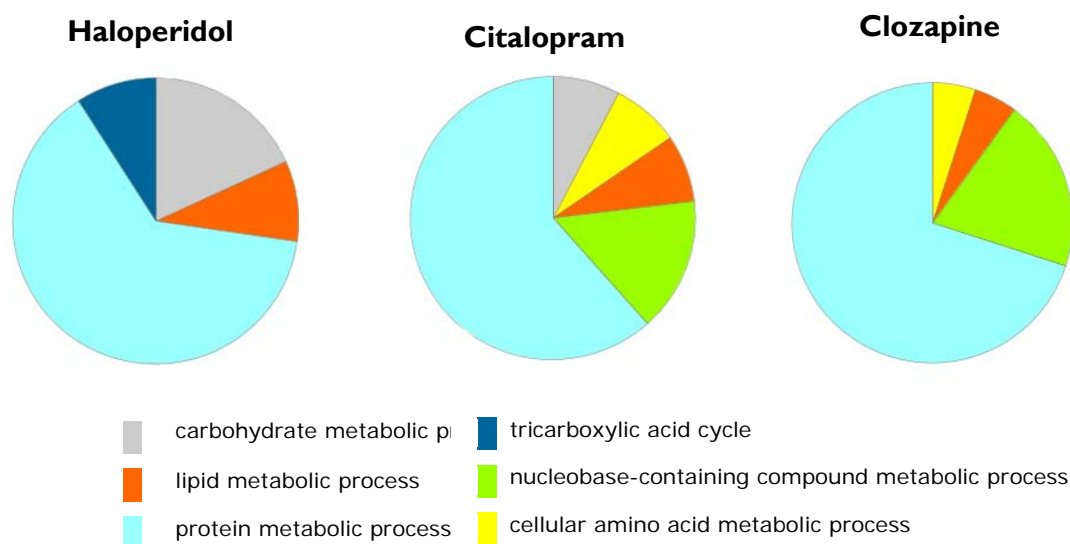
Figure 5.12: Pie charts illustrating the biological processes of the proteins differently regulated in the three drugs conditions. Proteins selected with a fold increase of 1.5 and fold decrease of 0.66 and/or p < 0.05 were used for this analysis. A pie chart section of primary metabolic process in previous figure (5.11) was selected to each condition.

Haloperidol   **Citalopram**   **Clozapine**

cellular protein modification process   ■ proteolysis

■ protein complex assembly   ■ translation

■ protein folding

Figure 5.13: Pie charts illustrating the biological processes of the proteins differently regulated in the three drugs conditions. Proteins selected with a fold increase of 1.5 and fold decrease of 0.66 and/or $p <$ 0.05 were used for this analysis. A pie chart section of protein metabolic process in previous figure (5.12) was selected to each condition.

The results in the figure 5.10, show that the majority of the differentially regulated proteins were integrated into two functional processes, namely metabolic (grey part) and cellular pro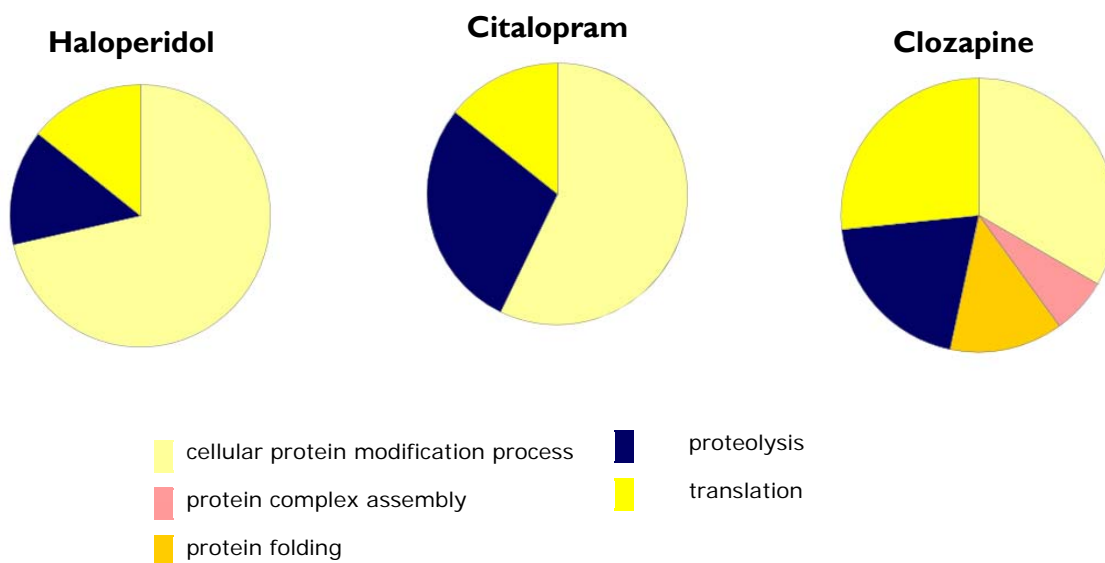cess (blue part). In the cellular process the proteins were classified into two groups, protein phosphorylation and cell communication (data not shown). In metabolic process the majority of the proteins belong to the primary metabolic process (orange part) for the three drugs (figure 5.11), but in relation on the rest of the functional groups there are differences between the three drugs. In the haloperidol condition the proteins also belong to generation of precursor metabolites and energy, phosphate-containing compound metabolic process and coenzyme metabolic process. In the citalopram condition the functional groups are only two: the primary metabolic process, common for the three drugs, and the coenzyme metabolic process. For the clozapine conditions the proteins belong to the groups mentioned above and also to the biosynthetic process and nitrogen compound metabolic process.

Also in primary metabolic process there are differences between the three drugs (figure 5.12). The majority of the proteins belong to the protein metabolic process (blue part) for the three conditions. The proteins, although in less quantity, that belong to lipid metabolic process (orange part) are common for all the conditions, but proteins of carbohydrate metabolic process were regulated only by haloperidol and citalopram drugs, while proteins of

nucleobase-containing compound metabolic process and cellular amino acid metabolic process were regulated by citalopram and clozapine. Haloperidol is the only that regulated proteins that belong to the tricarboxylic acid cycle.

Inside of protein metabolic process there are also differences between the drugs (figure 5.13). The majority of the proteins belong to the cellular protein modification process and were regulated by the three drugs. Although in less quantity the proteins that belong to the proteolysis and translation were also regulated by the three drugs, and proteins belonging to protein complex assembly and protein folding only were regulated by clozapine.

Many studies have reported antipsychotic drugs may affect several metabolic pathways (Thomas *et al.*, 2003), and this is the main path altered by the drugs in this study, but several other processes seems to be affected. Proteins belonging to the apoptotic pathways were altered in this study by the three drugs (figure 5.10), inducted expression of this proteins was already showed by haloperidol (Ahmed *et al.*, 2012) and genome-wide analyses have implicated apoptotic pathways in the genetics of schizophrenia (Sequeira, Martin and Vawter, 2012; Catts and Weickert, 2012). Proteins from immune system also were related here as altered by the drugs, and recent genetic association studies have provided evidence for the deregulation of the immune system, since immune abnormalities endure into adulthood and anti-inflammatory agents appear to be beneficial to the disease (Michel, Schmidt and Mirnics, 2012).

Inside the metabolic processes affected by the drugs, the glucose and lipid metabolisms are the most referred in the literature (Thomas *et al.*, 2003; Lieberman and Stroup, 2005) and the results of this study present the lipid metabolism as an altered pathway by the three drugs. Although these pathways have not yet been reported as altered by drugs or in the disease cellular protein modifications, translation and proteolysis processes were altered by the drugs in this study and these may be of particular importance in the mechanisms of psychotic drugs action and in the pathophysiology of disorder.

Proteins as **Calcineurin subunit B type 1** and **Calcium/calmodulin-dependent protein kinase type II subunit alpha**, both differently regulated by the three drugs, as well as, **Calretinin** protein down regulated by clozapine, are involved in calcium pathways or dependent on it, which confirms the involvement of the drugs in calcium homeostasis. These findings are in line with the fact that several proteins related to calcium signaling have already been found regulated by antipsychotic medication (Kashem *et al.*, 2009; Thomas *et al.*, 2003). Alterations of the intracellular calcium in schizophrenia has also been reported in the literature (Martins-de-Souza, 2011; Melkersson, 2010), which means that the proteins changes mentioned above due to the drugs could influence the outcome in SCZ disease.

Calcium/Calmodulin-dependent Kinase type II (CaMKII) is one of the most densely expressed proteins in the central nervous system. The intracellular signaling pathways that are controlled by CaMKII have been shown to be important for memory formation by controlling synaptic plasticity. The CaMKII holo-enzyme is essential for pre- and post-synaptic mechanisms at both excitatory and inhibitory synapses in hippocampal, amygdalar, cortical, and cerebellar neurons, which highlights the importance of this molecule for proper neuronal functioning (Gao *et al.*, 2014). In this study the **CaMKII subunit alpha** was found up regulated by the treatment of the three drugs. Several studies reported this protein as down regulated in SCZ model animals, according (Zhou *et al.*, 2012) **CaMKIIα** was greatly down regulated after the MK-801 treatment both in the synaptosomal fraction and in the cerebral cortex. Another study proved that mice heterozygous for a null mutation of the alpha-isoform of calcium/calmodulin-dependent protein kinase II (alpha-CaMKII+/-) have profoundly dysregulated behaviours and impaired neuronal development in the dentate gyrus. The behavioral abnormalities include a severe working memory deficit and an exaggerated infradian rhythm, which are similar to symptoms seen in schizophrenia, bipolar mood disorder and other psychiatric disorders (Yamasaki *et al.*, 2008). Therefore, the results present in this study suggest that the increase of **CaMKIIα** protein by all the drugs could be an important mechanism of action to antagonize the low levels of this protein in psychiatric disorders.

According to (Walton *et al.*, 2012) an emerging class of mouse models for SCZ and bipolar disorders (BPD) display similar cognitive impairments to those observed in human patients. The hippocampus of these mice possess a conserved pathophysiological alteration; the given term is the 'immature dentate gyrus' (iDG). The animals possessing an iDG are defined by increased expression of immature neuronal markers (including doublecortin and **calretinin**) and reduced levels of mature neuronal markers, most notably calbindin. With the objective to validate this class of mouse model the authors of this study confirmed that human SCZ and BPD patients displayed significantly elevated **calretinin** expression in the dentate gyrus and trending declines in calbindin expression (in BPD patients) when compared with control subjects, and patients suffering from major depression, meaning that **calretinin** overexpression in both SCZ and BPD patients was closely associated with a psychosis diagnosis and suicide risk (Walton *et al.*, 2012). Thus, the down regulation of the **calretinin** protein by the Clozapine drug observed in this project proves to be significant, once this decrease could contribute to the outcomes of the SCZ disease.

The proteins **L-lactate dehydrogenase B chain** and **creatine kinase B-type** down regulated by haloperidol and clozapine, respectively, also have been reported as altered in

more than one study of the human proteome of subjects with Schizophrenia (Dean, 2011; Deng *et al.*, 2011).

In the case of **excitatory amino acid transporter 2** (**EAAT2**) it was found up regulated by clozapine (figure 5.9), while (Schmitt *et al.*, 2003) observed the opposite effect where clozapine significantly down regulated **EAAT2** in hippocampus, temporal, cingulate and frontal cortex compared to the control. **EAAT2** belongs to a family of Na^+ dependent glutamate transporters that maintain a low synaptic concentration of glutamate by removing glutamate from the synaptic cleft into astroglia and neurons (Shan *et al.*, 2014). It also contributes to energy metabolism in the brain, by transporting glutamate into astrocytes for conversion into glutamine (Spangaro *et al.*, 2012). The glutamate hypothesis of schizophrenia is based on the observation that phencyclidine, a NMDAR antagonist leading to a glutamatergic hypofunction, gives rise to a schizophrenia-like psychosis (Schmitt *et al.*, 2003). A glutamatergic deficit can be due to defective receptors, inadequate glutamate release or hyperactive glutamate transporters. Glutamate transporters control glutamatergic neurotransmission by removal of glutamate from the synaptic cleft.

Different studies focused on **EAAT2** alterations among subjects affected by schizophrenia, reporting a decreased expression in the parahippocampal region and in the dorsolateral prefrontal cortex (Spangaro *et al.*, 2012). This protein, as well as, excitatory amino acid transporters 1 and 3, were found down regulated in the superior temporal gyrus, and in the hippocampus of patients with schizophrenia and the authors of the same study did not detect an effect of antipsychotic medication on expression of this protein in the temporal association cortex or hippocampus in rats treated with haloperidol for 9 months (Shan, 2014). Another study found evidence for less glycosylation of the EAAT1 and **EAAT2** proteins in schizophrenia (Bauer *et al.*, 2010). Therefore, the results in the present study suggest that the increased expression of **EAAT2** in consequence of clozapine administration could be important, once it may be a compensatory mechanism of the decrease observed in the disease. An increase in this transporter could lead to the stabilization of the glutamate levels in the brain which could lead to the benefic effects of this drug observed in SCZ patients.

CONCLUSION AND FUTURE PRESPECTIVES

6. CONCLUSION AND FUTURE PERSPECTIVES

The main goal of this study was to identify the proteomic medication-associated changes of prefrontal cortex from mice treated with Haloperidol, Clozapine and Citalopram, as the molecular mechanisms responsible for the differences in the clinical profile of the drugs mentioned above remain unclear.

A subproteome fractionation of the tissue was successfully accomplished and the membrane protein fraction was separate from soluble protein fraction. The proteins NMDAR and VDAC-1 were used as membrane markers; and the protein DJ-1 as soluble marker, confirming that were an enrichment of membrane and soluble proteins in membrane and soluble fractions, respectively.

In order to focus on the intracellular proteomic changes, in this project only the soluble proteins were analyzed. Firstly the identification of the proteins was performed by LC-MS/MS in the four conditions (control and the three pharmacological treatments). The total number of proteins identified was similar in the four conditions (around 1500), although the citalopram group present a slightly higher number, and the proteins identified in the four groups belonged all to the same cellular, molecular and biological processes.

Then, a recently developed label free quantitative method (SWATH) was used to allow the quantification of an elevated number of proteins with a high confidence (489 proteins). After the outlier analysis, three of the replicates samples (CT4, HA1 and HA5) were eliminated, once several proteins appeared as outliers in these samples.

Significant altered proteins were considered outside of the 1.5 fold factor (1/1.5 - 1×1.5 i.e. below 0.66 and above 1.5) and/or with a $p < 0.05$. In the three drug conditions 14 proteins presented a $p < 0.05$ and 3 of them present a $p < 0.01$. Clozapine presented a higher number of differentially regulated proteins according to these criteria (39 proteins), followed by citalopram (23 proteins), and then by haloperidol (19 proteins). This could explain the different effects observed by the drugs revealed different mechanisms of action.

The Panther analysis revealed that the use of these drugs has a major effect in proteins involved in the metabolism, although other processes related with SZC were identified, namely: apoptotic, immune pathways and calcium homeostasis.

Finally, the results in the present study suggest that the increased expression of the proteins **CaMKIIα** by all the drugs and the **EAAT2** in consequence of clozapine

administration, as well as, the down regulation of the **Calretinin** by the use of clozapine could be important, once it may be a compensatory mechanism of the regulation in the disease.

In the future, the most interesting proteins must be validated in a targeted analysis for example, by western blot, as well as, quantify these proteins in post-mortem tissue of individuals with and without these therapies. Also, considering the availability of the other tissues, protein fractions (enrichment membrane proteins) and a metabolites fraction (not mentioned), the analysis and combination of all results can contribute to elucidate the overall changes induced by these drugs.

Altogether, these findings can give new insights of future strategies for the treatment and prevention of the progression of SCZ once it shows new directions for recognizing disease-related changes.

REFERENCES

7. REFERENCES

ABBOTT, C.; KEITH, S. - **Antipsychotic treatment and adherence in schizophrenia.** (2010) 1–22.

ABI-DARGHAM, A. *et al.* - **Baseline and amphetamine-stimulated dopamine activity are related in drug-naïve schizophrenic subjects**. Biological psychiatry. ISSN 1873-2402. 65:12 (2009) 1091–3. doi: 10.1016/j.biopsych.2008.12.007.

ABI-DARGHAM, A.; LARUELLE, M. - **Mechanisms of action of second generation antipsychotic drugs in schizophrenia: insights from brain imaging studies.** European psychiatry : the journal of the Association of European Psychiatrists. ISSN 0924-9338. 20:1 (2005) 15–27. doi: 10.1016/j.eurpsy.2004.11.003.

ABLES, A. Z.; BAUGHMAN, O. L. - **Antidepressants: update on new agents and indications.** American family physician. ISSN 0002-838X. 67:3 (2003) 547–54.

ACKENHEIL, M.; WEBER, K. - **Developments in antipsychotic therapy with regard to hypotheses for schizophrenia.** Pharmacological aspects. 4. (2002) 426–431.

AGUILAR, M. - **HPLC of Peptides and Proteins**. 122–127 p. ISBN 0896039773.

AHMED, E. U. *et al.* - **Antipsychotic induced alteration of growth and proteome of rat neural stem cells.** Neurochemical research. . ISSN 1573-6903. 37:8 (2012) 1649–59. doi: 10.1007/s11064-012-0768-3.

AKDENIZ, C.; TOST, H.; MEYER-LINDENBERG, A. - T**he neurobiology of social environmental risk for schizophrenia: an evolving research field.** Social psychiatry and psychiatric epidemiology. ISSN 1433-9285. 49:4 (2014) 507–17. doi: 10.1007/s00127-014-0858-4.

BAKHTIAR, R.; NELSON, R. W. - **Electrospray ionization and matrix-assisted laser desorption ionization mass spectrometry.** Biochemical Pharmacology. ISSN 00062952. 59:8 (2000) 891–905. doi: 10.1016/S0006-2952(99)00317-2.

BAN, T. A.; HEALY, D.; SHORTER, E. - **Reflections on twentieth-century psycopharmacology.** 4:(2004) 35–44.

BARAK, Y. *et al.* - **Age-related differences in the side effect profile of citalopram.** Progress in neuro-psychopharmacology & biological psychiatry. ISSN 0278-5846. 27:3 (2003) 545–8. doi: 10.1016/S0278-5846(03)00041-1.

BARCH, D. M.; CEASER, A. - **Cognition in schizophrenia: core psychological and neural mechanisms.** Trends in cognitive sciences. ISSN 1879-307X. 16:1 (2012) 27–34. doi: 10.1016/j.tics.2011.11.015.

BAUER, D. *et al.* - **Abnormal glycosylation of EAAT1 and EAAT2 in prefrontal cortex of elderly patients with schizophrenia.** Schizophrenia research. ISSN 1573-2509. 117:1 (2010) 92–8. doi: 10.1016/j.schres.2009.07.025.

BERTOLINO, A; BLASI, G. - **The genetics of schizophrenia.** Neuroscience. . ISSN 1873-7544. 164:1 (2009) 288–99. doi: 10.1016/j.neuroscience.2009.04.038.

BOB, P.; MASHOUR, G. A - **Schizophrenia, dissociation, and consciousness.** Consciousness and cognition. . ISSN 1090-2376. 20:4 (2011) 1042–9. doi: 10.1016/j.concog.2011.04.013.

BOŠKOVIĆ, M. *et al.* - **Oxidative stress in schizophrenia patients treated with long-acting haloperidol decanoate.** Psychiatry research. . ISSN 1872-7123. 2013). doi: 10.1016/j.psychres.2013.08.035.

BOŽOVIĆ, A.; KULASINGAM, V. - **Quantitative mass spectrometry-based assay development and validation: from small molecules to proteins.** Clinical biochemistry. . ISSN 1873-2933. 46:6 (2013) 444–55. doi: 10.1016/j.clinbiochem.2012.09.024.

BRAY, N. J. *et al.* - **The neurobiology of schizophrenia: new leads and avenues for treatment.** Current opinion in neurobiology. . ISSN 1873-6882. 20:6 (2010) 810–5. doi: 10.1016/j.conb.2010.09.008.

BROOME, M. R. *et al.* - **What causes the onset of psychosis?** Schizophrenia research. . ISSN 0920-9964. 79:1 (2005) 23–34. doi: 10.1016/j.schres.2005.02.007.

BRØSEN, K.; NARANJO, C. A - **Review of pharmacokinetic and pharmacodynamic interaction studies with citalopram.** European neuropsychopharmacology : the journal of the European College of Neuropsychopharmacology. . ISSN 0924-977X. 11:4 (2001) 275–83.

CACABELOS, R.; HASHIMOTO, R.; TAKEDA, M. - **Pharmacogenomics of antipsychotics efficacy for schizophrenia.** Psychiatry and clinical neurosciences. . ISSN 1440-1819. 65:1 (2011) 3–19. doi: 10.1111/j.1440-1819.2010.02168.x.

CARPENTER, W. T.; TANDON, R. - **Psychotic disorders in DSM-5: summary of changes**. Asian journal of psychiatry. . ISSN 1876-2026. 6:3 (2013) 266–8. doi: 10.1016/j.ajp.2013.04.001.

CATTS, V. S.; WEICKERT, C. S. - **Gene expression analysis implicates a death receptor pathway in schizophrenia pathology.** PloS one. . ISSN 1932-6203. 7:4 (2012) e35511. doi: 10.1371/journal.pone.0035511.

CHANA, G. *et al.* - **Biomarker investigations related to pathophysiological pathways in schizophrenia and psychosis.** Frontiers in cellular neuroscience. . ISSN 1662-5102. 7:June (2013) 95. doi: 10.3389/fncel.2013.00095.

CHANDRAPPA, P.; HO, L. - **Case reports of patients with treatment-resistant schizophrenia and related psychotic disorders intolerant to clozapine responding to high doses of quetiapine.** Therapeutic advances in psychopharmacology. . ISSN 2045-1253. 2:5 (2012) 207–9. doi: 10.1177/2045125312451265.

CHEN, C.-H. W. - **Review of a current role of mass spectrometry for proteome research.** Analytica chimica acta. . ISSN 1873-4324. 624:1 (2008) 16–36. doi: 10.1016/j.aca.2008.06.017.

CHEN, G.; PRAMANIK, B. N. - **Application of LC/MS to proteomics studies: current status and future prospects.** Drug discovery today. . ISSN 1878-5832. 14:9-10 (2009) 465–71. doi: 10.1016/j.drudis.2009.02.007.

CHIEN, W. T. *et al.* - **Current approaches to treatments for schizophrenia spectrum disorders, part II: psychosocial interventions and patient-focused perspectives in psychiatric care.** Neuropsychiatric disease and treatment. . ISSN 1176-6328. 9:(2013) 1463–1481. doi: 10.2147/NDT.S49263.

CHIEN, W. T.; YIP, A. L. - **Current approaches to treatments for schizophrenia spectrum disorders, part I: an overview and medical treatments.** Neuropsychiatric disease and treatment. . ISSN 1176-6328. 9:2013) 1311–1332. doi: 10.2147/NDT.S37485.

CONTI, F. - **Localization of NMDA receptors in the cerebral cortex: a schematic overview.** Brazilian journal of medical and biological research . . ISSN 0100-879X. 30:5 (1997) 555–60.

CRAFT, G. E.; CHEN, A.; NAIRN, A. C. - **Recent advances in quantitative neuroproteomics.** Methods (San Diego, Calif.). . ISSN 1095-9130. 61:3 (2013) 186–218. doi: 10.1016/j.ymeth.2013.04.008.

CRITCHLOW, H. M. *et al.* - **Clozapine and haloperidol differentially regulate dendritic spine formation and synaptogenesis in rat hippocampal neurons.** Molecular and cellular neurosciences. . ISSN 1044-7431. 32:4 (2006) 356–65. doi: 10.1016/j.mcn.2006.05.007.

CROWLEY, J. J. *et al.* - **Brain levels of the neurotoxic pyridinium metabolite HPP+ and extrapyramidal symptoms in haloperidol-treated mice.** Neurotoxicology. . ISSN 1872-9711. 39:2013) 153–7. doi: 10.1016/j.neuro.2013.09.005.

CUENCA, P. J.; HOLT, K. R.; HOEFLE, J. D. - **Seizure secondary to citalopram overdose.** The Journal of emergency medicine. . ISSN 0736-4679. 26:2 (2004) 177–81. doi: 10.1016/j.jemermed.2003.06.005.

DASS, C. - **FUNDAMENTALS OF CONTEMPORARY**. ISBN 9780471682295. (2007). 80-139.

DAWES, S. E. *et al.* - **Does antidepressant treatment improve cognition in older people with schizophrenia or schizoaffective disorder and comorbid subsyndromal depression?** Neuropsychobiology. . ISSN 1423-0224. 65:3 (2012) 168–72. doi: 10.1159/000331141.

DEAN, B. - **Dissecting the Syndrome of Schizophrenia: Progress toward Clinically Useful Biomarkers**. Schizophrenia research and treatment. . ISSN 2090-2093. 2011:2011) 614730. doi: 10.1155/2011/614730.

DENG, M. Y. *et al.* - **Frontal-subcortical protein expression following prenatal exposure to maternal inflammation**. PloS one. . ISSN 1932-6203. 6:2 (2011) e16638. doi: 10.1371/journal.pone.0016638.

DLABOGA, D.; HAJJHUSSEIN, H.; O'DONNELL, J. M. - **Chronic haloperidol and clozapine produce different patterns of effects on phosphodiesterase-1B, -4B, and -10A expression in rat striatum.** Neuropharmacology. . ISSN 0028-3908. 54:4 (2008) 745–54. doi: 10.1016/j.neuropharm.2007.12.002.

DUNCAN, G. E. *et al.* - **Comparison of the effects of clozapine, risperidone, and olanzapine on ketamine-induced alterations in regional brain metabolism.** The Journal of pharmacology and experimental therapeutics. . ISSN 0022-3565. 293:1 (2000) 8–14.

EBRAHIMZADEH, H. *et al.* - **Determination of haloperidol in biological samples using molecular imprinted polymer nanoparticles followed by HPLC-DAD detection**. International journal of pharmaceutics. . ISSN 1873-3476. 453:2 (2013) 601–9. doi: 10.1016/j.ijpharm.2013.05.054.

EGGERS, A. E. - **A serotonin hypothesis of schizophrenia.** Medical hypotheses. . ISSN 1532-2777. 80:6 (2013) 791–4. doi: 10.1016/j.mehy.2013.03.013.

ELIS, O.; CAPONIGRO, J. M.; KRING, A. M. - **Psychosocial treatments for negative symptoms in schizophrenia: Current practices and future directions.** Clinical psychology review. . ISSN 1873-7811. 33:8 (2013) 914–928. doi: 10.1016/j.cpr.2013.07.001.

ELLENBROEK, B. A - **Psychopharmacological treatment of schizophrenia: what do we have, and what could we get?** Neuropharmacology. . ISSN 1873-7064. 62:3 (2011) 1371–80. doi: 10.1016/j.neuropharm.2011.03.013.

ENGLISH, J. A *et al.* - **The neuroproteomics of schizophrenia.** Biological psychiatry. . ISSN 1873-2402. 69:2 (2011) 163–72. doi: 10.1016/j.biopsych.2010.06.031.

EYLES, D.; FELDON, J.; MEYER, U. - **Schizophrenia: do all roads lead to dopamine or is this where they start? Evidence from two epidemiologically informed developmental rodent models**. Translational psychiatry. . ISSN 2158-3188. 2:2 (2012) e81. doi: 10.1038/tp.2012.6.

FITZGERALD, K. T.; BRONSTEIN, A. C. - **Selective serotonin reuptake inhibitor exposure**. Topics in companion animal medicine. . ISSN 1938-9736. 28:1 (2013) 13–7. doi: 10.1053/j.tcam.2013.03.003.

FÖCKING, M. *et al.* - **Common proteomic changes in the hippocampus in schizophrenia and bipolar disorder and particular evidence for involvement of cornu ammonis regions 2 and 3**. Archives of general psychiatry. . ISSN 1538-3636. 68:5 (2011) 477–88. doi: 10.1001/archgenpsychiatry.2011.43.

FRANGOU, S. - **Schizophrenia.** Medicine. . ISSN 13573039. 36:8 (2008) 405–409. doi: 10.1016/j.mpmed.2008.05.007.

FUSAR-POLI, P.; POLITI, P. - **Paul Eugen Bleuler and the birth of schizophrenia (1908).** The American journal of psychiatry. . ISSN 1535-7228. 165:11 (2008) 1407. doi: 10.1176/appi.ajp.2008.08050714.

GAEBEL, W.; ZIELASEK, J.; CLEVELAND, H.-R. - **Psychotic disorders in ICD-11.** Asian journal of psychiatry. . ISSN 1876-2026. 6:3 (2013) 263–5. doi: 10.1016/j.ajp.2013.04.002.

GAO, Z. *et al.* - **Distinct roles of α- and βCaMKII in controlling long-term potentiation of GABAA-receptor mediated transmission in murine Purkinje cells.** Frontiers in cellular neuroscience. . ISSN 1662-5102. 8:February (2014) 16. doi: 10.3389/fncel.2014.00016.

GERACE, E. *et al.* - **Evidence of Haldol (haloperidol) long-term intoxication.** Forensic science international. . ISSN 1872-6283. 215:1-3 (2012) 121–3. doi: 10.1016/j.forsciint.2011.01.038.

GILLET, L. C. *et al.* - **Targeted data extraction of the MS/MS spectra generated by data-independent acquisition: a new concept for consistent and accurate proteome analysis.** Molecular & cellular proteomics : MCP. . ISSN 1535-9484. 11:6 (2012) O111.016717. doi: 10.1074/mcp.O111.016717.

GORDON, M. - **Selective serotonin re-uptake inhibitors.** Australian family psysician. 42:9 (2013) 620–623.

GYGI, S. P.; AEBERSOLD, R. - **Mass spectrometry and proteomics.** Current opinion in chemical biology. . ISSN 1367-5931. 4:5 (2000) 489–94.

HAN, K.; KIM, E. - **Synaptic adhesion molecules and PSD-95**. Progress in neurobiology. . ISSN 0301-0082. 84:3 (2008) 263–83. doi: 10.1016/j.pneurobio.2007.10.011.

HAN, X.; ASLANIAN, A.; YATES, J. R. - **Mass spectrometry for proteomics.** Current opinion in chemical biology. . ISSN 1367-5931. 12:5 (2008) 483–90. doi: 10.1016/j.cbpa.2008.07.024.

HAREN, N. E. VAN *et al.* - **The course of brain abnormalities in schizophrenia: can we slow the progression?** Journal of psychopharmacology (Oxford, England). . ISSN 1461-7285. 26:5 Suppl (2012) 8–14. doi: 10.1177/0269881111408964.

HARRISON, P. J. - **The hippocampus in schizophrenia: a review of the neuropathological evidence and its pathophysiological implications.** Psychopharmacology. . ISSN 0033-3158. 174:1 (2004) 151–62. doi: 10.1007/s00213-003-1761-y.

HELMUT BUSCHMANN, J. L. D.; JÖRG HOLENZ, A. P.; VELA, A. T. And J. M. **Antidepressants, Antipsychotics, Anxiolytics.** ISBN 9783527310586. (2007) 297-586

HIEMKE, C.; HÄRTTER, S. - **Pharmacokinetics of selective serotonin reuptake inhibitors**. Pharmacology & therapeutics. . ISSN 0163-7258. 85:1 (2000) 11–28.

HIRVONEN, J.; HIETALA, J. - **Dysfunctional brain networks and genetic risk for schizophrenia: specific neurotransmitter systems.** CNS neuroscience & therapeutics. . ISSN 1755-5949. 17:2 (2011) 89–96. doi: 10.1111/j.1755-5949.2010.00223.x.

HOFFMANN, E. De;; STROOBANT, V. - **Mass Spectrometry Principles and Applications**. 85–167 p. ISBN 9780470033104.

HONEA, R. *et al.* - **Reviews and Overviews Regional Deficits in Brain Volume in Schizophrenia : A Meta-Analysis of Voxel-Based Morphometry Studies.** i:2000) 2233–2245.

HOSAK, L. - **New findings in the genetics of schizophrenia**. World journal of psychiatry. . ISSN 2220-3206. 3:3 (2013) 57–61. doi: 10.5498/wjp.v3.i3.57.

HOWARD, P. *et al.* - **Antidepressant drugs.** Journal of pain and symptom management. . ISSN 1873-6513. 44:5 (2012) 763–83. doi: 10.1016/j.jpainsymman.2012.09.001.

IANCU, I. *et al.* - **Escitalopram in the treatment of negative symptoms in patients with chronic schizophrenia: a randomized double-blind placebo-controlled trial.** Psychiatry research. . ISSN 0165-1781. 179:1 (2010) 19–23. doi: 10.1016/j.psychres.2010.04.035.

JABLENSKY, A. - **Schizophrenia in DSM-5: Assets and liabilities.** Schizophrenia research. . ISSN 1573-2509. 150:1 (2013) 36–7. doi: 10.1016/j.schres.2013.07.037.

JEAN LUD CADET, SUBRAMANIAM JAYANTHI, MICHAEL T. MCCOY, GENEVIEVE BEAUVAIS, And N.; CAI, S. - **Dopamine D1 Receptors, Regulation of Gene Expression in the Brain, and Neurodegeneration.** CNS Neurol Disord Drug Targets. 9(5):2010) 526–538.

JUNN, E. - **Mitochondrial Localization of DJ-1 Leads to Enhanced Neuroprotection Eunsung.** Journal of Neurosci ence Research. 87:1 (2010) 123–129. doi: 10.1002/jnr.21831.Mitochondrial.

KANNAN, G.; SAWA, A.; PLETNIKOV, M. V - **Mouse models of gene-environment interactions in schizophrenia.** Neurobiology of disease. . ISSN 1095-953X. 57:2013) 5–11. doi: 10.1016/j.nbd.2013.05.012.

KAPUR, S.; REMINGTON, G. - **Atypical and antypical antipsycotic: New Directions and New Challenges in the Treatment of Schizophrenia.** 52:2001) 503–17.

KAPUR, S.; SEEMAN, P. - **Antipsychotic agents differ in how fast.** 2000) 0–5.

KARAM, C. S. *et al.* - S**ignaling pathways in schizophrenia: emerging targets and therapeutic strategies.** Trends in pharmacological sciences. . ISSN 1873-3735. 31:8 (2010) 381–90. doi: 10.1016/j.tips.2010.05.004.

KARL, T. *et al.* - **Behavioural effects of chronic haloperidol and risperidone treatment in rats.** Behavioural brain research. . ISSN 0166-4328. 171:2 (2006) 286–94. doi: 10.1016/j.bbr.2006.04.004.

KASAI, K. *et al.* - **Neuroanatomy and neurophysiology in schizophrenia.** Neuroscience research. . ISSN 0168-0102. 43:2 (2002) 93–110.

KASHEM, M. A *et al.* - **Effects of typical (haloperidol) and atypical (risperidone) antipsychotic agents on protein expression in rat neural stem cells.** Neurochemistry international. . ISSN 1872-9754. 55:7 (2009) 558–65. doi: 10.1016/j.neuint.2009.05.007.

KICMAN, A. T.; PARKIN, M. C.; ILES, R. K. - **An introduction to mass spectrometry based proteomics-detection and characterization of gonadotropins and related molecules.** Molecular and cellular endocrinology. . ISSN 0303-7207. 260-262:2007) 212–27. doi: 10.1016/j.mce.2006.02.022.

KINTER, M.; SHERMAN, N. E. - **PROTEIN SEQUENCING AND IDENTIFICATION USING TANDEM MASS SPECTROMETRY**. 29–61 p. ISBN 0471322490.

KIRBY, B. P.; WADDINGTON, J. L.; O'TUATHAIGH, C. M. P. - **Advancing a functional genomics for schizophrenia: psychopathological and cognitive phenotypes in mutants with gene disruption.** Brain research bulletin. . ISSN 1873-2747. 83:3-4 (2010) 162–76. doi: 10.1016/j.brainresbull.2009.09.010.

KONOPASKE, G. T. *et al.* - **Time-dependent effects of haloperidol on glutamine and GABA homeostasis and astrocyte activity in the rat brain.** Psychopharmacology. . ISSN 1432-2072. c:2013). doi: 10.1007/s00213-013-3136-3.

KONRADI, C.; HECKERS, S. - **Antipsychotic drugs and neuroplasticity: insights into the treatment and neurobiology of schizophrenia.** Biological psychiatry. . ISSN 0006-3223. 50:10 (2001) 729–42.

KRISHNAN, K. *et al.* - **Identification of glyceraldehyde-3-phosphate dehydrogenase (GAPDH) as a binding protein for a 68-kDa Bacillus thuringiensis parasporal protein cytotoxic against leukaemic cells.** Journal of biomedical science. . ISSN 1423-0127. 17:126 (2010) 86. doi: 10.1186/1423-0127-17-86.

LAKO, I. M. *et al.* - **The course of depressive symptoms and prescribing patterns of antidepressants in schizophrenia in a one-year follow-up study.** European psychiatry : the journal of the Association of European Psychiatrists. . ISSN 1778-3585. 27:4 (2012) 240–4. doi: 10.1016/j.eurpsy.2010.10.007.

LAMBERT, J.-P. - **Mapping differential interactomes by affinity purification coupled with data independent mass spectrometry acquisition**. Nature Methods. 10:12 (2013) 1–24. doi: 10.1038/nmeth.2702.Mapping.

LASCHET, J. J. *et al.* - **Glyceraldehyde-3-phosphate dehydrogenase is a GABAA receptor kinase linking glycolysis to neuronal inhibition.** The Journal of neuroscience : the official journal of the Society for Neuroscience. . ISSN 1529-2401. 24:35 (2004) 7614–22. doi: 10.1523/JNEUROSCI.0868-04.2004.

LIEBERMAN, J.; STROUP, T. - **Effectiveness of antipsychotic drugs in patients with chronic schizophrenia.** England Journal. 353:2005) 1209–1223.

LIN, D.; TABB, D. L.; YATES, J. R. - **Large-scale protein identification using mass spectrometry. Biochimica et Biophysica Acta (BBA) -** Proteins and Proteomics. . ISSN 15709639. 1646:1-2 (2003) 1–10. doi: 10.1016/S1570-9639(02)00546-0.

LIU, Y.; HÜTTENHAIN, R.; SURINOVA, S.; *et al.* - **Quantitative measurements of N-linked glycoproteins in human plasma by SWATH-MS.** Proteomics. . ISSN 1615-9861. 13:8 (2013) 1247–56. doi: 10.1002/pmic.201200417.

LIU, Y.; HÜTTENHAIN, R.; COLLINS, B.; *et al.* - **Mass spectrometric protein maps for biomarker discovery and clinical research.** Expert review of molecular diagnostics. . ISSN 1744-8352. 13:8 (2013) 811–25. doi: 10.1586/14737159.2013.845089.

LÔO, H. *et al.* - **Antidepressants. Psychiatrie**. . ISSN 17625718. 1:4 (2004) 246–254. doi: 10.1016/j.emcps.2004.06.004.

MA, D. *et al.* - **Antipsychotic Treatment Alters Protein Expression Associated with Presynaptic Function and Nervous System Development in Rat Frontal Cortex research articles.** 2009) 3284–3297.

MARAIS, L. *et al.* - **A proteomic analysis of the ventral hippocampus of rats subjected to maternal separation and escitalopram treatment**. Metabolic brain disease. . ISSN 1573-7365. 24:4 (2009) 569–86. doi: 10.1007/s11011-009-9156-3.

MARTI, T. *et al.* - **Molecular distinction of three N-methyl-D-aspartate-receptor subtypes in situ and developmental receptor maturation demonstrated with the photoaffinity ligand 125I-labele**d CGP 55802A. Proceedings of the National Academy of Sciences of the United States of America. . ISSN 0027-8424. 90:18 (1993) 8434–8.

MARTINS-DE-SOUZA, D.; HARRIS, L. W.; *et al.* - **The role of proteomics in depression research.** European archives of psychiatry and clinical neuroscience. . ISSN 1433-8491. 260:6 (2010) 499–506. doi: 10.1007/s00406-009-0093-2.

MARTINS-DE-SOUZA, D.; MACCARRONE, G.; *et al.* - **Proteome analysis of the thalamus and cerebrospinal fluid reveals glycolysis dysfunction and potential biomarkers candidates for schizophrenia.** Journal of psychiatric research. . ISSN 1879-1379. 44:16 (2010) 1176–89. doi: 10.1016/j.jpsychires.2010.04.014.

MARTINS-DE-SOUZA, D. - **Proteomics as a tool for understanding schizophrenia.** Clinical psychopharmacology and neuroscience : the official scientific journal of the Korean College of Neuropsychopharmacology. . ISSN 1738-1088. 9:3 (2011) 95–101. doi: 10.9758/cpn.2011.9.3.95.

MARTINS-DE-SOUZA, D. *et al.* - **Proteomic approaches to unravel the complexity of schizophrenia.** Expert review of proteomics. . ISSN 1744-8387. 9:1 (2012) 97–108. doi: 10.1586/epr.11.70.

MARTINS-DE-SOUZA, D. - **Proteomics tackling schizophrenia as a pathway disorder.** Schizophrenia bulletin. . ISSN 1745-1701. 38:6 (2012) 1107–8. doi: 10.1093/schbul/sbs094.

MEENT, M. H. M. VAN DE; JONG, G. J. DE - **Novel liquid-chromatography columns for proteomics research**. TrAC Trends in Analytical Chemistry. . ISSN 01659936. 30:11 (2011) 1809–1818. doi: 10.1016/j.trac.2011.06.012.

MEGGER, D. A *et al.* - **Label-free quantification in clinical proteomics.** Biochimica et biophysica acta. . ISSN 0006-3002. 1834:8 (2013) 1581–90. doi: 10.1016/j.bbapap.2013.04.001.

MELKERSSON, K. - **Introduction: clinical findings related to alterations of the intracellular calcium homeostasis in schizophrenia**. Progress in neuro-psychopharmacology & biological psychiatry. . ISSN 1878-4216. 34:8 (2010) 1365–6. doi: 10.1016/j.pnpbp.2010.10.002.

MICHEL, M.; SCHMIDT, M.; MIRNICS, K. - **Immune system gene dysregulation in autism and schizophrenia.** Developmental neurobiology. 72:10 (2012) 1277–1287. doi: 10.1002/dneu.22044.Immune.

MIYAMOTO, S. *et al.* - **Treatments for schizophrenia: a critical review of pharmacology and mechanisms of action of antipsychotic drugs.** Molecular psychiatry. . ISSN 1359-4184. 10:1 (2005) 79–104. doi: 10.1038/sj.mp.4001556.

MODINOS, G. *et al.* - **Molecular genetic gene-environment studies using candidate genes in schizophrenia: A systematic review.** Schizophrenia research. . ISSN 1573-2509. 2013). doi: 10.1016/j.schres.2013.09.010.

MOLTKE, L. L. VON *et al.* - **Citalopram and desmethylcitalopram in vitro: human cytochromes mediating transformation, and cytochrome inhibitory effects**. Biological psychiatry. . ISSN 0006-3223. 46:6 (1999) 839–49.

MONKS, S. *et al.* - **Further evidence for high rates of schizophrenia in 22q11.2 deletion syndrome.** Schizophrenia research. . ISSN 1573-2509. 153:1-3 (2014) 231–6. doi: 10.1016/j.schres.2014.01.020.

MUENCH, J.; HAMER, A. M. - **Adverse effects of antipsychotic medications.** American family physician. . ISSN 1532-0650. 81:5 (2010) 617–22.

MURRAY, C.; BARRETT, M.; EYK, J. Van - **Assessment of ProteoExtract subcellular fractionation kit reveals limited and incomplete enrichment of nuclear subproteome from frozen liver and heart tissue.** Proteomics. 9:15 (2009) 3934–3938. doi: 10.1002/pmic.200701170.Assessment.

NASH, J.; NUTT, D. - **Antidepressants.** Psychiatry. . ISSN 14761793. 6:7 (2007) 289–294. doi: 10.1016/j.mppsy.2007.04.005.

NGUYEN, T. V *et al.* - **Differential expression of c-fos and zif268 in rat striatum after haloperidol, clozapine, and amphetamine.** Proceedings of the National Academy of Sciences of the United States of America. . ISSN 0027-8424. 89:10 (1992) 4270–4.

NUTT, D. J. *et al.* - **Mechanisms of action of selective serotonin reuptake inhibitors in the treatment of psychiatric disorders.** European neuropsychopharmacology : the journal of the European College of Neuropsychopharmacology. . ISSN 0924-977X. 9 Suppl 3:1999) S81–6.

O'BRIEN, E. *et al.* - **Effects of chronic risperidone treatment on the striatal protein profiles in rats.** Brain research. . ISSN 0006-8993. 1113:1 (2006) 24–32. doi: 10.1016/j.brainres.2006.07.009.

O'TUATHAIGH, C. M. P. *et al.* - **Susceptibility genes for schizophrenia: characterisation of mutant mouse models at the level of phenotypic behaviour.** Neuroscience and biobehavioral reviews. . ISSN 0149-7634. 31:1 (2007) 60–78. doi: 10.1016/j.neubiorev.2006.04.002.

OHTANI, T. *et al.* - **Prefrontal cortex volume deficit in schizophrenia: A new look using 3T MRI with manual parcellation.** Schizophrenia research. . ISSN 1573-2509. d:2013). doi: 10.1016/j.schres.2013.10.026.

ONG, S.-E.; FOSTER, L. J.; MANN, M. - **Mass spectrometric-based approaches in quantitative proteomics.** Methods (San Diego, Calif.). . ISSN 1046-2023. 29:2 (2003) 124–30.

OS, J. VAN; KAPUR, S. - **Schizophrenia.** Lancet. . ISSN 1474-547X. 374:9690 (2009) 635–45. doi: 10.1016/S0140-6736(09)60995-8.

OWEN, M. J.; CRADDOCK, N.; O'DONOVAN, M. C. - **Schizophrenia: genes at last?** Trends in genetics : TIG. . ISSN 0168-9525. 21:9 (2005) 518–25. doi: 10.1016/j.tig.2005.06.011.

OWENS, S. F. et al. - **Prefrontal deviations in function but not volume are putative endophenotypes for schizophrenia.** Brain : a journal of neurology. . ISSN 1460-2156. 135:Pt 7 (2012) 2231–44. doi: 10.1093/brain/aws138.

PALMA, S. DI et al. - **Recent advances in peptide separation by multidimensional liquid chromatography for proteome analysis.** Journal of proteomics. . ISSN 1876-7737. 75:13 (2012) 3791–813. doi: 10.1016/j.jprot.2012.04.033.

PARK, E. J. et al. - **Long-acting injectable formulations of antipsychotic drugs for the treatment of schizophrenia.** Archives of pharmacal research. . ISSN 0253-6269. 36:6 (2013) 651–9. doi: 10.1007/s12272-013-0105-7.

PARK, J. et al. - **Haloperidol and clozapine block formation of autophagolysosomes in rat primary neurons.** Neuroscience. . ISSN 1873-7544. 209:2012a) 64–73. doi: 10.1016/j.neuroscience.2012.02.035.

PARK, J. et al. - **Haloperidol and clozapine block formation of autophagolysosomes in rat primary neurons.** Neuroscience. . ISSN 1873-7544. 209:2012b) 64–73. doi: 10.1016/j.neuroscience.2012.02.035.

PAULSON, L. et al. - **Proteome analysis after co-administration of clozapine or haloperidol to MK-801-treated rats**. Journal of neural transmission (Vienna, Austria : 1996). . ISSN 1435-1463. 114:7 (2007) 885–91. doi: 10.1007/s00702-007-0626-7.

RAO, J. S. et al. - **Dysregulated glutamte and dopamine transporters in postmortem frontal cortex from bipolar an schizophrenic patients.** 136:2012) 63–71. doi: 10.1016/j.jad.2011.08.017.Dysregulated.

RATAJCZAK, P.; WOZNIAK, A.; NOWAKOWSKA, E. - **Animal models of schizophrenia: developmental preparation in rats**. Acta neurobiologiae experimentalis. . ISSN 1689-0035. 73:4 (2013) 472–84.

ROSS, C. A et al. - **Neurobiology of schizophrenia.** Neuron. . ISSN 0896-6273. 52:1 (2006) 139–53. doi: 10.1016/j.neuron.2006.09.015.

RUMMEL, C.; KISSLING, W.; LEUCHT, S. - **Antidepressants as add-on treatment to antipsychotics for people with schizophrenia and pronounced negative symptoms: a systematic review of randomized trials.** Schizophrenia research. . ISSN 0920-9964. 80:1 (2005) 85–97. doi: 10.1016/j.schres.2005.07.035.

SCARR, E. et al. - **Cholinergic connectivity: it's implications for psychiatric disorders**. Frontiers in cellular neuroscience. . ISSN 1662-5102. 7:May (2013) 55. doi: 10.3389/fncel.2013.00055.

SCHINDLER, J. et al. - **Enrichment of integral membrane proteins from small amounts of brain tissue**. Journal of neural transmission (Vienna, Austria : 1996). . ISSN 0300-9564. 113:8 (2006) 995–1013. doi: 10.1007/s00702-006-0508-4.

SCHMETZER, A. D. - **Clinical Handbook of Schizophrenia**. 241–242 p. ISBN 9781593856526.

SCHMIDT, C. J. et al. - **The role of 5-HT2A receptors in antipsychotic activity**. 54:2 (1995).

SCHMITT, A. *et al.* - **Decreased gene expression of glial and neuronal glutamate transporters after chronic antipsychotic treatment in rat brain.** Neuroscience Letters. . ISSN 03043940. 347:2 (2003) 81–84. doi: 10.1016/S0304-3940(03)00653-0.

SCHMITT, A. *et al.* - **The impact of environmental factors in severe psychiatric disorders.** Frontiers in neuroscience. . ISSN 1662-4548. 8:February (2014) 19. doi: 10.3389/fnins.2014.00019.

SEEMAN, P. - **Clozapine, a fast-off-d2 antipsychotic.** ACS chemical neuroscience. . ISSN 1948-7193. 5:1 (2014) 24–9. doi: 10.1021/cn400189s.

SEQUEIRA, P.; MARTIN, M.; VAWTER, M. - **The first decade and beyond of transcriptional profiling in schizophrenia.** Neurobiology of disease. 45:1 (2012) 23–36. doi: 10.1016/j.nbd.2011.03.001.The.

SHAN, D. - **Abnormal Expression of Glutamate Transporters in Temporal Lobe Areas in Elderly Patients with Schizophrenia**. Schizophrenia research. 144:2014) 1–8. doi: 10.1016/j.schres.2012.12.019.Abnormal.

SHAN, D. *et al.* - **Abnormal partitioning of hexokinase 1 suggests disruption of a glutamate transport protein complex in schizophrenia.** Schizophrenia research. . ISSN 1573-2509. 154:1-3 (2014) 1–13. doi: 10.1016/j.schres.2014.01.028.

SHEREMATA, S.; CHEN, Y. - **Co-administration of atypical antipsychotics and antidepressants disturbs contrast detection in schizophrenia.** Schizophrenia research. . ISSN 0920-9964. 70:1 (2004) 81–9. doi: 10.1016/j.schres.2003.09.005.

SHOSHAN-BARMATZ, V. *et al.* - **VDAC, a multi-functional mitochondrial protein regulating cell life and death.** Molecular aspects of medicine. . ISSN 1872-9452. 31:3 (2010) 227–85. doi: 10.1016/j.mam.2010.03.002.

SPANGARO, M. *et al.* - **Cognitive dysfunction and glutamate reuptake: effect of EAAT2 polymorphism in schizophrenia.** Neuroscience letters. . ISSN 1872-7972. 522:2 (2012) 151–5. doi: 10.1016/j.neulet.2012.06.030.

TAKAHASHI, N.; ISOBE, T. - **Proteomic biology using LC-MS.** 1–147 p. ISBN 9780471662587.

TANDON, R. *et al.* - **Definition and description of schizophrenia in the DSM-5.** Schizophrenia research. . ISSN 1573-2509. 150:1 (2013) 3–10. doi: 10.1016/j.schres.2013.05.028.

TANDON, R.; KESHAVAN, M. S.; NASRALLAH, H. A - **Schizophrenia, "just the facts" what we know in 2008. Epidemiology and etiology.** Schizophrenia research. . ISSN 0920-9964. 102:1-3 (2008) 1–18. doi: 10.1016/j.schres.2008.04.011.

TANDON, R.; MAJ, M. - **Nosological status and definition of schizophrenia: Some considerations for DSM-V and ICD-11.** Asian journal of psychiatry. . ISSN 1876-2018. 1:2 (2008) 22–7. doi: 10.1016/j.ajp.2008.10.002.

TANDON, R.; NASRALLAH, H. A; KESHAVAN, M. S. - **Schizophrenia, "just the facts" 4. Clinical features and conceptualization.** Schizophrenia research. . ISSN 0920-9964. 110:1-3 (2009) 1–23. doi: 10.1016/j.schres.2009.03.005.

TATE, S. *et al.* - **Label-free quantitative proteomics trends for protein-protein interactions**. Journal of proteomics. . ISSN 1876-7737. 81:2013) 91–101. doi: 10.1016/j.jprot.2012.10.027.

THOMAS, E. A *et al.* - **Antipsychotic drug treatment alters expression of mRNAs encoding lipid metabolism-related proteins.** Molecular psychiatry. . ISSN 1359-4184. 8:12 (2003) 983–93, 950. doi: 10.1038/sj.mp.4001425.

TIFFIN, P. A; WELSH, P. - **Practitioner Review: Schizophrenia spectrum disorders and the at-risk mental state for psychosis in children and adolescents - evidence-based management approaches.** Journal of child psychology and psychiatry, and allied disciplines. . ISSN 1469-7610. 54:11 (2013) 1155–1175. doi: 10.1111/jcpp.12136.

UNCETA, N. *et al.* - **Enantioselective extraction of (+)-(S)-citalopram and its main metabolites using a tailor-made stir bar chiral imprinted polymer for their LC-ESI-MS/MS quantitation in urine samples.** Talanta. . ISSN 1873-3573. 116:2013) 448–53. doi: 10.1016/j.talanta.2013.07.004.

VERNON, A. C. *et al.* - **Contrasting effects of haloperidol and lithium on rodent brain structure: a magnetic resonance imaging study with postmortem confirmation**. Biological psychiatry. . ISSN 1873-2402. 71:10 (2012) 855–63. doi: 10.1016/j.biopsych.2011.12.004.

VIEWEG, W. V. R. *et al.* - **Citalopram, QTc interval prolongation, and torsade de pointes. How should we apply the recent FDA ruling?** The American journal of medicine. . ISSN 1555-7162. 125:9 (2012) 859–68. doi: 10.1016/j.amjmed.2011.12.002.

VOWINCKEL, J. *et al.* - **The beauty of being (label)-free: sample preparation methods for SWATH-MS and next-generation targeted proteomics.** F1000Research. . ISSN 2046-1402. 2013). doi: 10.12688/f1000research.2-272.v1.

WALTON, N. M. *et al.* - **Detection of an immature dentate gyrus feature in human schizophrenia/bipolar patients.** Translational psychiatry. . ISSN 2158-3188. 2:7 (2012) e135. doi: 10.1038/tp.2012.56.

WANG, M. *et al.* - **Label-free mass spectrometry-based protein quantification technologies in proteomic analysis.** Briefings in functional genomics & proteomics. . ISSN 1477-4062. 7:5 (2008) 329–39. doi: 10.1093/bfgp/eln031.

WENTHUR, C. J.; LINDSLEY, C. W. - **Classics in chemical neuroscience: clozapine.** ACS chemical neuroscience. . ISSN 1948-7193. 4:7 (2013) 1018–25. doi: 10.1021/cn400121z.

WESTON, A.; BROWN, P. R. - HPLC and CE Principles and Practice. 1997) 1–21.

WILLIAMSON, P. C.; ALLMAN, J. M. - **A framework for interpreting functional networks in schizophrenia.** Frontiers in human neuroscience. . ISSN 1662-5161. 6:June (2012) 184. doi: 10.3389/fnhum.2012.00184.

WU, E. Q. *et al.* - **The economic burden of schizophrenia in the United States in 2002.** The Journal of clinical psychiatry. . ISSN 0160-6689. 66:9 (2005) 1122–9.

WYSOCKI, V. H. *et al.* - **Mass spectrometry of peptides and proteins**. Methods (San Diego, Calif.). . ISSN 1046-2023. 35:3 (2005) 211–22. doi: 10.1016/j.ymeth.2004.08.013.

XIE, F.; SMITH, R. D.; SHEN, Y. - **Advanced proteomic liquid chromatography.** Journal of chromatography. A. . ISSN 1873-3778. 1261:2012) 78–90. doi: 10.1016/j.chroma.2012.06.098.

YAMASAKI, N. *et al.* - **Alpha-CaMKII deficiency causes immature dentate gyrus, a novel candidate endophenotype of psychiatric disorders.** Molecular brain. . ISSN 1756-6606. 1:2008) 6. doi: 10.1186/1756-6606-1-6.

YATES, J. R. - **Mass spectrometry from genomics to proteomics Large-scale DNA sequencing has stimulated the development of proteomics by providing a sequence.** 16:2000) 5–8.

ZHANG, F. *et al.* - **Genetic association between schizophrenia and the DISC1 gene in the Scottish population.** American journal of medical genetics. Part B, Neuropsychiatric genetics : the official publication of the International Society of Psychiatric Genetics. . ISSN 1552-4841. 141B:2 (2006) 155–9. doi: 10.1002/ajmg.b.30274.

ZHANG, F. *et al.* - **SWATH™- and iTRAQ-based quantitative proteomic analyses reveal an overexpression and biological relevance of CD109 in advanced NSCLC.** Journal of proteomics. . ISSN 1876-7737. 102:2014) 125–36. doi: 10.1016/j.jprot.2014.03.007.

ZHOU, K. *et al.* - **NMDA receptor hypofunction induces dysfunctions of energy metabolism and semaphorin signaling in rats: a synaptic proteome study.** Schizophrenia bulletin. . ISSN 1745-1701. 38:3 (2012) 579–91. doi: 10.1093/schbul/sbq132.

ZITO, K. - **NMDA Receptor Function and Physiological Modulation. (**2009) 1157–1164.
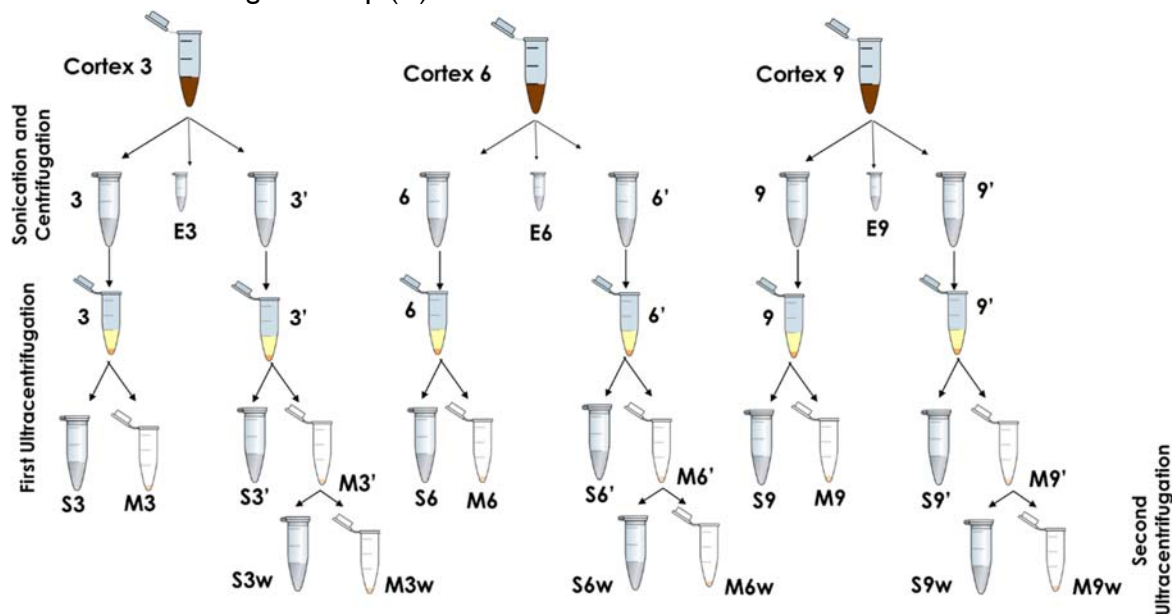
SUPPLEMENTARY DATA

8. SUPPLEMENTARY DATA

8.1. OPTIMIZATION OF THE SUBPROTEOME FRACTIONATION PROCEDURE

The goal in the subproteome fractionation procedure (see Experimental Procedure 4.2) was separate the maximun of membrane proteins from the other proteins simplifing the samples. A second ultracentrifugation step was performed in order to understand if the eficiency of the separation was increased.

In this procedure cortexes from rats that were not injected with any kind of drugs were used, kidly provided by Center for Neuroscience and Cell Biology of Coimbra. The Supplementary figure 8.1 shows a scheme of the subproteome fractionation procedure with a second ultracentrifugation step (w).

Supplementary Figure 8.1: Scheme of the membrane protein enrichment procedure with the second ultracentrifugation step. E3- extract from the cortex 3, obtained before subproteome fractionation, two other aliquots (3 and 3') were subjected to sonication, centrifugation to remove tissue debris, and the supernatant subjected to ultracentrifugation; M3- membrane protein fraction from cortex 3, obtained after the first ultracentrifugation step; M3w- membrane protein fraction from cortex 3, obtained after the second ultracentrifugation step; S3- soluble protein fraction from cortex 3, obtained after the first ultracentrifugation step; S3'- soluble protein fraction from cortex 2, obtained after the first ultracentrifugation step; S3w- soluble protein fraction from cortex 3, obtained after the second ultracentrifugation step. The same code applies to cortex 6 and 9.

Briefly, extract samples were obtained before the first ultracentrifugation step, these contained the membrane and soluble proteins. After the first hour of ultracentrifugation and the removal of supernatants (soluble fraction), it was added 2 mL of Tris 0.05 M to the pellets M3', M6' and M9' and a second ultracentrifugation at 144,000×g for 1 hour at 4°C was performed. The supernatant of these samples were taken again and 1 mL of TEAB 0.5 M was added to all the pellets. The pellets were then dissolved using the ultrasonicator with the 3 mm probe for 30 seconds at 40% to 50% amplitude with 1 second cycles, this step was repeated until total dissolution. Acetone was used for protein precipitation in all samples.

After the subproteome fractionation procedure protein concentration of each samples was obtained by 2-D Quant Kit (see Experimental Procedure 4.4). In the Supplementary table 8.1 the total amount of each sample and the percentage of recovery relative to each extract was calculated.

The amount of protein content in the extract samples was higher than in the other fractions, as expected, once the extract samples contain membrane and soluble proteins. The amount of protein content in the membrane fraction were superior than the soluble samples. Although the amount of membrane proteins in a cell is less than the other proteins, in this procedure cytoskeletal proteins also remain in the membrane fraction, increasing its protein content.

It was not possible to quantify the soluble fractions obtained after the second ultracentrifugation step (S3w, S6w and S9w) as the 2-D Quant Kit has a small range of absorvance values and the absorvance of these samples were outside the calibration curve meaning that the amount of protein in these fractions was very low.

The amount of protein in soluble and membrane fractions obtained after the first ultracentrifugation step (S3, S6, S9, M3, M6 and M9) was higher than the amount of protein in soluble and membrane fractions obtained after the second ultracentrifugation step (S3w, S6w, S9w, M3w, M6w and M9w), consequently with a second ultracentrifugation step the amount of protein that is separated is lower than the amount in the first step of ultracentrifugation.

Supplementary table 8.1: Protein concentration obtained by 2-D Quant Kit. The total amount of each sample and the percentage of recovery relative to each extract were calculated. [] – Concentration of protein.

Sample	[] (mg/mL)	Total amount (mg)	% Recovery	Sample	[] (mg/mL)	Total amount (mg)	% Recovery	Sample	[] (mg/mL)	Total amount (mg)	% Recovery
E3	1.88	37.64		E6	1.93	38.64		E9	1.37	27.37	
S3	7.25	7.25		S6	6.63	6.63		S9	5.19	5.19	
S3'	5.90	5.90	84.21	S6'	3.98	3.98	68.49	S9'	3.97	3.97	83.68
S3w	0.00	0.00		S6w	0.00	0.00		S9w	0.00	0.00	
M3	9.35	9.35		M6	8.79	8.79		M9	7	7.00	
M3w	8.25	8.25		M6w	6.10	6.10		M9w	6.06	6.06	

The percentage of recovery is the sum of the total amount of the samples of each cortex divided by total amount of the respective extract sample. In the cortex 3 and 9 the percentage of recovery was 84.21 and 83.68%, respectively, as expected, once is very difficult to achieve 100% of the protein recovery, since there are losses of protein is each step throughout the procedure. However, in the cortex 6 the percentage of recovery was 68.49%, slightly lower than the others cortexes, in that case the protein amount in the extract sample was similar with the other extracts samples but the protein amount in the membrane and soluble samples were lower, therefore it is probable that in these samples there was a greater loss of protein content.

In order to evaluate the subproteome fractionation procedure a SDS-PAGE followed by Coomassie staining was performed. The samples that were used to this procedure suffered the same subproteome fractionation process described in the Supplementary figure 8.1, the only difference is that the samples came from other rat cortexes specifically cortex 2, 5 and 8. The soluble samples (S5w and S8w) obtained after the second ultracentrifugation step were lost during the procedure. Briefly, samples (20 μg of total protein) were denatured with the addition of Laemmli Sample Buffer 6× to a 1× final concentration and boiled at 95°C for 5 minutes.

Afterwards the samples were electrophoretically separated in a 1.25 mm gel (12.5%) of SDS-polyacrylamide gel using a Mini-PROTEAN Tetra Electrophoresis System. To evaluate the SDS-PAGE profile the gel was stained with Colloidal Coomassie Blue (see Experimental Procedure 4.6). After successive washes with distilled water the gel was scanned to be visualized (Supplementary figure 8.2).
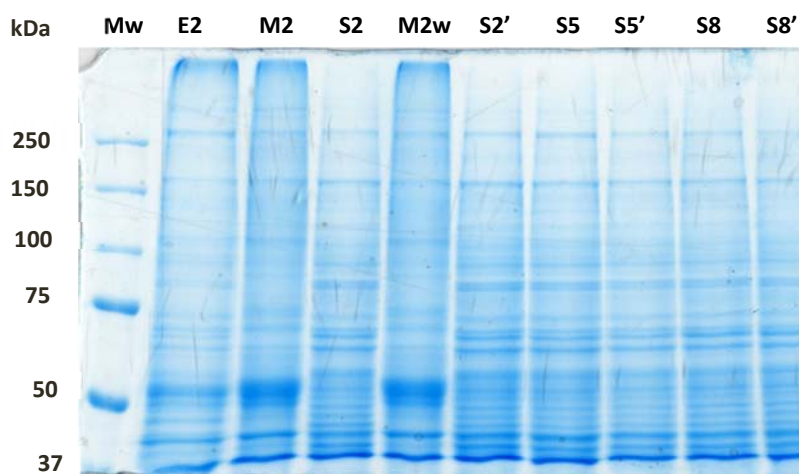
Supplementary Figure 8.2: Analysis of protein profile after membrane enrichment procedure by SDS-PAGE. SDS-PAGE followed by Coomassie staining. MW- molecular weight marker (BioRad). See supplementary figure 8.1 caption for further details.

In the upper part of the gel (Supplementary figure 8.2), it is possible to visualize that the profile of the membrane samples was very similar between them, and the same occurred with the soluble samples. As expected, the profile of the membrane, soluble and extract samples was different, an example is the intense band in the 50 kDa that only appears in the membrane fractions. It was possible to observe on top of the gel a deeper color in the membrane fractions than in the extract and soluble fractions, which means that there were more proteins with a high molecular weight in this samples (which are usually associated to membrane proteins). On the contrary a deeper color was observed in the bottom of the gel in the soluble fractions, so there were more proteins with a low molecular weight in these samples (possibility soluble proteins). The intense band (50 kDa) in the membrane fractions, but less intense in the extract sample, means that there was an enrichment of proteins in these samples. The sample is observed with the intense bands between (37 and 50 kDa) in the soluble fractions that were also less intense in the extract fraction, and in the membrane samples did not exist. It is possible to conclude that there was an enrichment of the proteins in the fractions comparing with the extract sample that were not subjected to a subproteome fractionation.

8.1.1. Evaluation of the subproteome fractionation procedure

In order to evaluate the subproteome fractionation procedure a comparison of the number of shared or unique proteins from samples that were identified by mass spectrometry was performed using a Venn diagram Supplementary figure 8.3, (Experimental procedure 4.10). The procedure for gel digestion was described in Experimental Procedure 4.6. The IDA conditions for gel digestion were similar to Experimental Procedure 4.8 except the parameters for search: Uniprot_SwissProt database for rat (updated in February 2014); trypsin digestion; acrylamide for gel digestion, as cysteine alkylating reagent.

The comparison between all gel digestion samples revealed that 313 proteins were shared by all the samples. The number of unique proteins in the membrane and soluble samples obtained after a first ultracentrifugation (M3 and S3) were higher relative to the rest of the samples.

As expected, the number of unique proteins in the extract sample was only 34, much lower than the unique proteins in the M3 and S3 samples, meaning that there is an enrichment of proteins in this two samples after the subproteome procedure. A very low number of unique proteins was identified in the samples that were obtained after a second ultracentrifugation step (M3w and S3w).

Total numer: 1540

Supplementary Figure 8.3: Venn diagram illustrating the number of shared or unique proteins from gel digestion that were identified by Mass spectrometry for all samples. There are 313 common proteins between all samples and the combined protein number is 1540.

These results, as well as the time required to perform a second ultracentrifugation step, are sufficient to consider that this step does not make the procedure more efficient and consequently was not applied to the final samples.

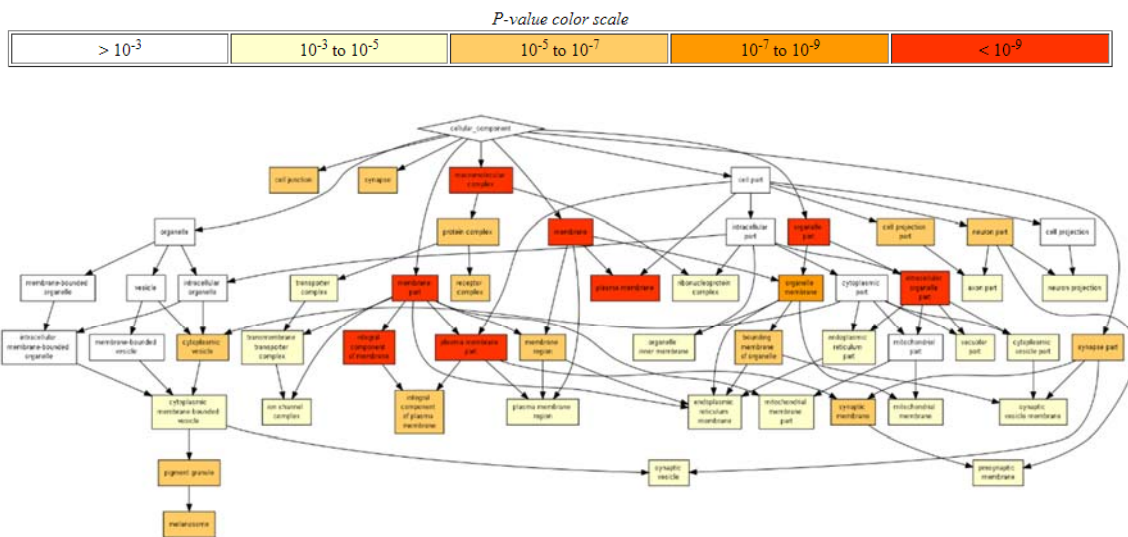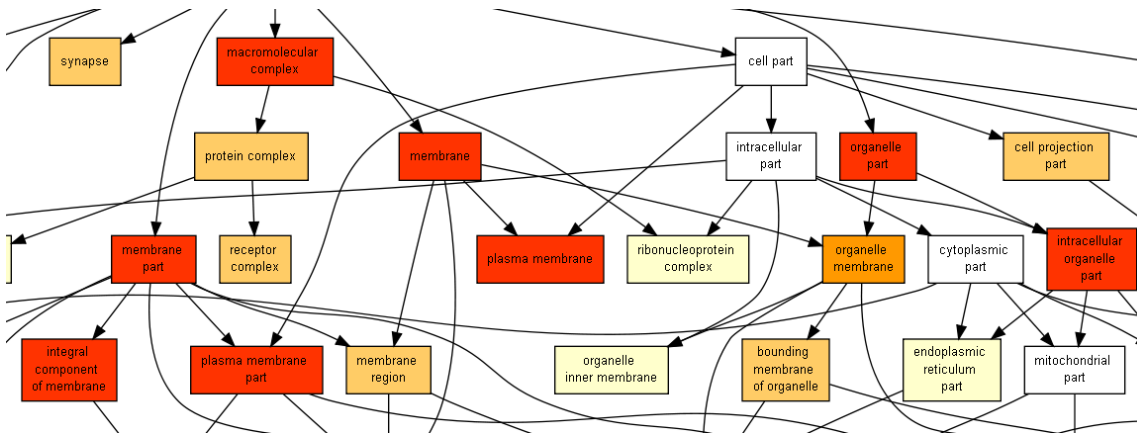In order to confirm if the membrane enrichment mentioned above was accomplish, a GO enrichment analysis of the identified proteins in gel digestion samples (E3, M3 and S3), respectively was performed (Supplementary figure 8.4). In this analyze two ranked lists were used i) the proteins from each sample against ii) all proteins that were identified in this procedure.

The GO enrichment analysis in the extract sample (Supplementary figure 8.4, A) indicates that the proteins statistically significant ($p < 10^{-9}$) in this sample belong to the extracellular region of the cell (red boxes) also cytoplasm and organelle protein present some statistical significance ($p < 10^{-5}$ to 10^{-9}) (orange and yellow boxes) in these samples. In the membrane fraction (B) the analysis indicates that the proteins statistically significant (red boxes in C) belong to the plasma membrane in the cell, while in the soluble fraction (D) the protein belongs to the cytoplasm, cytosol, nucleus and extracellular region of the cell (red boxes), as expected.

A   **E3**

B   **M3**

C   **M3**

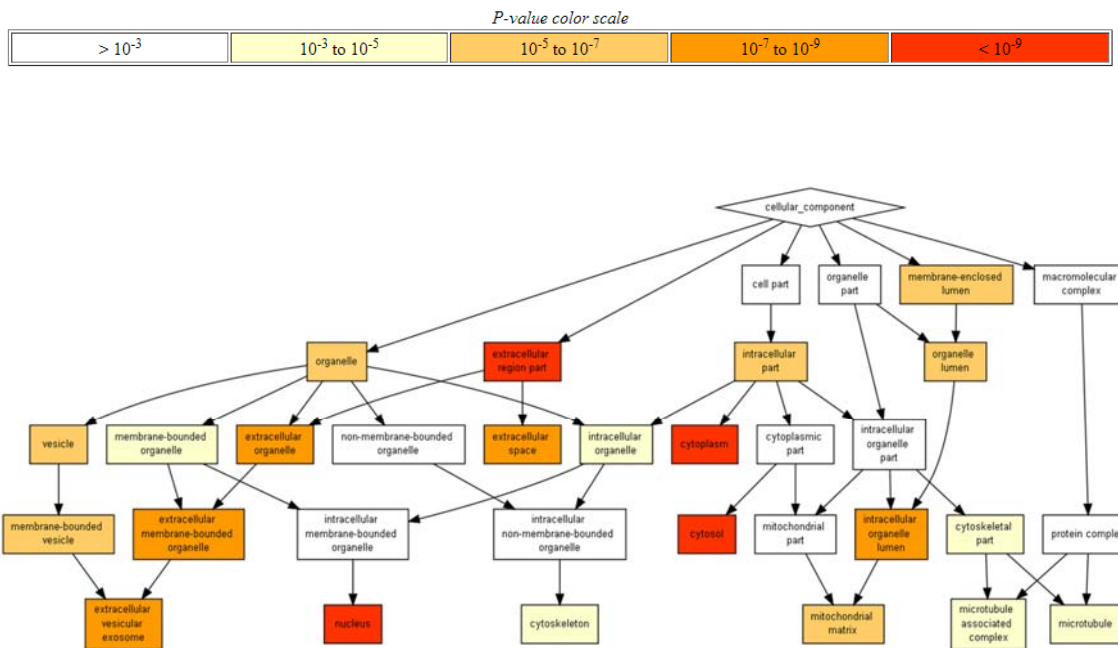**D**   **S3**

Supplementary Figure 8.4: Evaluation of the membrane enrichment procedure. Gene Ontology (GO) Enrichment of the identified proteins of the gel digested samples. A- proteins identified in the extract sample from cortex 3 (E3) against all the proteins that were identified; **B-** proteins identified in the membrane sample from cortex 3 (M3) against all the proteins that were identified **C-** zoom view of the red boxes of the M3 sample; **D-** proteins identified in the soluble sample from cortex 3 (S3) against all the proteins that were identified.

This results indicated that in the extract sample there was not an enrichment, as expected, once this sample did not suffered a subproteome fractionation, but in the membrane fraction an enrichment in membrane proteins was observed, as well as, an enrichment in other proteins mostly from cytoplasm was observed in the soluble fraction, as expected.

These results serve as proof-of-concept for membrane protein enrichment procedure, in the membrane fraction, and its depletion from the soluble fraction.

8.2. SOLVENTS FOR THE PROTEIN PRECIPITATION

In order to determine which solvent would be the best to precipitate the soluble and membrane proteins in the fractions, three different solvents were used namely: acetone (6 parts), methanol (4 parts) and methanol/chloroform (1.5 parts of MeOH and 3 parts of CHCl3).

The samples used to perform this analysis were processed using the same protocol as previous samples (see Supplementary Subchapter 8.1), but in the present procedure the three organic solvents were used to precipitate the proteins. A liquid digestion were performed to the samples (once this procedure is shorter) and the proteins were identified by mass spectrometry. In liquid digestion, samples were resuspended in a TEAB 0.5 M solution to a final volume of 45 µL and denatured using a sonicator with cuphorn during 1 min at 20% amplitude with 1 second cycles, after the addition of 4 µL Tris(2-carboxyethyl)phosphine (TCEP) 50 mM, a reducing agent. To promote the cysteine alkylation was added 2 µL of S-methyl methanethiosulfonate (MMTS) 200 mM were added and the samples were incubated at room temperature during 10 minutes. The reaction was quenched by the addition of TEAB at 0.5 M and Trypsin, at 0.5 µg/µL in TEAB 0.5 M, was added to a final ratio of 1:20 (w:w). The digestion was held at 37°C during 16 hours. After this period 2 µL of formic acid 100% were added to stop the trypsin's activity and the samples containing the peptides were concentrated on the Concentrator Plus at 60°C. The IDA conditions for liquid digestion were similar to Experimental Procedure 4.8 except the parameters for search: Uniprot_SwissProt database for rat (updated in February 2014); trypsin digestion; MMTS as cysteine alkylating reagent.

The total number of identified proteins in each sample is present in the Supplementary figure 8.5.
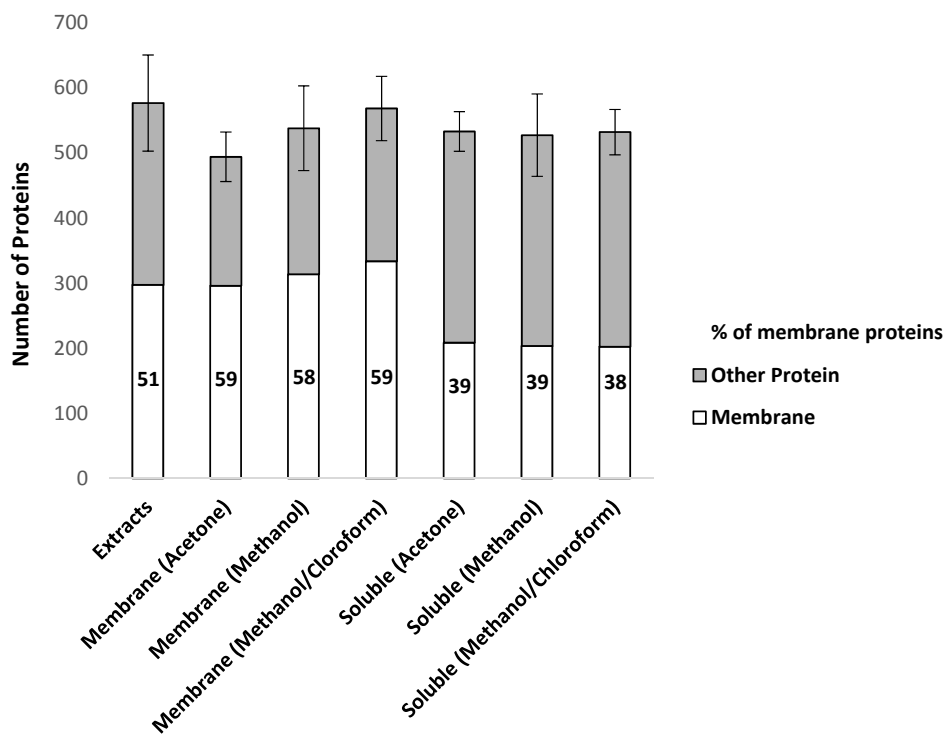
Supplementary Figure 8.5: Total number of proteins identified by Mass Spectrometry. Extracts-Extracts from cortex A, B and C; Membrane (Acetone)/ (Methanol)/ (Methanol/Chloroform) - Membrane protein fractions from cortex A, B and C precipitated with acetone, methanol and methanol/chloroform, respectively. Soluble (Acetone)/ (Methanol)/ (Methanol/Chloroform) **-** soluble protein fractions from cortex A, B and C precipitated with acetone, methanol and methanol/chloroform. The results represent mean values ± SEM.

As it can be seen, the number of proteins identified was approximately the same in each sample. In the membrane fraction where acetone was used the number of proteins identified was less than the other membrane fractions, and the membrane fractions where methanol were used also had less proteins identified than in the case of membrane fractions where it was used methanol/chloroform. The percentage of membrane proteins that were identified in the membrane fractions was similar (approximately 59%) for the three organic solvents. Although the results for samples that were processed using methanol/chloroform were slightly better, the procedure with this solvent was more laborious and prone more variability. The samples presented a phase separation disc (membrane fraction) instead of a rigid pellet, which difficult the removal of the soluble fraction and the elimination of the solvent, therefore methanol is the solvent suggested to be used in the processing of membrane fractions.

In the soluble samples the difference is even smaller, the number of the identified protein and the percentage of the membrane proteins is very similar for the three organic solvents.

Consequently, for the soluble fraction the solvent acetone was chosen to be used in the final samples, once it presents a smaller standard deviation.

8.3. OPTIMIZATION OF THE WESTERN BLOTS FOR THE EVALUATION OF THE SUBPROTEOME FRACTIONATION PROCEDURE

8.3.1. PSD-95 and GAPDH as protein markers

PSD-95 is a synaptic scaffolding protein with multiple protein–protein interaction domains that is enriched in the postsynaptic density, an electron-dense specialization of postsynaptic membrane that contains macro-molecular protein complexes. PSD-95 has diverse synaptic functions. One such function is to interact with membrane proteins and regulate their synaptic localization. PSD-95 seems to stabilize interacting membrane proteins at synapses by suppressing their lateral diffusion or internalization (Han, K. and Kim, 2008).

GAPDH is an enzyme with metabolic function, in particular in glycolysis process, thus serves to break down glucose for energy and carbon molecules (Krishnan *et al.*, 2010). This protein is commonly used as a cytoplasmic marker in proof-of-concept of subproteome fractionations procedures (Murray, Barrett and Eyk, 2009), cell fractionation kit (Abcam®) and nuclear and cytoplasmic extraction reagents (Thermo Fisher Scientific).

Therefore, PSD-95 and GAPDH were tested as membrane and soluble markers, respectively, for the evaluation of the subproteome fractionation procedure.

The sample "N" was used for normalization, these contained 10 µg of protein from all samples that were used in SDS-PAGE procedure. The samples used were the same used in the procedure above (Supplementary Data 8.1).

The samples (30 µg of protein) were denatured with the addition of Laemmli Sample Buffer 6× [0.35M Tris-HCl, pH 6.8 with 0.4% SDS (v/v), 30% glycerol (v/v), 10% SDS (w/v), 9.3% DTT (w/v) and 0.01% bromophenol blue (w/v)] to a 1× final concentration and boiled at 95°C for 5 minutes. Samples were electrophoretically separated on a 10% SDS-polyacrylamide gel using a Mini-PROTEAN Tetra Electrophoresis System. After the transference to the membrane (see Experimental Procedure 5.1.2) these were incubated with the antibodies goat Anti-PSD95 C-20 (1:500) [Santa Cruz Biotechnology, Inc. (sc-8575)], mouse Anti-GAPDH G-9 (1:500) [Santa Cruz Biotechnology, Inc. (sc-365062)] and their respective secondary antibodies. The molecular weight of PSD-95 and GAPDH antibodies were 95 kDa and 37 kDa, respectively. The volume applied in the soluble samples S3w, S6w

and S9w were the maximum possible, once it was not possible to determine the protein concentration on these samples (Supplementary Data 8.1, table 8.1).

As expected, intense bands could be observed in all membrane and extract samples, as well as, in the N sample, for PDD-95 detection (figure 8.6), while bands with less intensity were detected in soluble samples. The results for GAPDH were not expected, since bands were observed for all the samples, in that case would be expected bands only in the soluble, extract and N samples, whereas the GAPDH is used here as a soluble marker.
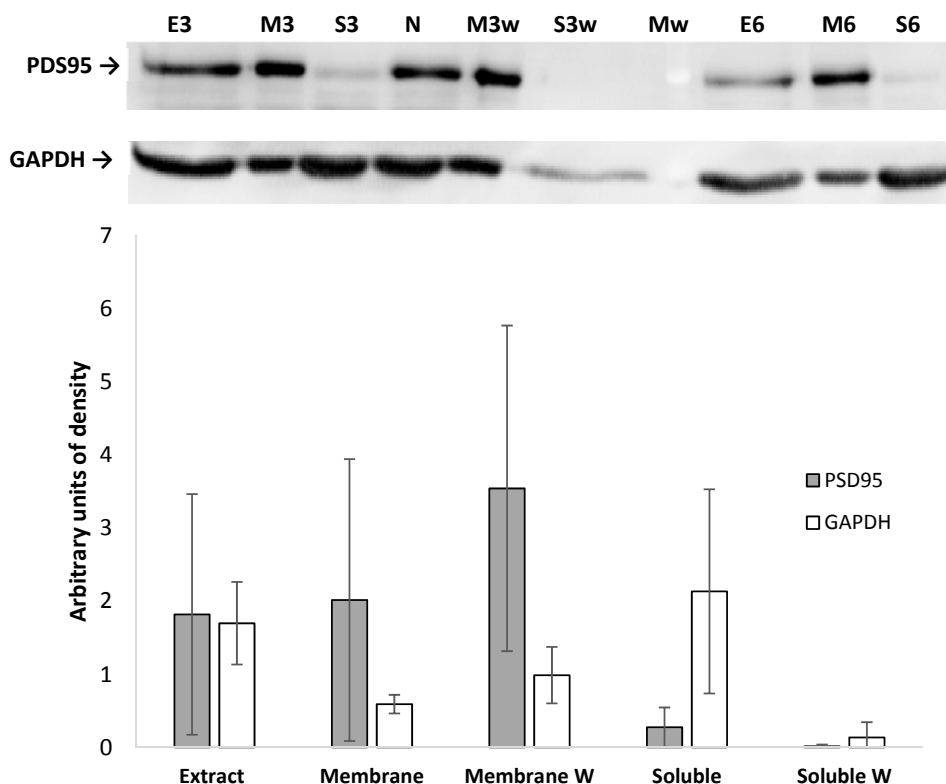
Supplementary Figure 8.6: Evaluation of the subproteome fractions procedure. Imunodetection of PSD95 as a membrane marker and GAPDH as a soluble marker. Extracts- extracts from the cortex 3, 6 and 9; Membrane- membrane protein fractions from cortex 3, 6 and 9, obtained after the first ultracentrifugation step; Membrane w- membrane protein fractions from cortex 3, 6 and 9, obtained after the second ultracentrifugation step;   Soluble- soluble protein fractions from cortex 3, 6 and 9, obtained after the first ultracentrifugation step; Soluble w- soluble protein fractions from cortex 3, 6 and 9, obtained after the second ultracentrifugation step. The results represent mean values ± SEM.

The PSD-95 detection (grey bars) was higher for membrane samples (both, membrane and membrane w) than soluble samples (soluble and soluble w). In the extract samples the detection of PSD-95 was higher than the soluble samples but less comparing with the membrane samples, as expected. These results indicate that the PSD-95 could be found in

higher quantity in the membrane samples, as expected, but their higher standard deviation indicates that the data were spread over a range of values, lowering the confidence in these data. These results combined with the fact that PDS-95 protein interacts with membrane proteins but is not a real membrane protein decreases the confidence on this protein as a membrane marker.

Although the detection of GAPDH was higher in the soluble samples (white bars), the detection of GAPDH in all samples, mainly in membrane samples indicated that this protein was not a good soluble marker for the evaluation of this procedure. In the literature GAPDH is mentioned several times as a cytoplasmic protein that innerves in metabolic processes but some studies showed that GAPDH could be found as a binding protein on the plasma membrane (Krishnan *et al.*, 2010; Laschet *et al.*, 2004), which could justify the results obtained in this study. Antibodies for the detection of EGFR (epidermal growth factor receptor) and Shank 3 (SH3 and multiple ankyrin repeat domains 3) were tested (membrane and soluble markers, respectively) but the results were not in accordance to their use as fraction markers (data not shown).

8.3.2. NMDA as a membrane marker

The NMDA protein was used as a membrane marker to evaluate the subproteome fractionation procedure, but the results of western blot showed that the bands were in the area of the membrane correspondent to the stacking gel, it means that this protein could not enter in the running gel to be separated and the analysis was not possible (data not shown). These results indicate that the NMDA protein had not been correctly denatured, probably due to its complex structure, as it was previously reported (Results and Discussion 5.2).

The denatured conditions applied to the samples before, were used to denatured the majority of the proteins in the lab and until this moment with excellent results, but in that case using Laemmli Sample Buffer 6× [0.35M Tris-HCl, pH 6.8 with 0.4% SDS (v/v), 30% glycerol (v/v), 10% SDS (w/v), 9.3% DTT (w/v) and 0.01% bromophenol blue (w/v)] to a 1× final concentration and at 95°C during 5 minutes did not permit a correct denaturation of the NMDA receptor in the samples, consequently there was the need to optimize this procedure.

Denaturation is a process in which the protein lose the quaternary, tertiary and secondary structure which is present in their native state. For detection and analysis of the protein in a western blot procedure, firstly the proteins are denatured to be separated by gel electrophoresis. The application of the external stress or compounds as acid or base,

concentrated inorganic salt, organic solvent, radiation or heat leads to denaturation of proteins. Denatured proteins can exhibit a wide range of characteristics, from loss of solubility to communal aggregation. Therefore, the temperature condition of 95°C during 5 minutes could cause the denaturation of the NMDA protein in the samples but due its complex structure the subunits were aggregated, which justify the bands in the staking gel region.

To try to overcome this, a 60°C temperature during 10 minutes was tested, such that the denaturation occurs slowly and to avoid the aggregation of the NMDA protein in the samples. Therefore, extract from membrane and soluble fractions (30 µg of protein) were used (Supplementary Subchapter 8.1). The 1× Laemmli Sample Buffer was used to each sample and the temperatures of 60°C during 10 minutes or 95°C for 5 minutes were applied to different samples. The electrophoretic separation was performed on a 10% SDS-polyacrylamide gel using a Mini-PROTEAN Tetra Electrophoresis System. The antibodies used for NMDAR detection were described in Experimental Procedure 4.5.2.

As it can be seen in figure 8.7 the detection of the NMDAR was observed only for the extract and membrane samples, for both temperatures conditions, as expected, but the bands in these samples were not clear. A smear can be seen in the stacking gel, which was not supposed, and bands in the molecular weight (115 kDa) correspondent of NMDA protein. These results indicate that the temperature decrease alone is not sufficient to denature properly the NMDA protein in these samples.
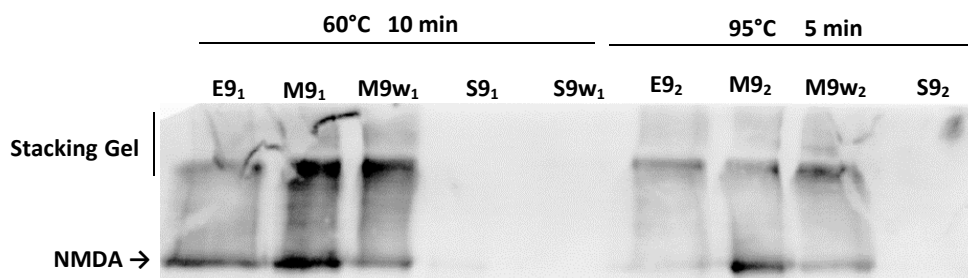
Supplementary Figure 8.7: Immunodetection of the NMDAR as a membrane marker. E9- extract from the cortex 9, obtained before subproteome fractionation/membrane enrichment procedure, M9-membrane protein fraction from cortex 9, obtained after the first ultracentrifugation step; M9w- membrane protein fraction from cortex 9, obtained after the second ultracentrifugation step; S9- soluble protein fraction from cortex 9, obtained after the first ultracentrifugation step; S9w- soluble protein fraction from cortex 9, obtained after the second ultracentrifugation step. The 1 samples were denatured at 60°C during 10min and the 2 samples were denatured at 95°C during 5 min.

Therefore, 37°C of temperature during 30 minutes also were tested and the reagents concentration on the Laemmli buffer were changed. This time, only the membrane samples

were used, 30 µg of protein of M9 sample denatured with different conditions, as could be seen in Supplementary figure 8.8. The sample $M9_1$ was denatured at 37°C during 30 minutes with SDS concentration increased to 12% and 4 M of NaCl added in the buffer 6×, in the $M9_2$ sample the conditions were the same except this time NaCl was not added, in $M9_3$ and $M9_4$ samples the temperature used was 60°C during 10 minutes, with SDS increase to 12% and NaCl addition in the $M9_3$ and without the addition of NaCl in the $M9_4$, lastly in the $M9_5$ and $M9_6$ samples, urea 6 M were added in the buffer 6× and 60°C during 10 minutes of temperature was tested for the $M9_5$ sample. In this procedure also the percentage of acrylamide in the gel were lower (7.5%) to help the NMDA protein to enter and to run through the gel.

In the figure 8.8, the bands for 115 kDa could be observed for all samples in the different denaturation conditions. The bands in the stacking gel region that were observed in previous results were not observed here. And the bands in the samples there were denatured with the increase of the SDS concentration and the addition of the NaCl present a better intensity for both temperatures than the bands of the samples that were denatured only with a SDS concentration increase.

SDS is an anionic detergent that denatures secondary and non–disulfide–linked tertiary structures, and additionally applies a negative charge to each protein in proportion to its mass, the increase of its concentration was essential to obtain a better denaturation of the NMDA protein. Proteins are biomolecules which occur in physiological environment with a delicate balance of salt concentrations. Too high or too low salt conditions can lead to precipitation of a protein, suggesting its denaturation, so NaCl addition was also essential to help the denaturation of the NMDAR in the samples. Urea is used in high concentrations (> 6 M) to denature proteins. It is a chaotropic agent that destroy is the tertiary and secondary structure of proteins by influencing hydrophobic effects hydrogen bonds and others. Nonetheless, in this procedure the samples that were denatured with urea did not present bands as intense as the bands observed in the rest of the conditions.

As in the $M9_3$ sample the smearing of the signal in the lane was lower than the $M9_1$ samples and with 60°C it is possible save to time in the procedure, the denaturation conditions that were applied on the $M9_3$ samples showed better results for the NMDAR detection.
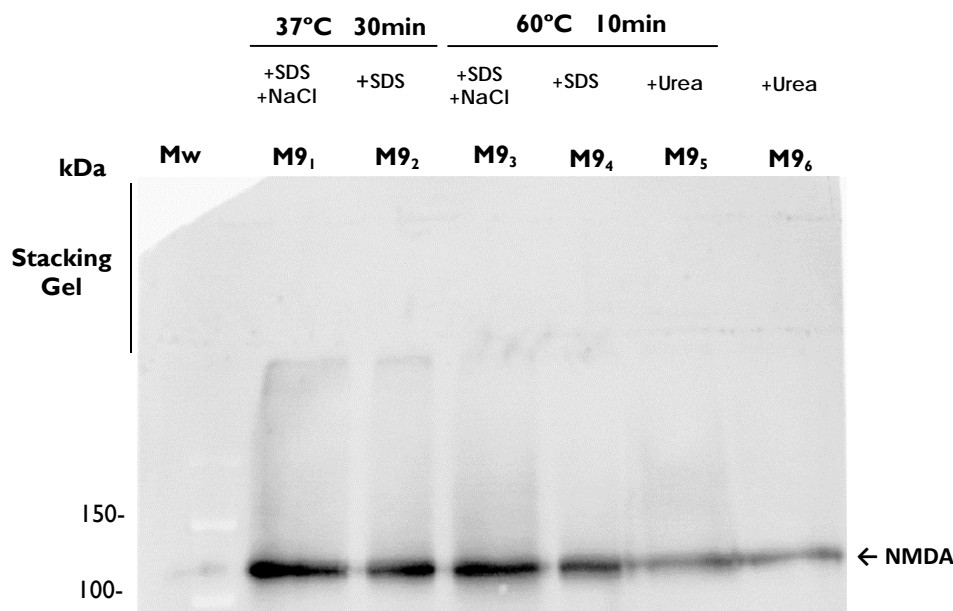
Supplementary Figure 8.8: Immunodetection of the NMDAR as a membrane marker. Mw- molecular weight marker; M9$_1$- Membrane protein fraction, denatured at 37°C for 30 min with NaCl and SDS; M9$_2$- Membrane protein fraction, denatured at 37°C for 30 min with SDS; M9$_3$- Membrane protein fraction, denatured at 60°C for 10 min with SDS and NaCl; M9$_4$- Membrane protein fraction, denatured at 60°C for 30 min with SDS; M9$_5$- Membrane protein fraction, denatured at 60°C for 10 min with urea; M9- Membrane protein fraction, denatured with urea.

The next step was to test other samples (extract, membrane and soluble) with the denaturation conditions previously chosen, so samples (30 µg of protein) that were process as the samples in Supplementary Subchapter 8.1 were used. The samples "N" was used as normalization of the samples between membranes and GFP protein was added to each sample to the normalization of the samples between each well, to account for pipetting errors. The denature conditions applied were the following: Laemmli Sample Buffer 6× [0.35M Tris-HCl, pH 6.8 with 0.4% SDS (v/v), 30% glycerol (v/v), 12% SDS (w/v), 9.3% DTT (w/v), 0.01% bromophenol blue (w/v) and 1.2 M NaCl] to a 1× final concentration, 60°C of temperature during 10 min (Supplementary figure 8.9).

Despite the presence of a labeling signal with the bands, intense bands were observed only in the extract, N and membrane samples, while in the soluble fractions very weak bands were observed, as expected. However, for GFP detection several nonspecific bands were observed, meaning that this new denaturation conditions was not indicated for the GFP protein.
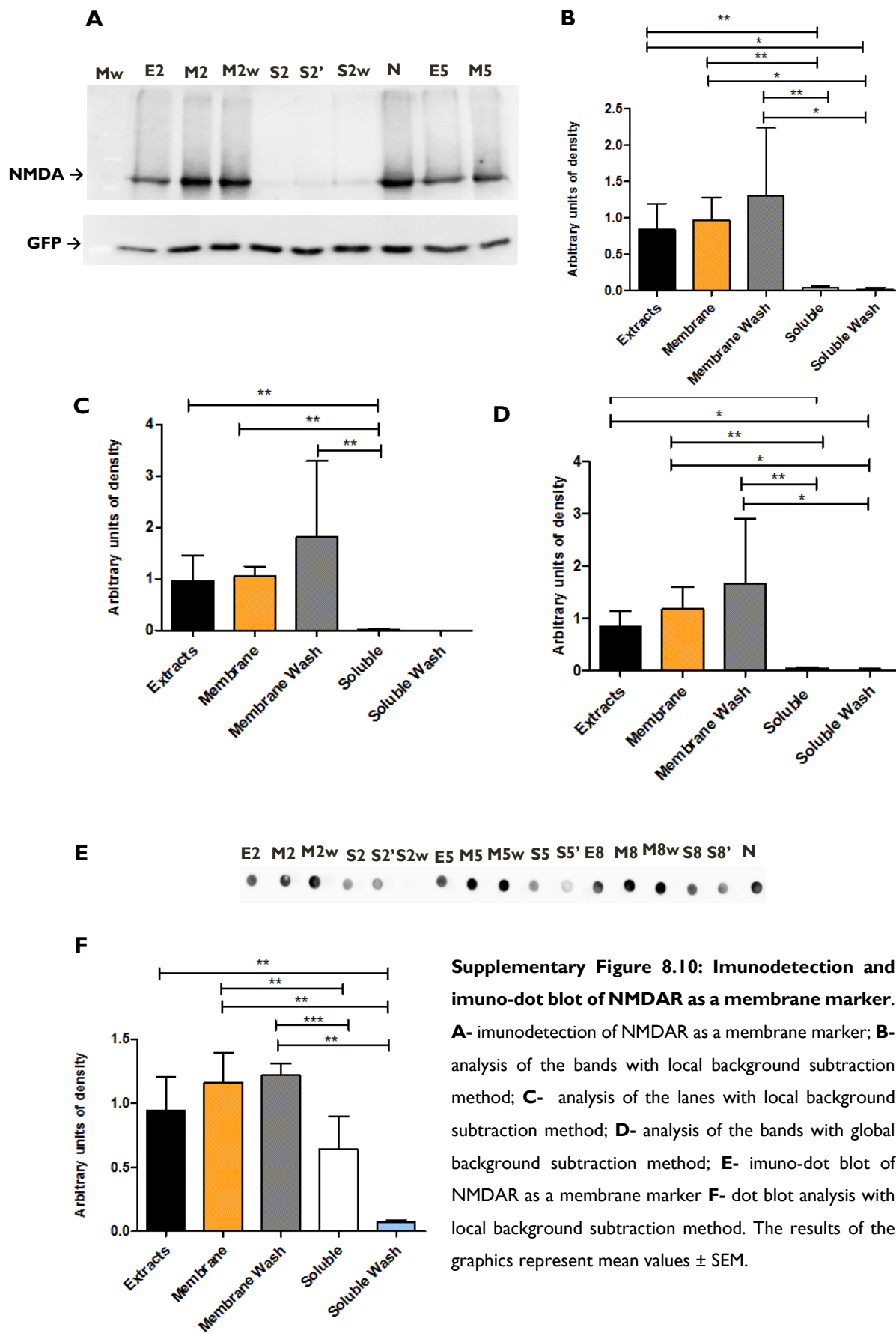
Supplementary Figure 8.9: Immunodetection of the NMDA as a membrane marker with GFP protein as a standard normalization. For more details see Supplementary figure 8.2.

Thus, the samples (30 μg of protein) were denatured with the denaturation condition described above and GFP protein was denatured separately with Laemmli Sample Buffer 6× [0.35M Tris-HCl, pH 6.8 with 0.4% SDS (v/v), 30% glycerol (v/v), 10% SDS (w/v), 9.3% DTT (w/v) and 0.01% bromophenol blue (w/v)] to a 1× final concentration and boiled at 95°C for 5 minutes. After this, 0.84 ng of GFP protein was added to each sample and the SDS-PAGE procedure was performed in a 7.5% acrylamide gel. The western blot detection was performed as described in Experimental Procedure 4.5.2 for NMDA detection. Firstly, the analysis of the bands and the lanes with local background subtraction method were performed, as well as, the bands with global background, using Quantity One software (Supplementary figure 8.10).

Once the smearing of the signal in the lane continued to exist, a dot blot was performed using the same samples (Supplementary figure 8.10, E) and compared with different band data processing (Supplementary figure 8.10). Briefly, samples (2 μg of protein) were added directly to a pre-activated, with methanol, PVDF membranes. The membranes were blocked for 1 hour at room temperature with 5% (w/v) skimmed milk powder dissolved in PBS with 0.1% (v/v) Tween-20. Then the membranes were incubated with primary goat antibodies against Anti-NMDAR C-20 (1:500) in 5% (w/v) skimmed milk powder dissolved in PBS-T, overnight at 4°C followed by 1 hour at RT. The antibodies incubation and detection was performed with the same conditions as the western blot procedure mentioned in Experimental Procedure 4.5.2.

A

B

C

D

E

F

Supplementary Figure 8.10: Imunodetection and imuno-dot blot of NMDAR as a membrane marker. **A-** imunodetection of NMDAR as a membrane marker; **B-** analysis of the bands with local background subtraction method; **C-** analysis of the lanes with local background subtraction method; **D-** analysis of the bands with global background subtraction method; **E-** imuno-dot blot of NMDAR as a membrane marker **F-** dot blot analysis with local background subtraction method. The results of the graphics represent mean values ± SEM.

As expected, intense bands are observed for the extract, membrane and N samples, while less intense bands could be seen in the soluble samples, also, only one band is observed for each sample in GFP detection (Supplementary figure 8.10, A). The graphic B and C represent bands and lane analysis, respectively, with a local background subtraction method (i.e., the final density in the selected area (bands or lanes) were obtained by subtraction of the intensity in this selected area by the intensity in the surrounding region) while in the Supplementary figure 8.10 D the bands were analyzed with global background subtraction method (i.e., a clean and small region of the membrane background was selected and used to the comparison of the bands intensity). The bands were analyzed with global background because the smearing of the signal in the lanes could influence the results of the analysis with local background, thus the selection of a clean region of the membrane could be better for the results. Besides the analysis of the bands, it was also performed the analysis of the lanes because of the same reasons mentioned above, the labeling of the signal in lanes could influence the analysis of the bands.

As can be seen in the three analysis the NMDAR detection (Supplementary figure 8.10 A-D) were higher in membrane and extract samples than the soluble fractions and the intensity was higher in membrane samples comparing with the extracts samples, as expected. The profile of the three analysis was similar, except in the analysis of the lanes (Supplementary figure 8.10 C), where the density of the soluble fractions that were obtained after the second ultracentrifugation step (soluble wash) was 0 (Supplementary table 8.2), and therefore it did not have any statistical difference between the soluble fractions and the other samples. This results indicated that the smearing did not influence the results, and it won't be needed to perform an analysis with a global background.

The dot blot procedure does not require a separation in a gel and therefore to the NMDAR complications referred above did not exist. Intense dots were observed in the membrane samples (Supplementary figure 8.10, E) comparing with the other samples, and the intensity of the NMDAR was higher in the extracts and membrane samples (black, orange and grey bars) comparing with soluble samples (white and blue bars) (Supplementary figure 8.10, F).

In the Supplementary table 8.2 the results for the extracts samples for the 4 analysis (0.84, 0.96, 0.84 and 0.94), as well as, the average for the membrane samples (0.96, 1.05, 1.18 and 1.16) were similar between the samples. In the membrane wash samples the average for the lanes and bands with global background analysis was superior (1.81 and 1.66, respectively) than the bands and dot blot analysis (1.30 and 1.22, respectively). The average of the soluble

samples in the western blot analysis were similar for soluble samples (0.04, 0.01 and 0.05) and 0.02 for soluble wash samples, while the average for the dot blot analysis was superior (0.64 for soluble and 0.07 for soluble wash samples).

However the standards deviations and the percentage of coefficient of variation were much lower for all samples in the dot blot analysis comparing with the other three analysis.

The results indicate that although the dot blot analysis present best standard deviations and percentage of CV thereby making them more reliable results, a higher detection of NMDAR in soluble samples comparing with the other analysis could lead to the conclusion that the separation of membrane and soluble samples in subproteome fractionation procedure were not efficient, which was not in line with the results by western blots and the mass-spectrometry analysis (Supplementary Data 8.1.1). This increase in NMDA detection of soluble samples for dot blot analysis may be due to the fact that a high protein amount (2 µg of protein) were used which could lead to a signal saturation in the membrane samples.

**Supplementary table 8.2: Imunodetection and imuno-dot blot of NMDAR as a membrane marker**. The average, standard deviation and the percentage of coefficient of variation were calculated using GraphPad software for the samples in different analysis (lanes and bands analysis with local background subtraction method, bands analysis with global background subtraction method and imuno-dot blot analysis).

Samples	Mean	SD	%CV	
Extracts	0.84	0.36	42.82	Western Blot (Bands)
Membrane	0.96	0.32	33.40	
Membrane Wash	1.30	0.93	71.86	
Soluble	0.04	0.02	59.21	
Soluble Wash	0.02	0.03	125.32	
Extracts	0.96	0.49	51.31	Western Blot (Lanes)
Membrane	1.05	0.20	18.65	
Membrane Wash	1.81	1.48	81.57	
Soluble	0.01	0.02	150.07	
Soluble Wash	0.00	0.00	0.00	
Extracts	0.84	0.30	35.68	Western Blot (Bands with Global Background)
Membrane	1.18	0.43	36.06	
Membrane Wash	1.66	1.25	75.21	
Soluble	0.05	0.02	48.08	
Soluble Wash	0.02	0.03	173.21	
Extracts	0.94	0.26	27.97	Dot Blot
Membrane	1.16	0.24	20.39	
Membrane Wash	1.22	0.10	7.85	
Soluble	0.64	0.25	39.45	
Soluble Wash	0.07	0.02	23.52	

8.4. COMPARISON OF LIQUID AND IN-GEL DIGESTIONS

To cleave the proteins in peptides, liquid and gel digestions were performed, in order to evaluate with which one more proteins would be identified by mass spectrometry. The samples (Supplementary subchapter 8.1) (30 μg of protein) were used for both digestions, except in the S3w, S6w and S9w samples, once a protein quantification was not possible, that was used the maximum volume to make sure that the amount of protein was sufficient. The procedure for gel digestion was described before in Supplementary Subchapter 8.1.1 and for liquid digestion in Supplementary Subchapter 8.1.2.

The Supplementary figure 8.11 represents the total amount of proteins identified by mass spectrometry for liquid and gel digestions, as well as, the percentage of membrane proteins in each sample.
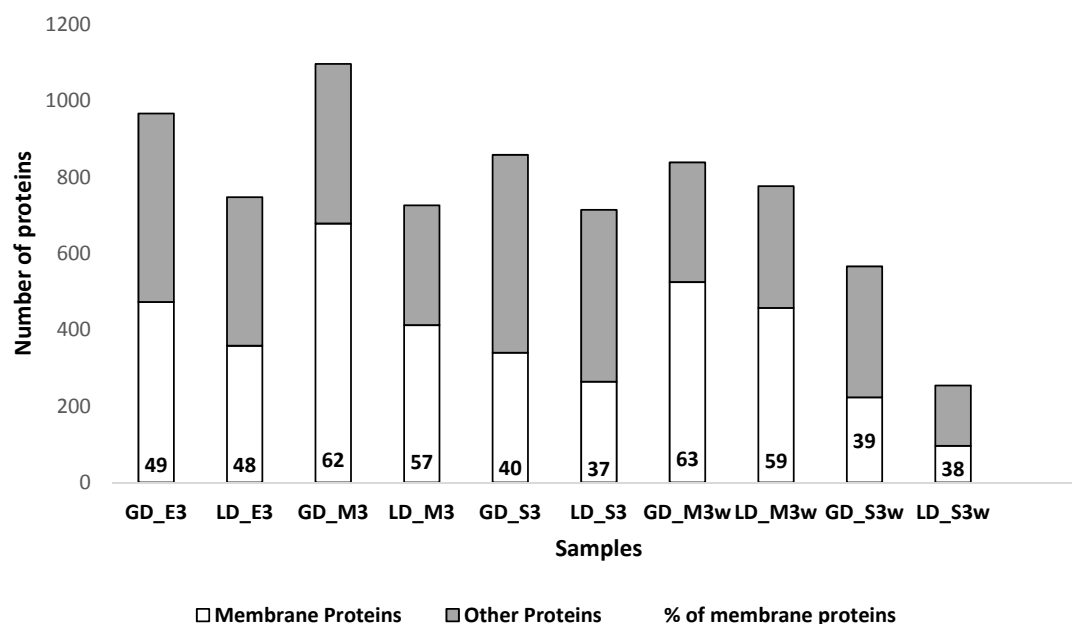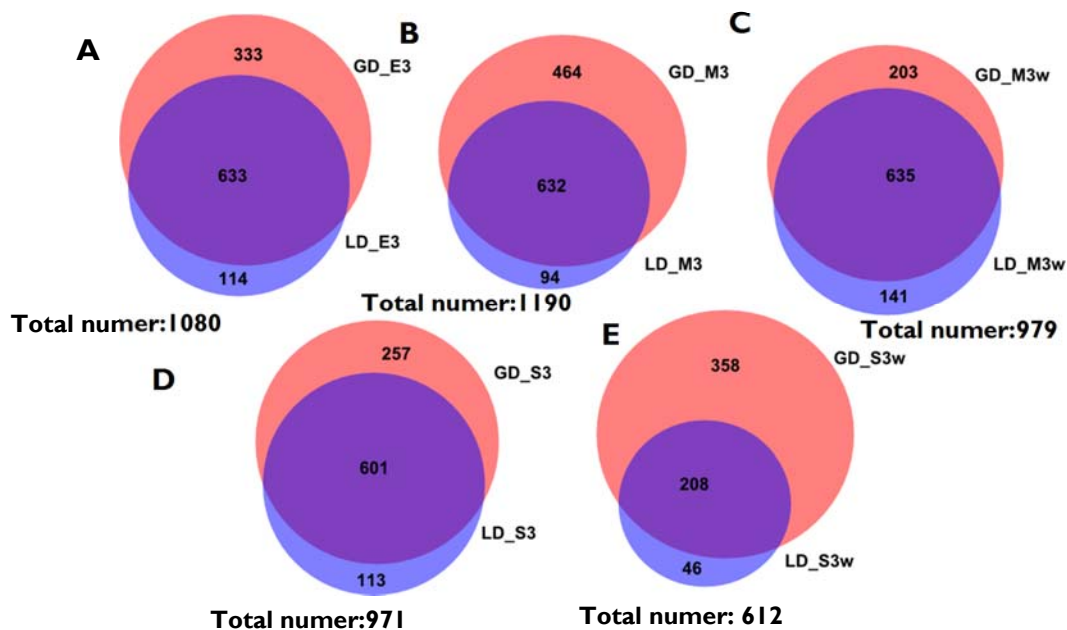

Supplementary Figure 8.11: Total number of proteins identified by Mass Spectrometry. Samples were digested either using the gel digestion (GD) or the liquid digestion (LD) protocol. E3- extract from cortex 3, obtained before the subproteome fractionation; M3- membrane fraction from cortex 3, obtained after the first ultracentrifugation step; S3- soluble fraction from cortex 3, obtained after the first ultracentrifugation step; M3w- membrane fraction from cortex 3, obtained after the second ultracentrifugation step; S3w- soluble fraction from cortex 3, obtained after the second ultracentrifugation step.

The results showed that the number of membrane proteins (white part of the bars) that were identified in the extract samples, for both liquid and gel digestions, were approximately 50%, as expected, once the extract samples contained membrane and soluble proteins, before

the subproteome fractionation. The membrane proteins in the membrane samples (M3 and M3w), for both digestions, were superior of the soluble proteins (grey part of the bars), approximately 63% and 59% for the gel digestion and liquid digestion samples, respectively. The contrary could be observed for the soluble samples (S3 and S3w), for both digestions, since the percentage of membrane proteins were lower comparing with soluble proteins, approximately 40% of membrane proteins in all soluble samples. This result was also expected, once during the subproteome fractionation procedure there was an enrichment of membrane proteins in the pellets (membrane samples).

In Supplementary figure 8.12 are represented the Venn Diagrams illustrating the number of shared or unique proteins from liquid and gel digestion that were identified by mass spectrometry. BioVenn software analysis was performed (http://www.cmbi.ru.nl/cdd/biovenn/) using diagrams with area-proportional to the number of identifications. The Venn Diagrams showed that approximately 630 proteins were commonly identified between gel and liquid digestion for samples E3, M3 and M3w, in the S3 samples 601 proteins were common and for S3w only 208 once the total number were lower (612 proteins) comparing with the other samples. The results obtained revealed that the number of identified proteins for all samples that were digested by in-gel digestion was higher comparing with the samples digested by the liquid approach. In gel digestion samples were also identified with a higher number of unique proteins comparing with liquid digestion. Although gel digestion being a more time consuming procedure, this results showed that for a higher protein identification by mass spectrometry the in-gel digestion procedure is a better technique comparing with a liquid digestion procedure. A similar comparison between liquid and gel digestions was already done by a colleague in the group and the conclusion was the same, plus the reproducibility of the gel digestion technique was higher too, as well as, the results presented a lower coefficient of variation (Anjo *et al*, 2014, accepted).

Supplementary Figure 8.12: Venn Diagrams illustrating the number of shared or unique proteins from liquid and gel digestion that were identified by Mass spectrometry. A- Venn diagram showing the distribution of the shared and unique proteins between E3 sample digested in gel and E3 sample digested by the liquid approach. The combined protein number is 1080. **B-** Venn diagram showing the distribution of the shared and unique proteins between M3 sample digested in gel and M3 sample digested by the liquid approach. The combined protein number is 1190; **C-** Venn diagram showing the distribution of the shared and unique proteins between M3w sample digested in gel and M3w sample digested by the liquid approach. The combined protein number is 979; **D-** Venn diagram showing the distribution of the shared and unique proteins between S3 sample digested in gel and S3 sample digested by the liquid approach. The combined protein number is 971; **E-** Venn diagram showing the distribution of the shared and unique proteins between S3w sample digested in gel and S3w sample digested by the liquid approach. The combined protein number is 612.